



**Impact of Pericardial and Paracardiac Fat on the Cardiovascular Structure
and Function in HIV Infected Persons: A Cardiovascular Magnetic Resonance
Study**

by

Patricia Maishi

Student no: 217295363

**Thesis submitted in fulfilment of the requirement for the
degree Master of Science: Radiography
in the Faculty of Health and Wellness Sciences
at the Cape Peninsula University of Technology
Bellville
South Africa**

Supervisor: Dr. A. Speelman (Internal)

Supervisor: Prof. N. A. B. Ntusi (External)

Co-supervisor: Mrs. E. Herbert

ABSTRACT

Introduction: Cardiovascular disease (CVD) is the major contributor to morbidity and mortality in people living with human immunodeficiency virus (PLHIV). Approximately 8.2 million South Africans live with the human immunodeficiency (HIV) infection. The widescale availability and use of ART has dramatically decreased the number of HIV/acquired immunodeficiency syndrome (AIDS)-related deaths and improved quality of life. However, ART is associated with the development of CVD leading to heart failure with preserved ejection fraction, myocardial inflammation, myocardial fibrosis, and myocardial steatosis are common phenotypes in ART-treated PLHIV. Increased visceral and pericardiac adipose tissue is associated with poor cardiovascular outcomes, including elevated risk of incident heart failure, atrial fibrillation, myocardial infarction, and sudden cardiac death. While the pathophysiology of HIV-associated CVD is complex and multifactorial, including varying evidence for direct viral effect of HIV, metabolic changes induced by antiretroviral therapy (ART), opportunistic infections, systemic inflammation and subclinical immune activation, mitochondrial dysfunction, and endothelial dysfunction, the role of pericardial and paracardiac adiposity to development of HIV-associated CVD is unknown. Cardiovascular magnetic resonance (CMR), through its high spatial and temporal resolution, is the ideal technique for quantification of pericardial adipose tissue (PAT) and paracardiac adipose tissue (ParaAT). The current study hypothesised that fat around the heart has detrimental effects on the myocardium in PLHIV on ART. Therefore, this study is aimed to investigate the effect of pericardial and paracardiac fat deposits on cardiovascular structure and function in PLHIV using CMR.

Methods: This was a retrospective, cross-sectional study design including 3 groups of participants: (1) PLHIV on ART; (2) untreated PLHIV; and (3) matched HIV uninfected controls. CMR was performed on a Siemens Magnetom Skyra 3Tesla between February 2017 and March 2020. Images were postprocessed and analysed with proprietary software from circle Cardiovascular Imaging (CVI)42[®]. PAT and ParaAT volumes were obtained manually using Simpson's method, by contouring the borders of PAT and the ParaAT with regions of interest at end-diastole, from base to the apex of the heart. Late gadolinium enhancement (LGE) images were acquired with a phase-sensitive inversion-recovery sequence. PAT and ParaAT volumes from different short-axis slices were summed to obtain whole-heart PAT and ParaAT volumes. Left (LV) and right (RV) ventricular volumes, LV mass (LVM), and function, T2 short Tau inversion-recovery imaging,

strain and strain rates, T1 and T2 mapping, LGE, and extracellular volume (ECV) were also assessed.

Results: 198 participants were included: PLHIV on ART (n=131), PLHIV naïve to ART (n=19), and matched HIV uninfected controls (n=48). PLHIV on ART were older (44.9 ± 8.3 years) than untreated PLHIV (36.4 ± 8.2 years) and uninfected controls (41.7 ± 11.5 years), respectively ($p<0.001$). A large distribution of our study cohort was female. PLHIV on ART were on antiretroviral combination therapy treatment including nucleoside reverse transcriptase inhibitors, non-nucleoside reverse transcriptase inhibitor and protease inhibitor. PLHIV on ART had greater whole-heart PAT volumes 43.1 cm^3 (30.7-54.8 IQR) compared to untreated PLHIV 32.1 cm^3 (22.8-52.8 IQR) or uninfected controls 22.99 cm^3 (17.2-31.7 IQR), $p<0.001$. PLHIV on ART had higher whole-heart ParaAT volume 9.0 cm^3 (3.8-13.4 IQR) compared to untreated PLHIV 0 cm^3 (0.0-10.8 IQR) or uninfected controls 0 cm^3 (0.0-5.2 IQR), $p<0.001$ (Figure 2). PLHIV on ART (100.9 ± 28.5 g) and untreated PLHIV (103.2 ± 29.7 g) had elevated LVM compared to uninfected controls (87.6 ± 19.3 g), $p<0.01$ (Table 1). Untreated PLHIV had higher T1, T2 times and ECV (1301 ± 58 ms; 42 ± 4 ms; $32\pm 5\%$) compared to PLHIV on ART (1251 ± 47 ms; 39 ± 3 ms; $31\pm 5\%$) and untreated controls (1224 ± 48 ms; 39 ± 2 ms; $29\pm 9\%$), respectively. Similarly, untreated PLHIV had the largest burden of LGE (Figure 3) and the greatest impairments in myocardial strain and strain rates. On univariate regression analysis in the pooled population, ParaAT demonstrated weak negative correlation with peak global circumferential strain ($r=-0.23$, $p<0.001$) and longitudinal strain ($r=-0.21$, $p<0.01$), while PAT showed a weak negative correlation with peak circumferential strain ($r=-0.18$, $p<0.01$) and moderate positive correlation with LVM ($r=0.45$, $p<0.001$) (Figure 4).

Conclusion: The study suggests that pericardial and paracardial fat can drive cardiometabolic risk factors and directly promote cardiac dysfunction in HIV patients. CMR offers a non-invasive means of assessing ventricular function, anatomical structure, tissue characterisation and the presence of LGE in asymptomatic HIV-infected patients by assessing myocardial structure, inflammation, fibrosis, deformation, and weak association between the burden of pericardial and paracardiac fat, and tissue characteristics in PLHIV.

Keywords: Cardiovascular magnetic resonance (CMR), human immunodeficiency virus (HIV), antiretroviral therapy (ART), pericardial and paracardiac fat.

DEDICATION

“Two are better than one, because they have a good reward for their labour. For if they fall, one will lift up his fellow. But pity anyone who falls and has no one to help them up”.

Ecclesiastes 4 vs 9-10

To my husband Bonginkosi Maishi, my two boys, Thabiso and Lindani and daughter, Khumsa.
Thank you for all the support and encouragement.

ACKNOWLEDGEMENTS

- This work is based on the research conducted by Professor N.A Ntusi, Head of Department of Medicine at Groote Schuur Hospital.
- A special appreciation to Prof N.A. Ntusi and Dr A Speelman. Your guidance and mentorship has been invaluable. My appreciation is also extended to my co-supervisor Mrs Estelle Herbert for her contributions.
- UCT-CUBIC radiographers Petronella Samuels, Ingrid Op't Hof and Mariaan Japhta, who performed all the CMR scans, and Stephen Jermy for assisting with CVI analysis;
- Prof Ntusi's research group, Pheletso Letuka, Solomon Alukayode, Daniel Mutithu, Tasmin Bana, Sango Skelem, Noleen Williams and Lionel Chinhoyi for advice, guidance and friendship;
- Thanks to Dr Tess Petersen, Dr Justin Mbalabu, Dr Mpiko Ntseko, Dr Jason Baker, and Dr Hadil Saad who assisted me with the CMR data;
- I would like to thank my church home group and friends whose prayers have been instrumental to my progress;
- I would like to thank the HWSETA for financial support in year 2022;
- I would like to acknowledge the National Research Foundation, Medical Research Council of South Africa, Lily and Ernst Hausmann Trust for funding support (2020-2021);
- Finally, I am very grateful to my husband Bonginkosi Maishi, my two boys Thabiso and Lindani and daughter Khumsa for their unwavering support and encouragement through my master's journey and life in general.

DECLARATION

I, **Patricia Maishi**, declare that the contents of this dissertation/thesis represent my original work, and that neither the whole nor part of this thesis has been submitted for academic examination towards any qualification. Furthermore, this work represents my own opinions and not necessarily those of the Cape Peninsula University of Technology.

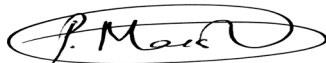
Signed: 

Date: 08/02/2023

PLAGIARISM DECLARATION

I, **Patricia Maishi**, confirm that this thesis is my own work and is not from any other person's work (published or unpublished). Where required, I have referenced the appropriate sources on whose work parts of this thesis part was based.

Signed

A handwritten signature in black ink, enclosed in a hand-drawn oval. The signature appears to read "P. Maishi".

Date: 08/02/2023

LIST OF FIGURES

<u>Figure 1.</u> Prevalence estimates of HIV and number of PLHIV in South Africa.....	2
<u>Figure 2.1.</u> Schematic demonstration of the internal anatomy of the heart showing the outer pericardium, myocardium, and endocardium	8
<u>Figure 2.2.</u> CMR image showing four chamber view (a) demonstrating pericardium, (b) paracardiac fat, (c) pericardial fat of an adult HIV+ patient, and (d) CMR of a normal heart in the control group	10
<u>Figure 2.3.</u> Classification of ART regimens and risk factors.....	12
<u>Figure 3.1.</u> CMR T2 STIR image of the heart showing quantitative analysis by comparing the LV myocardium (1) in short axis against adjacent skeletal muscle (2) excluding non-suppressed blood pool signal.....	27
<u>Figure 3.2.</u> CMR cine images of the normal heart of our study participants with myocardial point overlay (yellow dots) to perform global strain analysis. (A) 2 chamber view (B) 4 chamber view (C) LVOT view and (D) short-axis view with endocardial (red line) & epicardial (green line) contours.....	27
<u>Figure 3.3.</u> CMR native T1 mapping (A) and (B) post-contrast T1 mapping of the normal heart of our study participants showing endocardial (red circle), epicardial (green circle), and blood pool (orange circle) contours.....	28
<u>Figure 3.4.</u> Short axis T2 map of LV myocardium. The region of interest (ROI) is used to define the epi- and endocardial borders and partition the myocardium into segments.....	28
<u>Figure 3.5.</u> CMR T1-weighted fast spin-echo image on the short-axis showing quantitative analysis by comparing the LV myocardium (1) against adjacent skeletal muscle (2).....	29
<u>Figure 3.6.</u> CMR PSIR LGE sequence of short-axis stack images (A-F) (from base to apex) demonstrating volumetric measurements of pericardial and paracardiac fat mass.....	30
<u>Figure 3.7.</u> The LGE image in the PSIR sequence with high signal intensity enhancement of an HIV-untreated participant (a), the same LGE image with colour overlay in the area of enhancement (yellow outline) (b), quantification of LGE volume fraction for region of interest by comparing normal myocardium (blue outline) to abnormal area (purple outline) (c).....	31
<u>Figure 4.1.</u> Box plot comparison of PATi (A) and ParaATi (B) fat between the three sub-groups, including HIV on ART, HIV not on therapy and uninfected controls.....	39
<u>Figure 4.2.</u> Bar graph illustrating percentage of patterns of late gadolinium enhancement amongst participants with HIV and on ART, those not on therapy and uninfected controls.....	41
<u>Figure 4.3.</u> Scatter plots illustrating the correlation between (a) ParaAT and peak circumferential strain, (b) PAT and peak circumferential strain, (c) PAT and peak longitudinal strain and (d) PAT and LV mass in HIV-infected sub-groups and HIV-uninfected controls.....	45

LIST OF TABLES

Table 3.1. Inclusion and exclusion criteria.....	24
Table 4.1. Demographic characteristics separated by HIV infection status and uninfected controls.....	35
Table 4. 2. Clinical characteristics separated by HIV infection status and uninfected controls....	36
Table 4. 3. CMR functional characteristics of HIV- infected participants and uninfected controls.	37
Table 4. 4. Myocardial deformation characteristics.....	38
Table 4. 5. Myocardial tissue characteristics.....	39
Table 4.6. Quantification of pericardial and paracardiac adipose tissue in HIV-infected participants and uninfected controls	40
Table 4.7. LGE patterns in HIV-infected participants and uninfected controls.....	41
Table 4. 8. Classification of PLHIV by ART regimens	42
Table 4.9. Correlation between PATi and CMR parameters in HIV-infected participants and uninfected controls.....	43
Table 4. 10. Correlation between ParaATi and CMR parameters in HIV-infected participants and uninfected controls.....	44

LIST OF ABBREVIATIONS

AIDS	Acquired immunodeficiency syndrome
ANOVA	Analysis of variance
ART	Antiretroviral treatment/therapy
ASCVD	Atherosclerotic cardiovascular disease
b-SSFP	Balanced steady state free precession
BMI	Body mass index
BSA	Body surface area
CAD	Coronary artery disease
CD4	Cluster of differentiation 4
cm	Centimetre
CMR	Cardiovascular magnetic resonance
CPUT	Cape Peninsula University of Technology
CUBIC	Cape Universities Body Imaging Centre
CV	cardiovascular
CVD	Cardiovascular disease
CVI	Cardiovascular imaging
DCM	Dilated cardiomyopathy
DNA	Deoxyribonucleic acid
ECG	Electrocardiogram
ECM	extracellular matrix
ECV	Extracellular volume
EDV	End diastolic volume
EF	Ejection fraction
EGE	Early gadolinium enhancement
eGFR	Estimated glomerular filtration rate
ESV	End systolic volume
FLASH	Fast low angle shot
Gad	Gadolinium
GFR	Glomerular filtration rate
GRE	Gradient recall echo
GSH	Groote Schuur Hospital
HAART	Highly Active Antiretroviral Therapy
HASTE	Half-Fourier Acquired Single-shot turbo spin-echo
HDL	High-density lipoprotein
HIV	Human immunodeficiency virus
HLA	Horizontal long axis
HREC	Human Research Ethics Committee
ID	Identification
IFN- α	Interferon alfa
INIs	Integrase inhibitors
IQR	interquartile range

kg	Kilogram
LGE	Late gadolinium enhancement
LV	Left ventricle/ventricular
LVEDV	Left ventricular end-diastole volume
LVEDVi	Left ventricular end-diastole volume index
LVESV	Left ventricular end-systolic volume
LVESVi	Left ventricular end-systolic volume index
LVM	Left ventricular mass
LVMi	Left ventricular mass index
LVOT	Left ventricular outflow tract
LVSV	Left ventricular stroke volume
LVSVi	Left ventricular stroke volume index
mL	millilitre
MRC	Medical Research Council
MRI	Magnetic resonance imaging
ms	milliseconds
NMR	Nuclear magnetic resonance
NNRTIs	Non-nucleoside reverse transcriptase inhibitors
NRTIs	Nucleoside reverse transcriptase inhibitors
ParaAT	Paracardiac adipose tissue
ParaATi	Paracardiac adipose tissue index
PAT	Pericardial adipose tissue
PATi	Pericardial adipose tissue index
PIs	Protease inhibitors
PLHIV	People living with HIV
Prof	Professor
PSIR	Phase-sensitive inversion recovery
REC	Research Ethics Committee
RNA	Ribonucleic acid
ROI	Region of interest
RV	Right ventricle/ventricular
SA	Short axis
SA-CMR	South African Cardiovascular Magnetic Resonance
SD	Standard deviation
SE	Spin-echo
SI	Signal intensity
SPSS	Statistical Package for the Social Sciences
STATS SA	Statistics South Africa
STIR	Short Tau inversion recovery
SV	Stroke volume
T1-w	T1-weighted
T2-w	T2-weighted
T	Tesla

TE	echo time
TRUFI	True fast imaging
TSE	Turbo spin-echo
UCT	University of Cape Town
UNAIDS	The Joint United Nations Programme on HIV/AIDS
VLA	Vertical long axis
WHO	World Health Organization
WMA	World Medical Association

CONTENTS

ABSTRACT.....	ii
DEDICATION.....	iv
ACKNOWLEDGEMENTS.....	v
DECLARATION.....	vi
PLAGIARISM DECLARATION.....	vii
LIST OF FIGURES.....	viii
LIST OF TABLES.....	ix
LIST OF ABBREVIATIONS.....	x
CHAPTER ONE.....	1
INTRODUCTION.....	1
1.1 Introduction.....	1
1.2 Background.....	2
1.3 Research Rationale.....	4
1.4 Research question.....	5
1.5 Aim.....	5
1.6 Objectives.....	5
1.6.1 Primary objectives:.....	5
1.6.2 Secondary objectives:.....	5
1.7 Summary.....	5
1.8 A brief overview of the thesis structure:.....	5
1.8.1 Chapter 2: Literature review.....	6
1.8.2 Chapter 3: Research methodology.....	6
1.8.3 Chapter 4: Results.....	6
1.8.4 Chapter 5: Discussion.....	6
1.8.5 Chapter 6: Strengths, limitations, recommendations and conclusion.....	6
CHAPTER TWO.....	7
LITERATURE REVIEW.....	7
2.1 Introduction.....	7
2.2 The structure and function of the heart.....	7
2.2.1 The endocardium.....	7
2.2.2 The myocardium.....	7
2.2.3 The pericardium.....	8
2.2.3.1 Physiology of pericardial fat.....	9
2.2.3.2 Physiology of paracardiac fat.....	9
2.2.3.3 Pericardial anatomy (as seen on MRI).....	10
2.3 Aetiology of HIV/AIDS.....	11

2.4 Antiretroviral treatment/therapy (ART).....	11
2.5 The burden of HIV-associated cardiovascular disease	13
2.6 Cardiovascular effects of ART treatment	13
2.7 Cardiovascular risk factors in PLHIV	14
2.7.1 Pericardial and paracardiac adipose tissue.....	14
2.7.2 Metabolic syndrome.....	14
2.7.3 Atherosclerosis.....	15
2.7.4 Inflammation	15
2.7.5 Myocardial Fibrosis.....	16
2.8 Cardiovascular magnetic resonance.....	16
2.8.1 Spin-echo sequences	17
2.8.1.1 T1-weighted sequences	17
2.8.1.2 T2-weighted short Tau inversion recovery	17
2.8.1.3 Half Fourier Acquired Single-shot spin-echo	18
2.8.2 Cine imaging.....	18
2.8.3 Native T1 mapping together with extracellular volume	18
2.8.4 T2 mapping	19
2.8.5 Strain imaging.....	19
2.8.6 Early gadolinium enhancement.....	20
2.8.7 Late gadolinium enhancement	20
2.8.8 Image quality	21
2.9 Summary	21
CHAPTER THREE.....	22
RESEARCH METHODOLOGY	22
3.1 Introduction.....	22
3.2 Study design.....	22
3.3 Study population	23
3.3.1 Inclusion and exclusion criteria for umbrella study.....	23
3.3.2 Inclusion and exclusion criteria for CMR images for the current study.....	24
3.4 Sample size.....	24
3.5 Image acquisition and data collection	24
3.6 Data management.....	25
3.7 Image analysis.....	25
3.7.1 Determination of ventricular parameters	25
3.7.2 T2-weighted short Tau inversion recovery images.....	26
3.7.3 Myocardial strain assessment	27
3.7.4 Myocardial T1 mapping and ECV.....	28

3.7.5 Myocardial T2 mapping.....	28
3.7.6 T1-weighted imaging.....	29
3.7.7 Measurements of the pericardial and paracardiac fat volume	29
3.7.8 Late gadolinium enhancement	30
3.8 Data statistical analysis and reporting.....	31
3.9 Ethical considerations	31
3.9.1 Informed consent (Umbrella study).....	32
3.9.2 Data confidentiality and management	32
3.9.3 Data integrity	32
3.10 Summary	33
CHAPTER FOUR.....	34
RESULTS	34
4.1 Introduction.....	34
4.2 Demographic characteristics	34
4.3 Clinical Characteristics	35
4.4 Cardiovascular magnetic resonance findings.....	36
4.4.1 Left and right ventricular function.....	36
4.4.2 Left ventricular deformational characteristics	37
4.4.3 Tissue characterisation.....	38
4.4.4 Pericardial and paracardiac adipose deposits.....	39
4.4.5 Late gadolinium enhancement	40
4.5 ART regimen.....	41
4.6 Bivariate correlates of myocardial function and tissue characteristics with pericardial adiposity.	43
4.7 Bivariate correlates of myocardial function and tissue characteristics with paracardiac adiposity.	43
4.8 Summary	45
CHAPTER FIVE.....	46
DISCUSSION	46
CHAPTER SIX	53
STRENGTHS, LIMITATIONS, RECOMMENDATIONS AND CONCLUSION.....	53
6.1 Introduction.....	53
6.2 Strengths.....	53
6.3 Limitations	53
6.4 Recommendations	53
6.5 Conclusion	54
REFERENCE LIST	55

APPENDICES

<u>APPENDIX 1:</u> MRI SAFETY SCREENING FORM.....	74
<u>APPENDIX 2:</u> CMR SCANNING PROTOCOL.....	75
<u>APPENDIX 3:</u> CMR SEQUENCES AND PARAMETERS USED TO SCAN PARTICIPANTS.....	76
<u>APPENDIX 4:</u> MICROSOFT EXCEL SPREADSHEET WITH PARTICIPANT INFORMATION AND CMR MEASUREMENTS.....	77
<u>APPENDIX 5:</u> UCT HREC ETHICAL APPROVAL.....	78
<u>APPENDIX 6:</u> CPUT HWS FACULTY RESEARCH ETHICS CERTIFICATE.....	79
<u>APPENDIX 7:</u> SUBJECT INFORMATION LEAFLET.....	80
<u>APPENDIX 8:</u> INFORMED CONSENT FORM.....	85

CHAPTER ONE

INTRODUCTION

1.1 Introduction

Cardiovascular diseases (CVD) are the major contributor to morbidity and mortality in people living with human immunodeficiency virus (PLHIV)(Ntusi, 2017;Bonou *et al.*, 2021). Consequently, both the human immunodeficiency virus (HIV) and antiretroviral treatment/therapy (ART) may be associated with complications leading to abnormalities in fat distribution, adiposopathy and disorders of glucose and lipid metabolism (Bune, Yalew & Kumie, 2019). Increased cardiac adipose tissue is considered an important contributor to HIV-associated CVD, in view of the complex interaction of the viral effect of HIV, metabolic changes induced by ART and underlying chronic inflammatory processes (Buggey *et al.*, 2020). There is a strong correlation between pericardial and paracardiac adipose tissue and the development of metabolic syndrome, insulin resistance and obesity (Goudis, Vasileiadis & Liu, 2018).

Thus, there is a need for renewed efforts to ensure eradication of HIV and to achieve sustainable health. The Joint United Nations Programme on HIV/acquired immunodeficiency syndrome (AIDS) (UNAIDS) encourages novel prevention strategies aimed at reducing new infections including the development of a preventative vaccine. In a recent Lancet Commission publication, the International AIDS Society highlights the need to assess the future of the HIV response in context of a more integrated approach to health (Bekker *et al.*, 2018), echoing the global call for advancing health in PLHIV.

Cardiovascular magnetic resonance (CMR) robustly and accurately detects cardiac involvement in HIV and assists in the clinical management thereof (Bièrè *et al.*, 2017). CMR has been successfully used to accurately assess left ventricular (LV) size and function, identify the distribution of scar patterns, and tissue characterisation (Marra, Lima & Iliceto, 2011). CMR is a powerful tool for diagnosis, risk stratification, and evaluating efficacy of therapeutic intervention. Late gadolinium enhancement (LGE) is a technique that enhances CMR capabilities by producing excellent contrast between diseased and normal myocardium (Ripley *et al.*, 2016). Moreover, LGE CMR is used to evaluate quantitatively for the absence or presence and regional distribution of cardiac scar enhancement patterns (Agoston-Coldea *et al.*, 2021). LGE is an independent predictor of adverse outcome in HIV-associated CVD (Karamitsos *et al.*, 2020). Early identification of cardiac

involvement in HIV improves treatment planning and prevents disease progression to arrhythmia and heart failure (Manga *et al.*, 2017).

The purpose of this study was to investigate the effect of cardiac fat deposits on the structure and function of the myocardium in PLHIV using CMR. In addition, the correlation between pericardial and paracardiac fat and myocardial inflammation, myocardial fibrosis, and myocardial strain was also assessed.

1.2 Background

HIV, which when untreated, leads to AIDS, and poses a major public health challenge in South Africa and globally according to Statistics South Africa (STATS SA) (2019). In 2020, approximately 37.7 million people globally were infected with HIV, with 1.5 million new infections and 680,000 AIDS-related deaths (UNAIDS, 2021). Africa has the largest HIV prevalence in the world, with an estimated 69% of PLHIV (Risher *et al.*, 2021). As can be noted from Figure one below, South Africa has the highest population rate for PLHIV than any other country (van Schalkwyk *et al.*, 2021). In South Africa, the estimated overall HIV prevalence is approximately 13,5% (van Schalkwyk *et al.*, 2021). In 2019, Statistics South Africa reported that approximately 8 million people were living with HIV, with about 126,805 HIV-related deaths (STATS SA, 2019). In addition, 19% of PLHIV are aged 15-49, of which 4% fall within the 15–24-year-old age range (Figure 1).

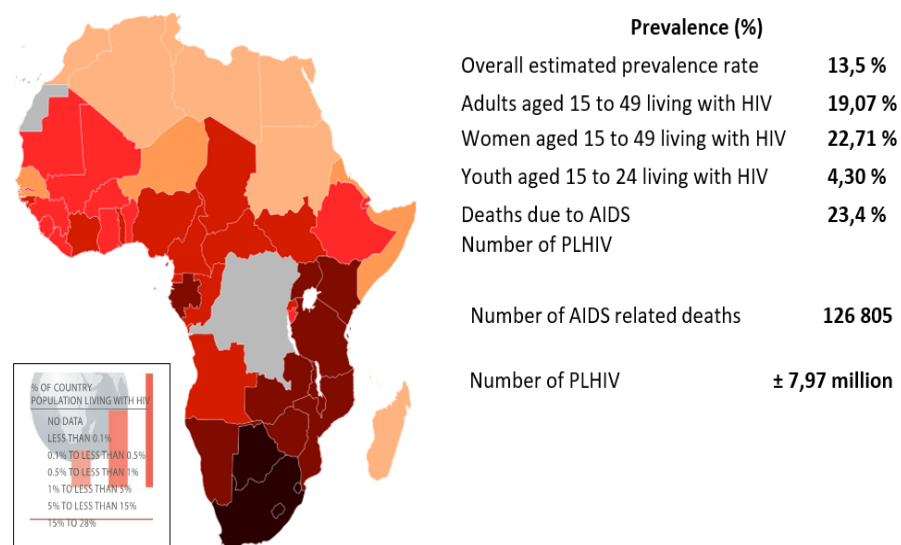


Figure 2. Prevalence estimates of HIV and number of PLHIV in South Africa (UNAIDS, 2021)

The increase in the roll-out of ART has dramatically decreased the proportion of HIV/AIDS-related deaths (Autenrieth *et al.*, 2018). However, ART has gained attention as one of the factors responsible for complications associated with heart failure, including coronary artery disease (CAD), cardiomyopathy, and pericardial disease (So-Armah & Freiberg, 2018). Although these complications are multi-factorial, a complex relationship of traditional risk factors, myocardial inflammation, myocardial fibrosis, myocardial steatosis, mitochondrial dysfunction and lipid metabolic abnormalities associated with CAD exists (Buggey & Longenecker, 2018). Aetiology and pathogenesis of fat deposition abnormalities is not fully understood, but may relate to specific effects of ART on adipocyte metabolism with consequent metabolic abnormalities, and from direct effects of ART on lipid and glucose metabolism (Hadigan *et al.*, 2003; Fricke *et al.*, 2019).

Higher volumes of epicardial and paracardiac fat resulting from fat redistribution may exert detrimental effects on the myocardium leading to the development of CAD, arrhythmias, and atrial fibrillation (Matloch, Kotulák & Haluzík, 2016; Belkin & Uriel, 2018). Importantly, pericardial fat is a source of proinflammatory cytokine stimulation; and elaboration of proinflammatory factors leads to endothelial dysfunction and CAD. Proinflammatory factors are known to play a role in the pathogenesis of cardiac adipose tissue (Castillo *et al.*, 2020).

Magnetic resonance imaging (MRI) is a non-invasive, versatile cross-sectional multi-planar imaging modality that can be used to gain insight into the pathogenesis of cardiac adipose tissue. CMR is an adapted form of MRI used to investigate structural and functional abnormalities of the cardiovascular system (Russo, Lovato & Ligabue, 2020). It has the added benefit of being able to measure treatment response; and has an unique ability to characterise myocardial tissue without any ionising radiation exposure (Lee *et al.*, 2011; Haaf *et al.*, 2016). CMR is a reference and accurate imaging technique for volumetric assessment, evaluation of myocardial function and detection of myocardial fibrosis in HIV-associated CVD (Salerno *et al.*, 2017; Cojan-Minzat, Zlibut & Agoston-Coldea, 2020). Therefore, to study the pathogenesis of cardiac adipose tissue in PLHIV the following CMR sequences were used such as:

- (i) A balanced steady-state free precession (b-SSFP) cine sequence which provides quantification of ejection fraction (EF), stroke volume (SV) and ventricular volumes.
- (ii) A T2-weighted with dark blood Short-Tau inversion recovery (STIR) sequence that can be used to detect inflammation in the myocardium by suppressing both blood and fat.
- (iii) A T1-weighted phase-sensitive inversion recovery (PSIR) LGE sequences used to identify the extent of myocardial injury.

- (iv) T1 maps and extracellular volume (ECV)-weighted sequences are used to identify fibrosis (Aldweib, Farah & Biederman, 2018).
- (v) LGE which also assists in visualisation of regional/focal patterns and delineation of infarcts in the myocardium (Ishida, Kato & Sakuma, 2009).

1.3 Research Rationale

The effect of HIV diagnosis, disease duration, ART use, cluster of differentiation 4 (CD4) count, viral load, opportunistic infections, and patient co-morbidity has not been explored, (Belkin & Uriel, 2018). However, ART is associated with complications leading to abnormalities in fat distribution (lipodystrophy) and disorders of the glucose and lipid metabolism (Deeks *et al.*, 2015). There is common agreement that lipodystrophy may be characterised by ectopic fat deposition, specifically, perivisceral accumulation of fat around the waist and heart (Barbaro & Boccara, 2005; Buggey & Longenecker, 2018; Fricke *et al.*, 2019). The pathogenesis of lipodystrophy syndrome is complex and poorly understood and includes direct effects of HIV and adipocytes on the heart, leading to the inflammatory response of the myocardium (Greenstein *et al.*, 2009; Buggey & Longenecker, 2018). Therefore, the importance of investigating vasoactive properties of perivascular adipose tissue as well as the inflammatory changes leading to cardiovascular disease in HIV is crucial.

Recent studies suggest that chronic inflammatory changes associated with pericardial fat-related cytokines and adipokines may be detrimental to coronary artery physiology and myocardial biology (Castillo *et al.*, 2020; Schiattarella, Sequeira & Ameri, 2020). One study reports myocardial injury related to pericardial adiposity may be secondary to inflammation and ischemia leading to irreversible cardiac dysfunction (Ma *et al.*, 2018). In addition, pericardial fat activates myocardial fibrosis, leading to diastolic dysfunction and heart failure (Patel *et al.*, 2017). The role of CMR in the diagnosis of cardiac involvement in HIV, including earlier detection of arrhythmia, diastolic dysfunction, and tissue characterisation, has been investigated (Rajiah *et al.*, 2019). Moreover, T1 mapping and ECV estimation are reliable techniques for quantifying the degree of myocardial fibrosis, whereas T2-weighted imaging is technically utilised in visualising myocardial oedema seen in disease pathologies (Haaf *et al.*, 2016; Salerno *et al.*, 2017). Versatility of CMR may be useful for a multiparametric assessment of cardiovascular phenotype in PLHIV and to evaluate the influence of pericardial and paracardiac adiposity on cardiovascular phenotypes and outcomes (Buggey & Longenecker, 2018).

1.4 Research question

Does adipose tissue around the heart in PLHIV have detrimental effects on myocardial structure and function?

1.5 Aim

The aim of this retrospective study was to investigate the effect of pericardial and paracardiac fat deposits on cardiovascular structure and function in PLHIV using CMR.

1.6 Objectives

1.6.1 Primary objectives:

- Assess myocardial structure and function in PLHIV.
- Assess the burden of pericardial and paracardiac fat in patients with HIV.

1.6.2 Secondary objectives:

- Assess myocardial inflammation in PLHIV.
- Assess myocardial fibrosis in PLHIV.
- Assess myocardial deformation in PLHIV.
- Correlate the burden of pericardial and paracardiac fat with the above parameters.

1.7 Summary

HIV is a major health challenge in South Africa. However, the use of ART has reduced HIV-related mortality. The paradox of ART is decreased mortality rates on one hand and an increase in cardiovascular (CV) morbidity on the other (Tsabedze *et al.*, 2018). CVD in PLHIV is increasingly related to a positive complex interaction of ART, hence extending lifespan. The complications of HIV have evolved from opportunistic infections to those leading to abnormalities in fat distribution and disorders of glucose and lipid metabolism. CMR is considered the most reliable means of phenotyping the spectrum of CV involvement in HIV and can be used in guiding management of cardiac complications in PLHIV (Ntusi, 2017).

1.8 A brief overview of the thesis structure:

A detailed description of the structure of this thesis is included in the section below.

1.8.1 Chapter 2: Literature review

Chapter 2 provides a literature review on the structure and function of the heart. The prevalence and pathophysiology of cardiac adipose tissue is discussed in depth. Additionally, the effects of HIV and ART on the cardiovascular system and complications will also be discussed. The chapter concludes with the role CMR plays in the assessment of cardiac adipose tissue and its impact on the cardiovascular structure and function in PLHIV.

1.8.2 Chapter 3: Research methodology

Chapter 3 provides a detailed description of the research methods and design. Furthermore, it describes the study population, inclusion, and exclusion criteria of the study. The sampling technique and sample size calculation for the study is explained. Furthermore, image acquisition and the data collection process are described, as well as the data analysis technique on CMR. Finally, the ethical considerations applicable to the data collection for this study are discussed.

1.8.3 Chapter 4: Results

Chapter 4 presents results from the study which include different data pertaining to the objectives of the study. This chapter describes clinical characteristics and demographics of the study population. PAT and ParaAT deposits, LV and right RV ventricular volumes, LVM, and function, T2 short Tau inversion-recovery imaging, strain and strain rates, T1 and T2 mapping, LGE, and ECV were also reported in the form of tables and graphs and concludes with a brief chapter summary.

1.8.4 Chapter 5: Discussion

Chapter 5 contains a comprehensive discussion that summarises the key observations of the study. The observation discussed included PAT and ParaAT, tissue characterisation, LV and RV function and strain; these were compared to previous publications. The chapter demonstrates the correlation between PAT/ParaAT and CMR parameters of the three sub groups. Further, this chapter also discuss the clinical implications of the observations within the context of other similar studies in literature.

1.8.5 Chapter 6: Strengths, limitations, recommendations and conclusion

Chapter 6 highlights strengths and limitations of the study. The chapter further, discusses recommendations for future research. A brief summary which concludes the study is presented.

CHAPTER TWO

LITERATURE REVIEW

2.1 Introduction

This study aimed to assess the impact of pericardial and paracardiac fat deposits on the cardiovascular structure and function in PLHIV who are untreated as well as a group receiving ART. In this chapter, a review of the literature is conducted to explain the burden of HIV-associated CVD on cardiovascular phenotypes and outcomes in PLHIV. Further, this chapter also reviews the pathophysiology of cardiac adiposity, the structure and function of the heart with a particular focus on the muscular layers, the aetiology of HIV/AIDS as well as the effect ART has on the structure and function of the heart. The literature review ends by describing the role of different CMR sequences in evaluation of myocardial function and structure in HIV-associated CVD.

2.2 The structure and function of the heart

The heart is a vital organ in the body and is a muscular pump (Weber *et al.*, 2013), which occupies the centre region of the thorax, with the great vessels suspended into and within the pericardium. The wall of the heart includes three principal layers: endocardium, myocardium and epicardium (Iaizzo, 2015).

2.2.1 The endocardium

The endocardium is the innermost layer of overlying connective tissue, which covers the valves, atrial and ventricular chambers (Emrich *et al.*, 2021). The endocardium consists predominantly of endothelial lining originating from the large blood vessels attached to the heart (Iaizzo, 2015).

2.2.2 The myocardium

The myocardium is the muscular, middle layer within the cardiac walls that plays a major role in cardiac contractility. It comprises a circular and spiral muscle fibre network arrangement, and connective tissue, that enables the heart to contract and relax, expelling blood between the heart chambers and into the great vessels. Further, the myocardium provides a scaffolding for the heart chambers and helps to anchor the four valves of the heart. The myocardium conducts electrostimulation through its own tissues and into the epicardium. Blood supply to the myocardium stems from the coronary circulation (Hegazy *et al.*, 2022). Thus, when the coronary arteries are occluded, oxygen and nutrient supply to the downstream myocardium is compromised, resulting in ischaemia (Iaizzo, 2015).

The muscle fibres of the heart are arranged to form fibrous rings around the atrioventricular openings, which separate the atrial upper chambers from the ventricular lower chambers. Moreover, the muscle fibres are arranged differently in the atria and ventricles. The myocardium in the atria has two layers: a superficial layer and a deep layer. The fibres of the superficial and deep layers are connected at the apex of the heart. At the LV, superficial fibres extend to the apex, forming a tight spiral known as the vortex cordis, turn inward and continue to the RV as deep muscle fibres. The myocardial wall of the LV is thicker than that of the RV, which ensures that the force needed to pump oxygenated blood into the aorta, and subsequently the rest of the body, is generated. The interventricular septum, separating the LV from the RV, forms part of the myocardium and bulges into the RV, giving the higher pressure LV a barrel-shaped appearance (Buckberg *et al.*, 2018).

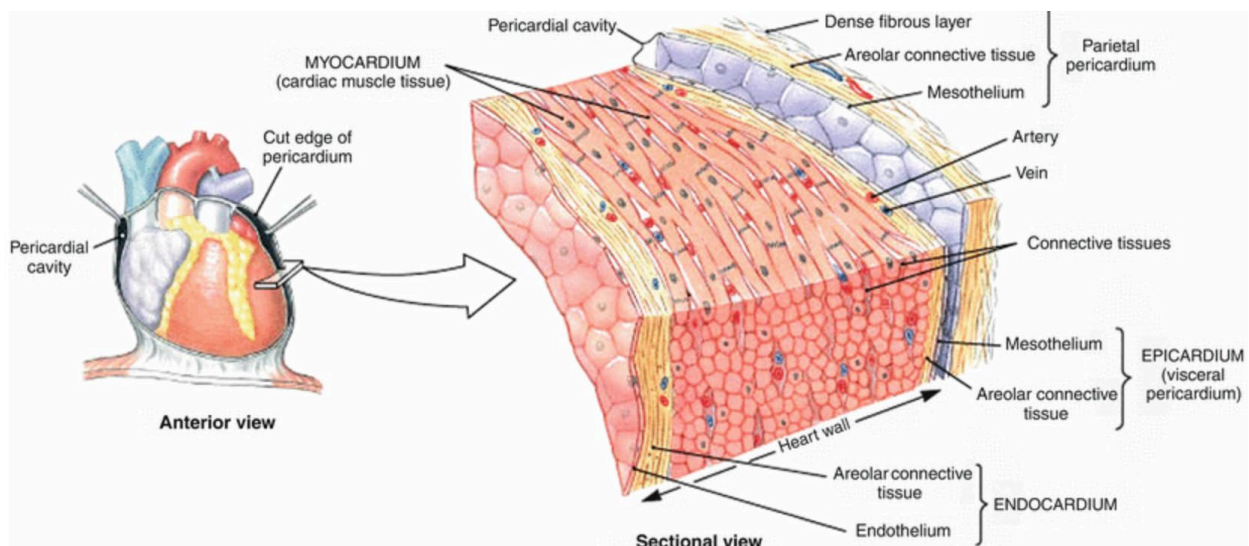


Figure 2.1. Schematic demonstration of the internal anatomy of the heart showing the outer pericardium, myocardium, and endocardium (Martini *et al.*, 2015).

2.2.3 The pericardium

The pericardium is a thin avascular two-layered sac covering the heart (Figure 2.1) and originates from the great vessels. The inner visceral layer is a delicate serous single membrane that firmly attaches to the heart wall and is termed the visceral lamina (Özer, Mehmet & Kirali, 2020; Elsaka *et al.*, 2022). According to Sacks and Fain (2007), the epicardium consists of mesothelial cells that originates from the diaphragm and later migrates to the septum of the heart, while the outer layer is composed of interwoven collagen and elastin, known as the parietal lamina. Between the visceral lamina and parietal lamina of the pericardium is a cavity known as the *cavitas pericardiaca*, which reduces friction during contractions. Under normal conditions the *cavitas pericardiaca* contains 15-

50ml serous fluid, which serves as a lubricant (Gagliardi *et al.*, 2021). Serous fluid from venous drainage occurs via the internal thoracic vein and right lymphatic ducts (Rodriguez & Tan, 2017). Additionally, the pericardium serves several important functions. These include:

- (i) anchoring the heart within the mediastinum,
- (ii) serves as a barrier to infection and malignancy from surrounding structures,
- (iii) restriction of excessive cardiac chamber dilation and maintenance of optimal pressure volume relationships,
- (iv) modulation of ventricular interdependence (Hutchison, 2009; Rodriguez & Tan, 2017).

While a small fraction of the population is born without a pericardium, this condition does not have adverse health consequences (Hoit, 2017). PLHIV are prone to develop high volume adipose tissue deposition around the heart and this redistribution of fat has been linked to the use of ART (Suliman, 2011; Butler *et al.*, 2018).

2.2.3.1 Physiology of pericardial fat

Pericardial fat is defined as fat delineating between the epicardium and the visceral pericardium (Figure 2.2c) (Bertaso *et al.*, 2013). Pericardial fat in the normal adult appears intense in the atrioventricular, interventricular grooves and around the coronary arteries (Kitterer *et al.*, 2015). There is less concentration of fat deposit around the atria, over the free wall of the LV and RV and apical region of the heart (Fricke *et al.*, 2019). Pericardial fat consists of a complex mixture of immune cells, nervous tissue, white adipocytes, and inflammatory stroma-vascular cells (Leo *et al.*, 2019). Pericardial fat shares the same embryological origins with the heart, which is splanchnopleuric mesoderm, which interestingly, gives rise to omental and mesenteric fat (Wong, Ganesan & Selvanayagam, 2017). As with the heart, pericardial fat receives its blood supply from the coronary arteries and plays an important role in cardiac physiology, particularly in the physiological and biochemical regulation of cardiac homeostasis (Antonopoulos & Antoniadis, 2017). Under normal conditions, pericardial fat buffers coronary arteries from torsion induced by arterial pulse waves and provides mechanical protection (Leo *et al.*, 2019). Epicardial fat and pericardial fat are terms that may be used interchangeably, but this excludes paracardiac fat (Kristoffersen *et al.*, 2013).

2.2.3.2 Physiology of paracardiac fat

Paracardiac fat is located within the mediastinum and the *pericardium fibrosum*, as shown below in Figure 2.2 (b) (Bertaso *et al.*, 2013). Blood supply to the pericardial fat originates from branches

of the coronary arteries; however, supply for paracardiac fat originates from the internal mammary and the pericardiophrenic arteries (Kroll *et al.*, 2021).

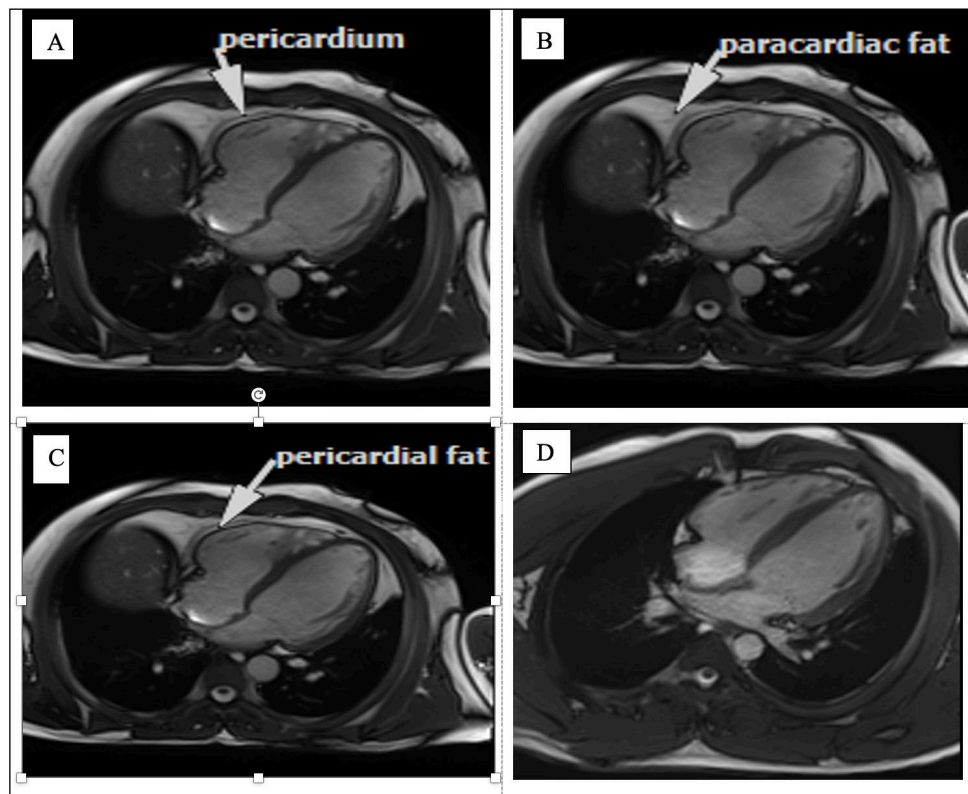


Figure 2.2. CMR image showing four chamber view (A) demonstrating pericardium, (B) paracardiac fat, (C) pericardial fat of an adult HIV+ patient, and (D) CMR of a normal heart in the control group.

2.2.3.3 Pericardial anatomy (as seen on MRI)

Black blood and bright blood sequences are useful in characterisation of adipose tissue. Four-chamber cine imaging and T1-weighted images are of major value for quantifying and visualising the epicardial and pericardial fat layer (Karamitsos *et al.*, 2020). On the 4-chamber view, pericardial fat is localised between the myocardium and the visceral pericardium as well as outside the parietal pericardium. The epicardial and pericardial fat layer is outlined to obtain the volumetric measurements for evaluation. Moreover, CMR allows for assessment of the atria, tricuspid and mitral valve, septum, apex, lateral and inferior walls of the LV and free wall of the RV (Krishnamurthy, Cheong & Muthupillai, 2014). T1-weighted imaging on CMR is the most reliable sequence to provide an excellent evaluation of the pericardium and demonstrate it as a low signal intensity curved line surrounded by high signal intensity of the epicardial and mediastinal fat pad (See Figure 2.2a). Additionally, in the presence of intense inflammation, pericardial thickness is seen on T1-weighted imaging and is associated with adhesions between the visceral lamina and

parietal lamina of the pericardium. Several studies have shown that inflammation on conventional T2-weighted imaging appears as a high signal intensity of the pericardial layer (de Leuw *et al.*, 2021; Rutka *et al.*, 2021).

2.3 Aetiology of HIV/AIDS

HIV transmission occurs through exposure to infected blood and bodily fluids and vertically through mother to child exposure. Like most modes of transmission, infectiousness is determined by viral load; the higher the viral load, the more likely that transmission will occur. HIV causes chronic infection with progressive impairment of the immune system by targeting CD4⁺ T cells (Osuji *et al.*, 2018). The HIV is a ribonucleic acid (RNA) retrovirus, belonging to the lentiviridae subfamily. HIV has characteristics that play a fundamental role in conversion of viral RNA into deoxyribonucleic acid (DNA) (Pejković, Stojić & Popovska-Jovičić, 2019). HIV is a fast-evolving organism due to high RNA genetic variability that emanates from its high mutation rate, high viral turnover, and retroviral recombination (Volberding, Joep & Joel 2013).

AIDS is the terminal phase of chronic HIV infection. In 1981, HIV/AIDS was first described amongst five individuals in the United States of America (de Cock, Jaffe & Curran, 2012). AIDS is diagnosed in people living with HIV with a total CD4 lymphocyte count of less than 200/mm³, as well as in those with AIDS-indicative disease (Pejković *et al.*, 2019). The main aim of ART is to suppress viral replication and significantly decrease progression from HIV to AIDS (de Cock *et al.*, 2012; World Health Organization (WHO), 2021).

2.4 Antiretroviral treatment/therapy (ART)

South Africa has the largest ART program in the world, and only 64% of those on ART are virally suppressed to <1,000 copies/mL. In the past few years, non-adherence to ART has become a challenging fact in public health care (WHO, 2021; Jennings *et al.*, 2022). ART regimens are divided into four treatment-based categories, including nucleoside reverse transcriptase inhibitors (NRTIs), non-nucleoside reverse transcriptase inhibitors (NNRTIs), protease inhibitors (PIs) and integrase inhibitors (INIs) (Table 1) (Hemkens & Bucher, 2014). At the beginning of the ART era, PLHIV were more likely to be on older generations of ART which were classified into two distinct categories: PIs and NRTIs. However, subsequently, the benefits of combination therapy have been demonstrated in several studies (Bangsberg *et al.*, 2006; Nachega *et al.*, 2007). Protease inhibitors function by inhibiting viral maturation through inhibition of cleavage of polyprotein. However, their exposure has been known to cause adverse effects such as lipodystrophy, insulin resistance

and hypertriglyceridemia and hyperlipidemia. NRTIs function differently: they inhibit viral replication by competitive binding to reverse transcriptase but increases the risk of developing cardiomyopathies (Singh *et al.*, 2021).

ART is associated with complications like accelerated coronary atherosclerosis and myocardial toxicity, which ultimately leads to LV dysfunction (Hsue & Waters, 2017), suggesting that ART has direct adverse effects on cardiac myocytes, endothelial cell function and disruption of mitochondria. On the other hand, the newer generation of ART reduces toxicity, but the risk for cardiometabolic disease is still elevated (Longenecker *et al.*, 2017). There are two important aspects to this new generation of ART (NNRTIs and INIs): they prevent viral replication by curbing the addition of new nucleotides to the growing DNA chain and inhibit HIV replication by preventing integration of the genome into the host, respectively (Belkin & Uriel, 2018). However, recent studies demonstrate that despite effective suppression of viral replication, ART has been associated with persistent inflammation that leads to myocardial fibrosis and organ damage (Ntusi & Ntsekhe, 2016; Pinto *et al.*, 2016).

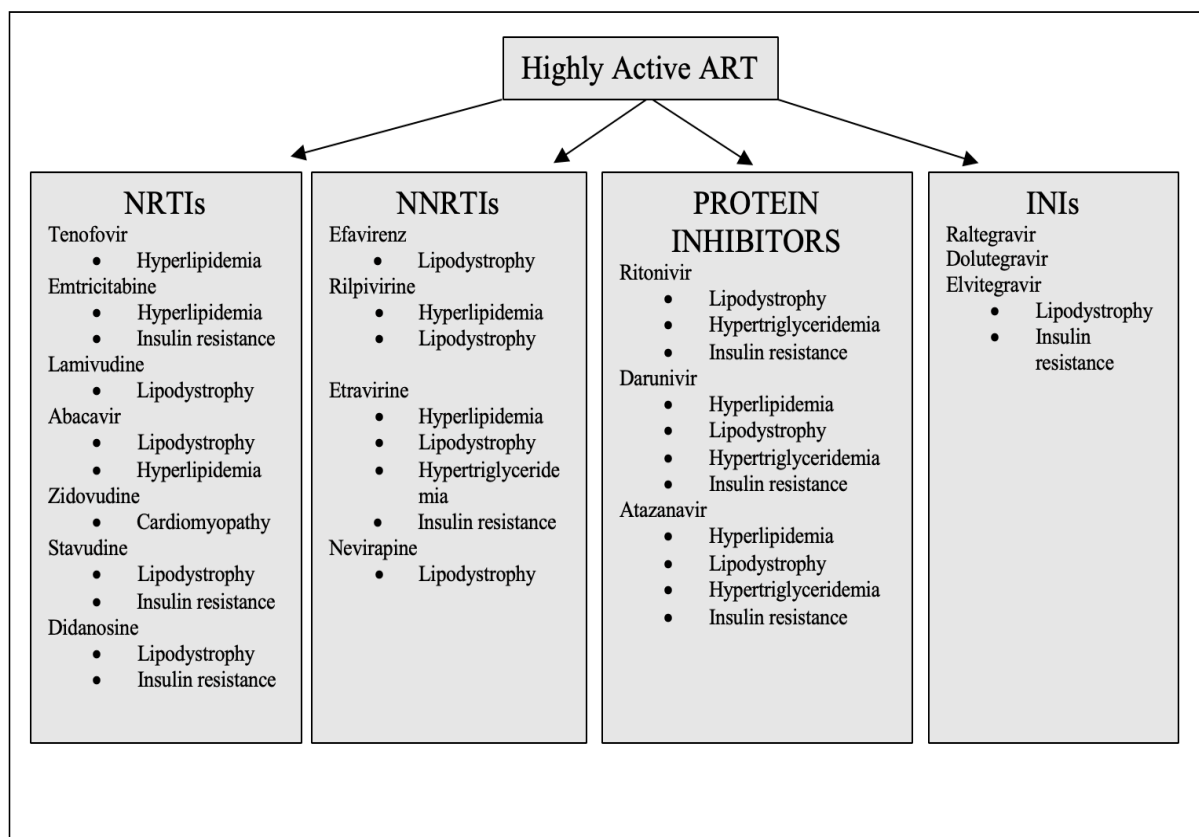


Figure 2.3. Classification of ART regimens and risk factors (Hemkens & Bucher, 2014).

2.5 The burden of HIV-associated cardiovascular disease

CVD is one of the major burdens in PLHIV and has increased dramatically over the past decade (Menacho *et al.*, 2020). Incidence of HIV-associated heart failure is increasing globally; and emerging evidence suggests that diastolic, rather than systolic dysfunction, is the predominant form of heart failure in the ART era (Ntusi & Ntsekhe, 2016). Since the widespread availability and use of ART, incidence of HIV-associated dilated cardiomyopathy (DCM) has substantially declined, while there has been a parallel increase in subclinical LV dysfunction (Sood *et al.*, 2017). HIV-associated CVD involves every segment of the cardiovascular tree and adversely affects all layers of the heart, including the myocardium, valves, pericardium, conduction system and coronary, pulmonary, and peripheral vasculature (Ntusi & Ntsekhe, 2016). While Ntusi (2017) identifies HIV as a CVD risk marker, pathophysiology of heart failure in PLHIV is multifactorial.

2.6 Cardiovascular effects of ART treatment

Consequently, ART is associated with complications arising from increases in epicardial fat deposition as well as disorders of the glucose and lipid metabolism (Hemkens & Bucher, 2014). Such changes are characterised by ectopic fat deposition, specifically perivisceral and accumulation of fat around waist circumference (Barbaro & Boccara, 2005). The aetiology of these abnormalities is not known but may relate to a specific effect of antiretroviral drugs on adipocyte metabolism with consequent metabolic abnormalities, and from direct effects of ART on lipid or glucose metabolism (Margolis *et al.*, 2014).

ART may result in further increased risk factors for metabolic syndrome and enhanced metabolic complications of the viral infection. It is important to identify persons at higher cardiovascular risk and prioritise them for clinical interventions (Ntusi & Ntsekhe, 2016). Thus, assessment of all PLHIV for presence of traditional CVD risk factors may be a good proposal when formulating new guidelines. ART has been responsible for development of adiposopathy, which is associated with complications leading to suboptimal immune recovery, myocardial inflammation and myocardial tissue fibrosis (Belkin & Uriel, 2018, Buggey & Longenecker, 2018; Fricke *et al.*, 2019). Importantly, morbidity and mortality are successfully reduced the use of ART in the HIV population (Whittaker *et al.*, 2020).

2.7 Cardiovascular risk factors in PLHIV

2.7.1 *Pericardial and paracardiac adipose tissue*

Adipose tissue changes and lipid metabolism abnormalities increase CVD risk (Hemkens & Bucher, 2014). The complications of excessive pericardial and paracardiac fat that confer mortality and morbidity are atherosclerosis, myocardial ischemia, LV dysfunction, and metabolic syndrome (Sacks & Fain, 2007; Homsí *et al.*, 2016). Subclinical immune activation and inflammation from HIV infection may directly contribute to CVD (Bertaso *et al.*, 2013; Rider *et al.*, 2014; Ntusi, 2017). Thus, an understanding of factors associated with metabolic perturbation and CVD risk is important in the development of vascular disease in PLHIV.

Pericardial and paracardiac fat are no longer perceived as a mere fat storage depot, but as an important biological active organ (Mazurek *et al.*, 2017). As pericardial fat volumes increase, due to ART effect, the balance of storage to facilitate the release of fatty acids is changing from production of adipokines to cytokines. Adipokines can be produced by immune cells (macrophages, neutrophils, lymphocytes, and monocytes/macrophages) and non-immune (endothelial cells and fibroblast) (Osuji *et al.*, 2018). Cytokines like interferon alfa (IFN- α) play an essential role in the control of homeostasis of the immune system. Cytokines can be classified as anti-inflammatory and pro-inflammatory, and infection with HIV can lead to deregulated production of both types of cytokines.

Higher volumes of epicardial and paracardiac fat resulting from fat redistribution may exert detrimental effects on the myocardium leading to development of CAD. The complications of excessive pericardial and paracardiac fat that confer mortality and morbidity are atherosclerosis, myocardial ischemia, LV dysfunction, and metabolic syndrome (Sacks & Fain, 2007; Homsí *et al.*, 2016). CAD has been associated with high rate of mortality and morbidity in PLHIV (Suliman, 2011).

2.7.2 *Metabolic syndrome*

Metabolic syndrome was first defined in 1977 as a cluster of factors associated with increased CVD risk (Nix, 2015). The American Heart Association has developed guidelines that define metabolic syndrome, and include parameters like abdominal obesity, triglycerides, high-density lipoprotein (HDL) cholesterol level and high blood pressure (Ntusi *et al.*, 2016). In more recent centuries, obesity has been identified as a chief contributor to development of CVD and plays a role in the development of metabolic syndrome (Thanassoulis *et al.*, 2010; Patel *et al.*, 2017). A strong

association between excess pericardial fat and atherosclerotic CVD exists (Buggey & Longenecker, 2018). Pericardial adipose tissue promotes inflammatory effects on the myocardium.

Metabolic syndrome is known to impair vascular function and needs to be managed well to reduce increasing vascular and myocardial disease in the population. HIV confers additive cardiovascular risk equivalent and equal in magnitude to metabolic syndrome (Rider *et al.*, 2014). Proper management of HIV-associated vasculopathy is of great concern and requires a multi-disciplinary approach (Ntusi & Ntsekhe, 2016). As ART plays an important role in preventing HIV disease progression, the choice of ART regimen must be carefully considered and minimise propensity for induction of dyslipidaemia and insulin resistance (Manga, 2017).

2.7.3 Atherosclerosis

Atherosclerosis is characterised by lipid plaque build-up inside the arteries. Plaque can narrow the coronary arteries leading to reduced flow of oxygen rich blood to the heart (Manga *et al.*, 2017). Endothelial dysfunction is a feature of atherosclerosis. Increased pericardial fat deposits cause endothelial dysfunction leading to macrophage infiltration and inflammatory effects on the myocardium and coronary arteries (Ntusi & Ntsekhe, 2016). Obstruction of blood vessels due to plaque deposits may lead to thrombus and embolus formation. Therefore, increased plaque volume has been recognised as a risk factor for myocardial infarction, stroke, and congestive heart failure (Cai *et al.*, 2002). Calcium oxalate crystal deposits within the plaque may be a complication of ART (Manga *et al.*, 2017). HIV-infected patients have altered vascular mechanisms, which have direct, diverse effects on vascular function, endothelial dysfunction and inflammation promoting atherosclerosis. There are direct effects of pericardial fat on the coronary vascular wall smooth muscle cell behaviour and extracellular matrix composition. Abnormal proliferation of smooth muscle cells, mixed with abundant elastic fibres, in HIV-infected patients may lead to endoluminal protrusion and therefore promote atherosclerosis (Ntusi & Ntsekhe, 2016; Manga *et al.*, 2017).

2.7.4 Inflammation

Inflammation is part of the complex biological response of the immune system to harmful stimuli, like pathogens, and eliminates the cause of injury to tissues by restoring homeostasis and healing damaged cells (Castillo, 2020). Inflammation has a protective response that involves mast cell, neutrophils, macrophages, epithelial cell, dendritic cell and natural killer cells (Urban, Lourido & Zychlinsky, 2006). Inflammation is characterised by rapid secretion of recruited cytokines and leukocytes leading to immune response activation which plays a major role in myocardium health.

When the myocardium initiates the healing process after injury, cytokines are activated and accumulate in the myocardium to remove stimuli leading to injury; however, failure to remove these stimuli can lead to further myocardium tissue destruction (Baker *et al.*, 2021). In the healthy myocardium, cardiac macrophages and mast cells help regulate homeostasis. Inflammation can be classified into two groups: acute and chronic. Acute inflammation is characterised by neutrophil infiltration leading to oedema, whereas chronic inflammation can be detrimental by causing advanced structural damage, resulting in cardiac fibrosis (Suthahar *et al.*, 2017). It has been suggested that after tissue damage has taken place and the repair process begins, one of two outcomes may be possible. First, after repair, cells of the same morphology and function replace the injured tissue leaving no evidence of damage. Secondly, connective tissue can replace the damaged tissue resulting in fibrosis (Liu, López de Juan Abad & Cheng, 2021).

2.7.5 Myocardial Fibrosis

Myocardial fibrosis poses a major health challenge and is associated with cardiovascular dysfunction in HIV. Myocardial fibrosis is defined as excessive deposition of collagen and net accumulation of extracellular matrix (ECM) in the myocardium (Tikhomirov *et al.*, 2020). The ECM of the heart is known for having a dynamic environment composed of collagen fibres, important for maintaining the optimum structure and plasticity of the myocardium. The myocardium as a highly organised structure that contains several cell types: fibroblast, smooth muscle cells, endothelial cells, and cardiomyocytes (Kong, Christia & Frangogiannis, 2014). The fibroblast produces the ECM and plays a major role in cardiac homeostasis. In diseased myocardium, the cardiac fibroblasts are activated by pathological stimuli, migrate to the site of injury, and transdifferentiate into myofibroblasts which are implicated as important mediators of fibrosis (Thomas & Grisanti, 2020). However, there are several other cells that are implicated as important mediators of fibrosis such as macrophages, mast cells, monocytes, T lymphocytes and endothelial cells (Cojan-Minzat *et al.*, 2020). Myocardial fibrosis occurs due to scar formation, after cardiomyocyte death (Frangogiannis, 2019).

2.8 Cardiovascular magnetic resonance

As mentioned before, CVD can be robustly and reproducibly detected using CMR in cardiac pathology, which can assist in clinical management. Different pulse sequences in the CMR protocols offer fast imaging with favourable performance in the assessment of anatomical structure, tissue characteristics, ventricular function and myocardial fibrosis, and viability (Philip *et al.*, 2021). Generally, most CMR protocols include spin-echo images (Turbo spin-echo (TSE) and

Half-Fourier single-shot spin-echo), cine images and tissue characterisation images such as T2 STIR, T1 mapping and ECV, and T2 mapping, strain imaging and LGE.

2.8.1 Spin-echo sequences

Spin-echo (SE) sequences are the work-horse sequences that were first used for evaluating cardiac morphology, as they provide good contrast between the myocardium and blood and thus are known as black blood imaging. However, SE takes a long time to acquire and has limited temporal resolution (Earls *et al.*, 2002). Nevertheless, SE produce high quality images when combined with electrocardiographic gating resulting in reduced motion artefacts (Saremi, Grizzard & Kim, 2008). SE is also less sensitive to susceptibility artefacts than gradient-echo sequences, especially when using a higher magnetic field strength like a 3 Tesla (T) MRI scanner. Further, SE image formation is influenced by relative T1 and T2 relaxation times of the tissue (Myerson, Francis & Neubauer, 2010). T1 differences are observed in sequences such as T1-weighted, with a short repetition time. In contrast T2 differences are emphasised in T2-weighted sequences and tends to have longer echo time (Krishnamurthy *et al.*, 2014).

2.8.1.1 T1-weighted sequences

T1-weighted dark blood sequence has been used in a standard CMR protocol for assessment of myocardial fibrosis and cardiac masses (Cai *et al.*, 2002). T1-weighted images provide rich myocardial structural and skeletal muscle information in the assessment of the change in T1 signal in the injured myocardium. T1-weighted images have the advantage of being able to provide high spatial resolution through the entire cardiac cycle (Myerson *et al.*, 2010).

2.8.1.2 T2-weighted short Tau inversion recovery

STIR sequence is used to suppress signals from specific tissues like moving blood and fat, making it useful in the detection of inflammation/oedema (Lintage *et al.*, 2020). A STIR sequence is strong at detecting myocardial oedema because myocardial oedema has long T2 values (Zhu *et al.*, 2019). Therefore, oedema can be robustly identified due to the excess interstitial fluid accumulation in the inflamed myocardial tissue. Moreover, a signal intensity ratio above 1.9 relative to both skeletal muscle and remote myocardium is indicative of elevated signal intensity which indicates the presence of myocardial oedema (Ntusi *et al.*, 2014).

2.8.1.3 Half Fourier Acquired Single-shot spin-echo

Half-Fourier acquired single-shot turbo spin-echo (HASTE) is one of the SE sequences based on a single-shot acquisition and can be achieved with or without fat suppression. This sequence is less sensitive to respiratory motion due to its short acquisition time therefore, the entire LV can be imaged with one breath-hold (Russo *et al.*, 2020). The acquisition is done with a short echo time (TE) due to the use of half-Fourier technique. The technique is robust in patients who are unable to hold their breath. HASTE images are first carried out in orthogonal (axial, coronal and sagittal) planes of the body for rapid survey of the entire heart as well as great vessels and provides lesion conspicuity by displaying tissue relationship between fluid and solid organs (Myerson *et al.*, 2010). Further, this technique is the most commonly used technique for assessment of incidental extra-cardiac pathology. The sequence can be particularly valuable to demonstrate the parietal pericardium as a thin dark line of 2mm thickness situated around the right atrium, RV, LV, aorta and pulmonary artery (Hassanabad *et al.*, 2021). However, HASTE does have limitations in the assessment of CVD because it has lower resolution compared to TSE.

2.8.2 Cine imaging

Cine sequences provide the advantage of assessing both cardiac morphology and function, and allow for qualitative assessment of the aorta (Ridgway, 2010). The assessment of LV function by cine imaging produces excellent contrast between blood and myocardium as well as epicardium and surrounding fat (Aldweib *et al.*, 2018). Cine imaging uses a balanced steady-state free precession technique combined with prospective electrocardiogram (ECG) gated technique during diastole and can demonstrate the motion of the entire heart in a single breath-hold (Emrich *et al.*, 2021). This technique performs optimally with the shortest repetition time, so making it possible to acquire fast imaging for capturing cardiac function (Bertaso *et al.*, 2013).

2.8.3 Native T1 mapping together with extracellular volume

Previous studies have shown native T1 mapping together with ECV as a useful technique for quantitative assessment of myocardial injury involving the myocyte and interstitium (Kramer *et al.*, 2013; Goebel *et al.*, 2016; Emrich *et al.*, 2021). More importantly, the use of gadolinium allows for measurement of the interstitial space. Therefore, to generate a parametric map of relaxation times, images of the same region of the myocardium are acquired with different sensitivity to the parameter of interest and the signal intensities of these images are fit to a model which describes the underlying physiology. A study looking at diffuse diseased myocardium in clinical CMR

suggests that parametric mapping has been based on nuclear magnetic resonance (NMR) properties such as T1 and T2 relaxation times to quantify tissue properties (Goebel *et al.*, 2016).

Moreover, native T1 mapping allows signal quantification on a standardised scale of each myocardial voxel for myocardial tissue characterisation (Captur, Manisty & Moon, 2016). Thus, T1 mapping has been useful in detecting the location and extent of myocardial injury. Additionally, this technique has been applied in several different studies, for its high diagnostic accuracy and superiority over LGE and T2-weighted imaging as it is based on pixel-wise measurement of the longitudinal relaxation time (aus dem Siepen *et al.*, 2018). Furthermore, T1 mapping has an ability to display the maps in colour and aids in the appreciation of the pathology (Butler *et al.*, 2018). A T1 value of the normal heart depends on the magnetic field strength and is approximately 1100 – 1250 milliseconds (ms) at 3T (Yang *et al.*, 2021). Additionally, an elevated myocardial T1 mapping value has been seen in diffuse fibrosis (Emrich *et al.*, 2021). T1 mapping can be performed prior to contrast administration and 15 minutes after, to obtain myocardial ECV fraction measurements (Haaf *et al.*, 2016). Native T1 and ECV mapping are useful in quantifying myocardial changes caused by diffuse fibrosis and inflammation (Butler *et al.*, 2018).

2.8.4 T2 mapping

T2 mapping has been used to quantify T2 values, which are useful in overcoming some of the limitations of detecting oedema and myocardial inflammation with T2-weighted sequences (Dastidar *et al.*, 2016). Myocardial T2 relaxation time decreases with fat infiltration and increases in the presence of oedema (Fernandez-Jimenez *et al.*, 2017), while T1 relaxation times increase in the presence of oedema (Higuchi *et al.*, 2014; Emrich *et al.*, 2021). T2 relaxation times was shown to be valuable parameters in CMR for the characterisation of myocardial tissue (Lee *et al.*, 2011). T2 mapping has an ability to display the maps in colour and aids in the evaluation of oedema and inflammation (Mahrholdt, Klem & Sechtem, 2007).CMR provides a rich resource for evaluating acute myocardial disease. And as such is well suited for characterising markers of cardiac dysfunction in PLHIV (Ntusi, 2017).

2.8.5 Strain imaging

Tagging has been used to examine diastolic dysfunction by assessing intramyocardial contractile function and detecting nondisjunction of the visceral and parietal pericardium throughout the cardiac cycle (Sood *et al.*, 2017). During tagging, the grid-like lines are superimposed on and embedded in the myocardium at the onset of a cine sequence. The deformation of the grid is used

to assess regional and global wall motion and strain (Ntusi *et al.*, 2016). PLHIV showed lower strain and strain rate than HIV-uninfected people (Bloomfield *et al.* 2014). Strain abnormalities assist in predicting the development of LV dysfunction in PLHIV (Sood *et al.*, 2017). However, tagging imaging is limited due to the loss of continuous tagging lines during cardiac contraction as a result of the shear motion between the visceral and parietal layers (Bloomfield *et al.*, 2014).

2.8.6 Early gadolinium enhancement

Early gadolinium enhancement (EGE) plays an important role in the diagnosis of intracardiac thrombus and acute inflammation because the inflammation increases blood flow to the tissues, which results in increased early uptake of gadolinium in inflamed areas. EGE on its own cannot be used as a clear indicator for the diagnosis of myocardial inflammation as image quality can be affected by factors such as breathing artefacts and irregular heart rhythm. EGE imaging adds value when used in combination with other tissue characterisation techniques, such as the T2 STIR, but its value has diminished with the introduction of mapping techniques (Vermes *et al.*, 2018).

2.8.7 Late gadolinium enhancement

Gadolinium-based contrast agents have been used as a tool to assess myocardial viability in CMR. Due to its strongly paramagnetic properties, gadolinium facilitates the process by altering the T1 recovery time of tissue, resulting in an increase in signal intensity on T1-weighted images (Sood *et al.*, 2017). Several studies have shown LGE to be useful for imaging focal scar tissue and is especially useful in determining the pattern and extent of the scar, as well as inflammation of the myocardial tissue (Lee *et al.*, 2011; Higuchi *et al.*, 2014). Moreover, utilisation of LGE allows a virtual histological assessment. LGE may have limitations, especially when it comes to distinguishing acute oedema from a chronic scar (Haaf *et al.*, 2016).

When compared to EGE and T2-w imaging, LGE typically reveals areas of irreversible damage, such as acute necrosis and chronic fibrosis (Karamitsos *et al.*, 2020). The advantage of this technique is that it detects focal processes but has its limitations in detection of diffuse processes. However, despite these limitations, LGE is still the most frequently used and best-established method for myocardial tissue characterisation and has been useful in both the diagnosis and prognosis of ischaemic and non-ischaemic cardiac diseases (Lintingre, 2020).

2.8.8 Image quality

Quality control checks need to be done by an experienced person familiar with different types of artefacts to avoid unreliable measurements and non-diagnostic images (Earls, 2002; van der Graaf *et al.*, 2014). Hence, both qualitative and quantitative measures should be defined to exclude images that may lead to erroneous quantification. Therefore, qualitative observation of artefacts in the images requires experience when scanning the participants because most artefacts can be corrected only during scanning. The most important factors to consider during scanning includes (i) breath-holds which are essential in ensuring adequate image quality because inconsistent breath-holds may lead to slice misregistration and ghosting artefact. (ii) Faster gradients are vital in the production of the best image quality scanning and spatial differentiation leading to high quality scanning. Rapid imaging techniques can help in the production of good image resolution because they are less sensitive to patient motion due to short acquisition time (Ripley *et al.*, 2016). Image quality can be assessed in terms of these artefacts namely, ripple, ghosting, geometric distortion, chemical shift, aliasing, metallic and off-resonance artefacts (Ripley *et al.*, 2016; Russo *et al.*, 2020).

2.9 Summary

HIV and ART contribute to the burden of CVD, resulting in considerable morbidity and mortality. PLHIV are prone to develop high volume adipose tissue deposition around the heart and this redistribution of fat has been linked to the use of ART. Through several different mechanisms, adipose tissue deposition leads to the development of CVD which causes adverse risks within the myocardium. These adverse factors in the myocardium influence the development of coronary artery atherosclerosis cardiac dysfunction and metabolism. CMR is the gold standard when it comes to providing key imaging characteristics that includes ventricular function, anatomical dimensions and tissue characterisation particularly the presence of fibrosis and inflammation. Additionally, CMR remains the most versatile imaging technique with the ability to examine the mechanisms of regression and progression of the HIV-associated CVD.

CHAPTER THREE

RESEARCH METHODOLOGY

3.1 Introduction

The research objectives of the study were to assess myocardial structure and function, as well as the burden of pericardial and paracardiac fat in PLHIV. The current study used secondary data from an umbrella study (Predictors of Diffuse Myocardial Fibrosis in HIV Infected Persons: A Multiparametric Cardiovascular Magnetic Resonance Study) which commenced in 2017 at the Cape Universities Body Imaging Centre (CUBIC) located within the Cape Metropole. This project was led by Professor (Prof) Ntusi: Head of Department of Medicine at GSH, Observatory, Cape Town. The ethical approval for the umbrella study and the study on which this thesis is based, is described under ethical consideration (Section 3.9 below). The targeted population for the larger umbrella study were HIV-positive participants that were recruited at the clinic where they received ART treatment and were at low risk for AIDS defining complications. The aim of the umbrella study was to (i) assess diffuse myocardial fibrosis and (ii) determine the effect of ART use on diffuse myocardial fibrosis in HIV-infected individuals on ART compared to untreated HIV-infected persons using CMR. The current study, which is a sub-component of the umbrella study, hypothesised that fat around the heart has detrimental effects on the myocardium in PLHIV who are on ART. In this chapter, the following aspects are described namely the study design, study population, inclusion and exclusion criteria, sample size, image acquisition and data collection process, data management, image quality, image analysis and ethical considerations relevant to the study.

3.2 Study design

The research design employed was a cross-sectional descriptive study, based on a comparison of the CMR imaging characteristics between three cohorts namely:

Group 1: HIV-infected participants receiving ART.

Group 2: HIV-infected participants not receiving ART.

Group 3: Matched HIV-uninfected controls.

Participants were both males and females (mean age 18 ± 60 years) that were scanned between February 2017 and September 2018. The participants were prospectively enrolled by the umbrella study 'Predictors of Diffuse Myocardial Fibrosis in HIV-Infected Persons: A Multiparametric Cardiovascular Magnetic Resonance Study' explained above. The main goal was to expand

understanding of the effects of HIV infection on cardiovascular disease among lower- to middle-income nations such as South Africa. Furthermore, the study explored whether HIV infection, despite effective treatment, leads to structural changes to the myocardium characterized by diffuse fibrosis that ultimately contributes to myocardial dysfunction.

Eligible participants were recruited from the Infectious Diseases and HIV clinics at GSH. Recruitment was performed by research medical officers from Prof. Ntusi's research group with the guidance of the nurses and doctors working at the sites. The research medical officers evaluated the participants' records and approached each participant during consultation. Furthermore, recruitment was done through posters and word of mouth for healthy controls. HIV-infected participants with CD4+ T-cell counts ≥ 350 cells/mm³ were recruited, with a focus on a target population with lower risk for AIDS-related complications, among whom morbidity and mortality from CVD-related complications are relatively more frequent.

3.3 Study population

The current study analysed retrospectively acquired data in a cohort of PLHIV, with a comparison between three groups which included: HIV-infected participants receiving ART, HIV-infected participants not receiving ART and HIV-negative controls. HIV-negative controls for the current study were drawn from the South African Cardiovascular Magnetic Resonance (SA-CMR) registry database available at CUBIC. The targeted population demographics for this study recorded included age, sex, heart rate, weight, body mass index (BMI) and body surface area (BSA) which were prospectively obtained from the participant's clinic folders. Further, the uninfected controls were matched to the HIV infection groups for sex, ethnicity, age and comorbidity. Participants included in this study were taken from the Predictors of Diffuse Myocardial Fibrosis in HIV-Infected Persons: A Multiparametric Cardiovascular Magnetic Resonance Study and the SA-CMR Registry (for controls). The study sampling technique was a purposive sampling of participants who had undergone comprehensive CMR imaging at the CUBIC-University of Cape Town (UCT) MRI scanner, which met the inclusion criteria described in Table 3.1 below.

3.3.1 Inclusion and exclusion criteria for umbrella study

The inclusion criteria for participant enrolment for the umbrella study were, males and females aged ≥ 18 years, ≤ 60 years; HIV antibody positive; uninterrupted ART for ≥ 1 years (treated group) or ART naïve (untreated group) and participants who were able and willing to give informed consent. Furthermore, the following were exclusion criteria: inability to tolerate MRI

(claustrophobia, inability to lie flat), arrhythmia, invasive malignancy or cancer treatment in the prior year, contraindications to MRI (hypersensitivity to gadolinium, implantable devices, metal implants, cranial aneurysm clips, metallic ocular foreign bodies), pregnancy, estimated glomerular filtration rate (eGFR) <30ml/min (Table 3.1).

3.3.2 Inclusion and exclusion criteria for CMR images for the current study

Table 3.1. Inclusion and exclusion criteria

Inclusion criteria:	Exclusion criteria:
Images of participants that were scanned at the CUBIC-UCT MRI scanner within the study period and were on the CUBIC-UCT database.	Non-diagnostic CMR images.
Participants with CMR images that were of diagnostic quality.	Incomplete CMR studies.
Images of all participants ranging from age 18 to 60 years.	Images of participants with inconclusive findings after CMR.
	Images of participants with pre-existing cardiovascular disease.

3.4 Sample size

A sample size of 159 participants was determined based on criteria used in similar studies together with a 95% confidence interval and a statistical power of 80% in addition to an assumed effect size using G* power 3.1.9.7 assuming a low effect size (effect size $f = 0.25$, Error probability = 0.05, and Power ($1-\beta$ error probability) = 0.08 (Cohen 2016).

3.5 Image acquisition and data collection

All participants underwent a CMR examination on a 3T Siemens Skyra MRI scanner (Erlangen, Germany) between February 2017 and September 2018 conducted at the CUBIC-UCT. Prior to scanning all participants were screened using an MRI screening checklist for participant safety (see **Appendix 1**). All participants were scanned using the same standardised CMR protocol with participants in supine position using a dedicated 18-channel body phase-array coil. ECG gated images were acquired using breath-holds (repeated end-expiration) (see **Appendix 2**). CMR sequences and details of parameters that were used for scanning are provided in **Appendix 3**. A dose of 0.2 mmol/kg gadolinium was administered intravenously for all research participants, and the duration of the scan was approximately one hour.

This retrospective analysis assessed the CMR images accessed from the CUBIC server where all data were stored from the umbrella study. In order to maintain confidentiality, all participants' data was anonymised by giving a unique identification (ID) code. The study ID code consisted of three digits between 001 and 159 and was chronologically assigned to participants. The variables recorded for this study included: patient study number, demographics (age, sex, race) and clinical characteristics (weight, height, BMI, BSA, heart rate), and medical history (HIV duration for the HIV+ group, CD4- count, co-morbidities) (**Appendix 4**). Only the researcher and supervisors had access to these images.

3.6 Data management

CMR studies were reported by experienced researchers, each with over five years' experience in CMR post-processing and analysis and with a keen interest in cardiac disease. At all times, CMR analysis was anonymised in keeping with the Protection of Personal Information Act (POPIA), (Staunton, 2020). Data was recorded on a Microsoft Excel spreadsheet (**Appendix 4**). Data were cleaned and double-checked for errors by the researcher under the guidance of Prof. Ntusi, in conjunction with another CUBIC colleague who had five years' of experience in CMR analysis. Quality control for the imaging data was done by Prof. Ntusi. Quality checks included: ripple, ghosting, geometric distortion, chemical shift, aliasing, and off-resonance artefact.

3.7 Image analysis

Post-processing and analysis of CMR images were undertaken by the researcher. Images and data analysis were reviewed by Prof. Ntusi. Data analysis was undertaken under the guidance of Prof. Ntusi, and was overseen by a biostatistician. For post-processing, data was transferred to a second computer, with Circle Cardiovascular imaging (CVI42)[®] software, for further image analysis. All image analysis was performed in a blinded manner (clinical information unknown, e.g. HIV status), with a random selection of participants, and HIV status only revealed after the analysis was completed. The following cardiac parameters were documented: LV volumes, mass, and function, T1- and T2- weighted imaging, strain imaging, T1 and T2 mapping, and ECV, pericardial and paracardiac fat volumes and late gadolinium imaging for viability and fibrosis assessment.

3.7.1 Determination of ventricular parameters

The quantitative and image analyses were performed using short- and long-axis b-SSFP images (Petersen *et al.*, 2017). The following steps were used for the assessment of LV and RV function, and mass: determine the quality of short- and long-axis cine images, assess the short-axis slices,

choose the end-diastolic and end-systolic phases, deciding on the basal and apical slices and manual contouring of the endocardial borders at end-diastole and end-systole and contouring of the epicardial borders at end-diastole. The ventricular volume parameters were derived using Simpson's rule which includes calculating end-diastolic volume (EDV) (ml), end-systolic volume (ESV) (ml), stroke volume (SV) (ml) and EF (%) in both the LV and RV and myocardial mass (g) in the LV. The EDV and ESV were used to calculate stroke volume ($SV=EDV-ESV$) and ejection fraction ($EF=SV/EDV \times 100\%$). LV myocardial mass was calculated by subtracting the LV endocardial volume from the LV epicardial volume in diastole; based on prior knowledge of the myocardial specific gravity (1.05 g/mL) the volume is then converted into mass. The measurements are corrected for BSA to give the indexed values: $EDVi$ (ml/m²), $ESVi$ (ml/m²), SVi (ml/m²) and mass index (Mi) (g/m²).

3.7.2 T2-weighted short Tau inversion recovery images

T2-weighted STIR sequences can be used to suppress signals from specific tissues, moving blood and fat, making it useful in the detection of oedema (Steckman *et al.*, 2012). Quantitative analysis was performed by comparing the signal intensity (SI) in the LV myocardium from the short-axis stacked against SI of the adjacent skeletal muscle in the same slice (Fig. 3.1). The formula used to calculate the T2 SI ratio was defined as follows: $T2\ SI_{\text{myocardium: skeletal}} = SI_{\text{myocardium}}/SI_{\text{skeletal muscle}}$ (Yang *et al.*, 2021). The inflammation was assessed on T2 STIR images for the presence of hyperintensities (Zhu *et al.*, 2019). These images were used to visualise inflammatory changes in the myocardium by suppression of pericardial fat. The CMR image that follows provides an overview of the quantitative analyses performed (Figure 3.1).

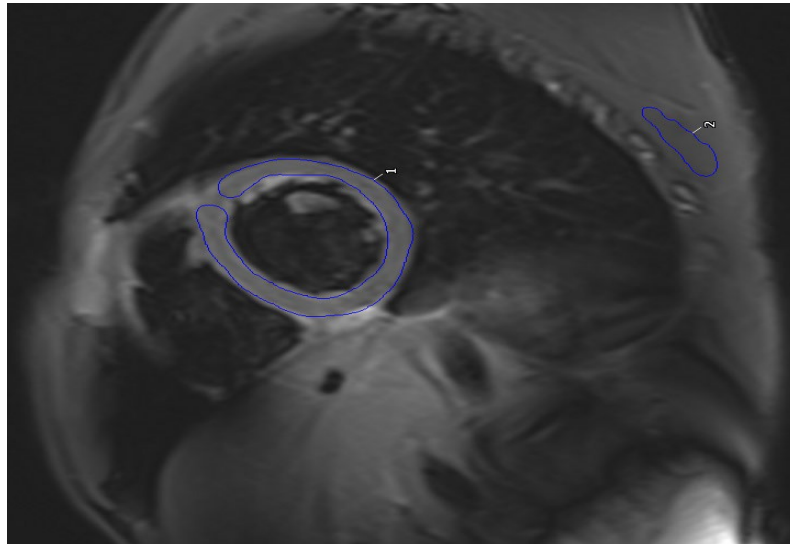


Figure 3.1. CMR T2 STIR image of the heart showing quantitative analysis by comparing the LV myocardium (1) in short axis against adjacent dorsal skeletal muscle (2) excluding non-suppressed blood pool signal.

3.7.3 Myocardial strain assessment

Quantitative strain analysis was performed in the LV myocardium to obtain information about wall strain and deformation. The feature tracking method was applied for the measurement of myocardial strain (Emrich *et al.*, 2021). Global longitudinal strain and strain rates were estimated from horizontal long-axis (HLA), vertical long-axis (VLA), and left ventricular outflow tract (LVOT) b-SSFP cine images while circumferential and radial strains and strain rates were derived from the short-axis cine images (Luetkens *et al.*, 2016) (Figure 3.2).

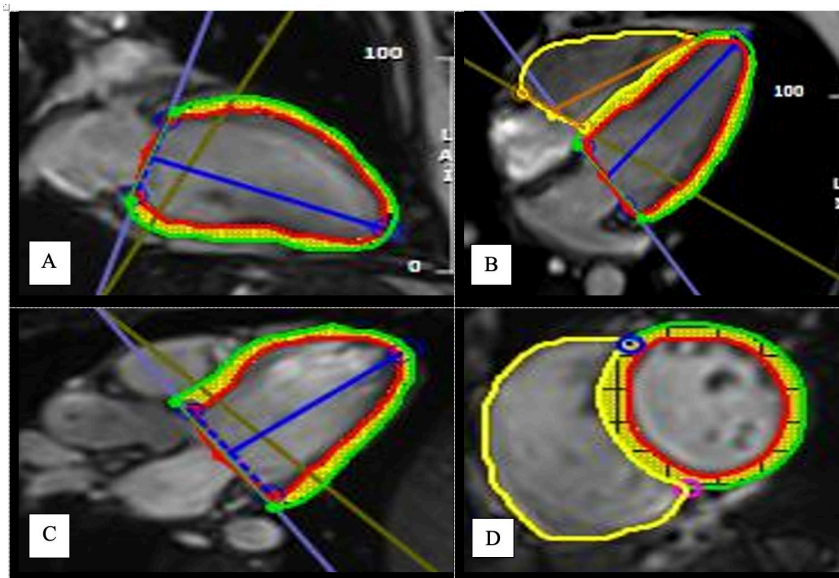


Figure 3.2. CMR Cine images of the normal heart with myocardial point overlay (yellow dots) to perform global strain analysis. (A) 2 chamber view (B) 4 chamber view (C) LVOT view and (D) short-axis view with endocardial (red line) & epicardial (green line) contours. The LV extent (blue line) defines the basal and apical boundaries of the left ventricle.

3.7.4 Myocardial T1 mapping and ECV

Quantitative analysis for myocardial fibrosis was performed using native T1 map and LGE T1 map images by manually contouring the area of interest, namely the endo- and epicardial borders and blood pool area. The estimation of ECV was calculated by a specific formula. An elevated ECV is associated with the elevated native T1 value and an indication of myocardial fibrosis (Mondy, Peter & Ravi, 2021).

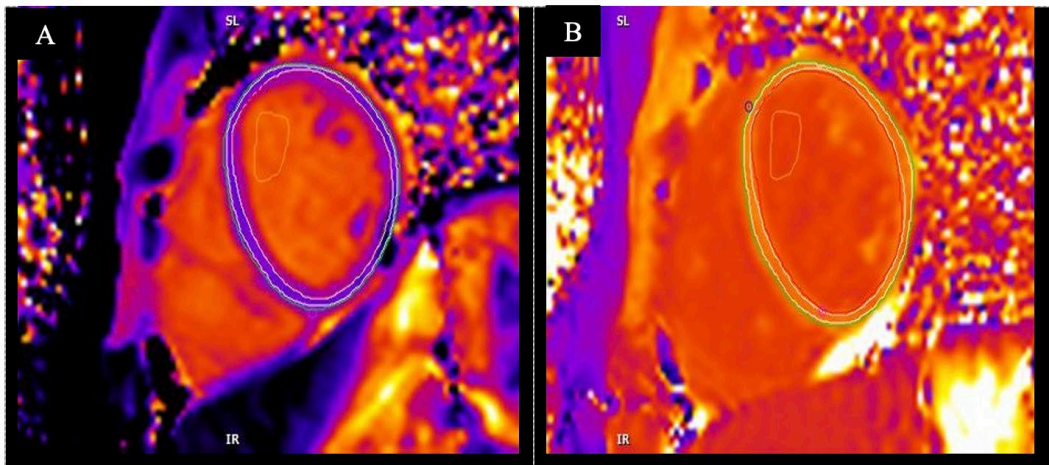


Figure 3.3. CMR native T1 mapping (A) and (B) post-contrast T1 mapping of the normal heart showing endocardial (red circle), epicardial (green circle), and blood pool (orange circle) contours excluding papillary muscles. The myocardial region of interest (ROI) (white) is offset from the endo- and epicardial borders to remove any partial volume effects from the surrounding blood pool.

3.7.5 Myocardial T2 mapping

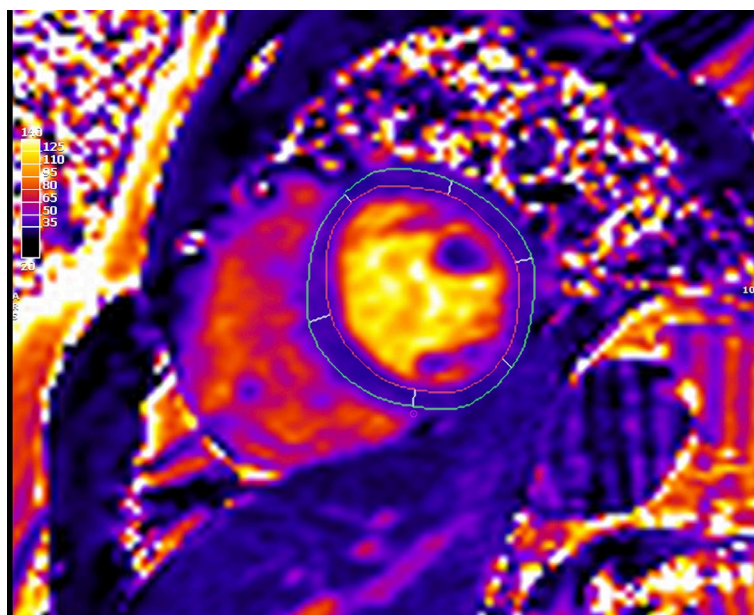


Figure 3.4 Short axis T2 map of LV myocardium. The region of interest (ROI) is used to define the epi- and endocardial borders and partition the myocardium into segments.

Quantitative T2 mapping analysis was performed by manually contouring the endo- and epicardial borders of the LV myocardium. The global T2 relaxation times are then calculated by averaging all the pixels in the entire area of interest. Quantitative T2 mapping can be used to detect myocardial oedema (Vermes *et al.*, 2018).

3.7.6 T1-weighted imaging

T1-weighted images were used for evaluating anatomical detail and pericardial fluid characterisation. T1-weighted sequences were used for assessing pericardial inflammation, fibrosis, and thickness.

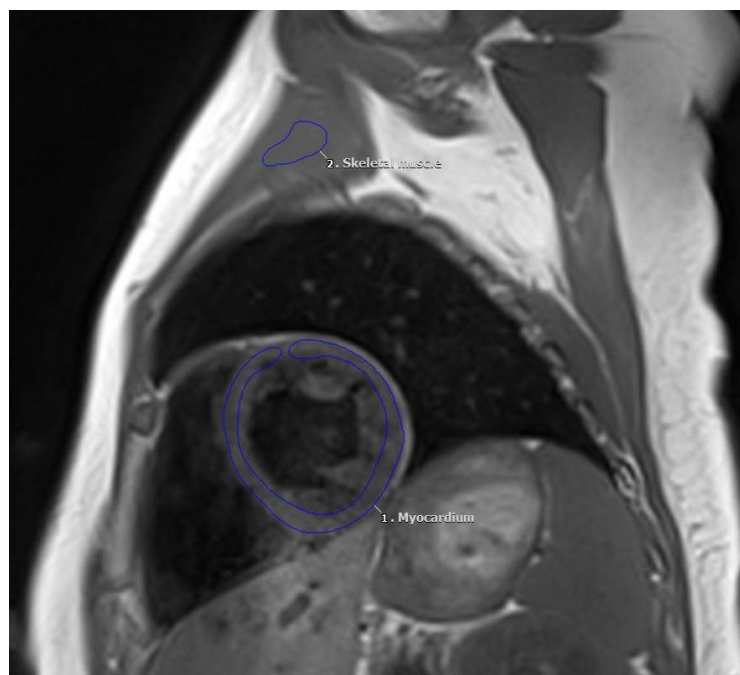


Figure 3.5. CMR T1-weighted fast spin-echo image on the short-axis showing quantitative analysis (Appendix 2) by comparing the LV myocardium (1) against adjacent skeletal muscle (2).

3.7.7 Measurements of the pericardial and paracardiac fat volume

For pericardial and paracardiac fat volumes, the measurements were also derived using Simpson's method rule by manually contouring the borders of pericardial fat with the pericardial contour and paracardiac fat with endocardial contour at end-diastole. The measurement was done in such a way that the heart is covered from base to apex (Figure 3.5). Analysis was performed from LGE imaging short-axis plane PSIR sequence because it is capable to differentiating effusion from fat by making effusion appear as low SI and fat as high SI (Rajiah *et al.*, 2019). Data from all slices were summed to obtain total pericardial and paracardiac volumes.

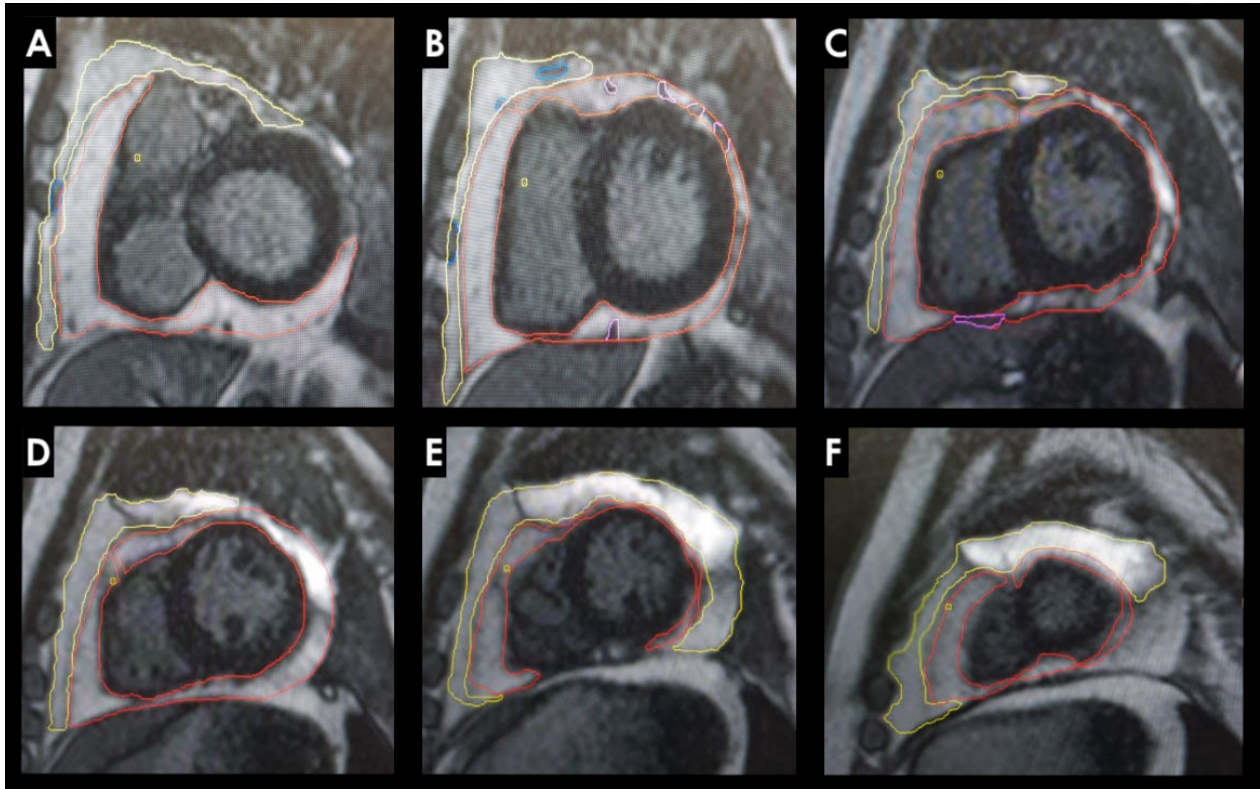


Figure 3.6. CMR PSIR LGE sequence of short-axis stack images (A-F) (from base to apex) demonstrating volumetric measurements of pericardial and paracardiac fat mass. The pericardial fat volume (area outlined in red) using epicardial contour and paracardiac fat volume (area outlined in yellow) using endocardial contour at end diastolic phase. The areas outlined in blue, and purple were excluded from the measurements using papillary muscle contours.

3.7.8 Late gadolinium enhancement

LGE images are acquired at approximately 10 – 15 minutes after the administration of gadolinium. This sequence allows for gadolinium to be washed out in normal myocardium, which is nulled. Areas with enlarged interstitial space, such as acute necrosis, chronic scar or fibrotic tissue will appear hyperintense on MRI images due to the delayed washed out of the contrast agent (Karamitsos *et al.*, 2020). Images were evaluated quantitatively for viability, presence, regional distribution and pattern of LGE. LGE can be useful in detecting the degree of myocardial fibrosis (Aldweib *et al.*, 2018). Moreover, volume fraction of LGE was calculated using a threshold of 3SDs.

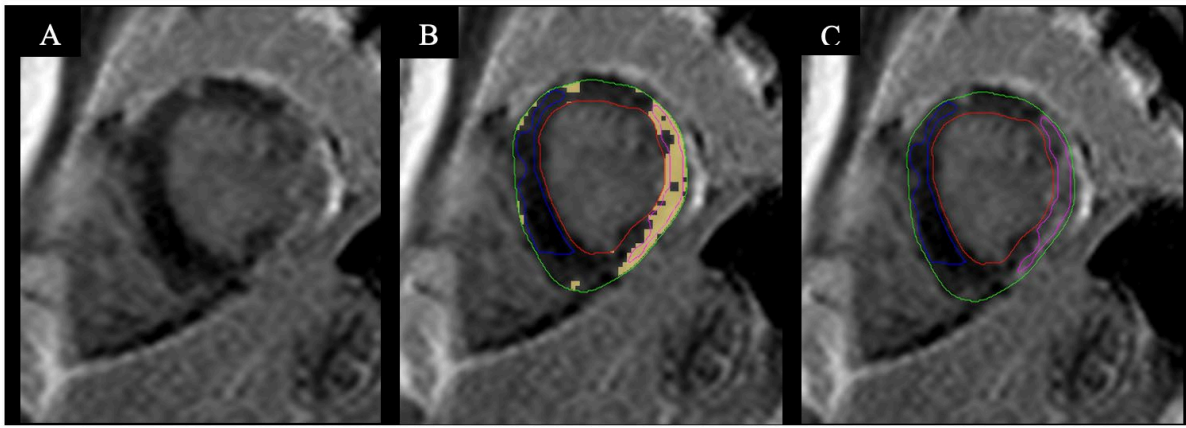


Figure 3.7. The LGE image in the PSIR sequence with high signal intensity enhancement of an HIV-untreated participant (A), The same LGE image with colour overlay in the area of enhancement (yellow outline) (B), quantification of LGE volume fraction for region of interest by comparing normal myocardium (blue outline) to abnormal areas (purple outline) (C).

3.8 Data statistical analysis and reporting

All statistical analysis was performed using the Statistical Package for the Social Sciences (SPSS) software (version 25; International Business Machines Corporation, New York, USA). Values were summarised as mean \pm SD or as percentages. BMI was calculated by using the following formula: $BMI = \text{weight (kg)}/\text{height (m)}^2$. Absolute values were indexed to BSA using the Mosteller formula, which is equal to the square root of the height in centimetres (cm) multiplied by the weight in kilograms (kg) divided by 3600 (Hafez & Missiri, 2021). Summary statistics were reported for CMR assessment baseline variables for group A, B and C was analysed using the Analysis of variance (ANOVA). Spearman's rank correlation coefficient was used to assess the impact of pericardial and paracardiac fat on myocardial volumes and function.

3.9 Ethical considerations

This retrospective study was approved by the Human Research Ethics Committee (HREC) of the Faculty of Health Sciences, at the University of Cape Town (HREC Reference number: 493/2020) to access retrospective CMR data (see **Appendix 5**). In addition, ethical approval was also granted by the Research Ethics Committee (REC) of the Faculty of Health and Wellness Sciences of the Cape Peninsula University of Technology (CPUT) (CPUT/HW-REC 2021/H4) (see **Appendix 6**). The research was conducted according to the ethical guidelines and principles of the Declaration of Helsinki (World Medical Association {WMA}, 2013) and the South African Good Clinical Practice Guidelines, based on the International Conference on Harmonization (1996), and the Medical Research Council (MRC) Ethical Guidelines for Research. The Declaration of Helsinki states "Research Investigators should be aware of the ethical, legal and regulatory requirements for

research on human subjects in their own countries as well as applicable international requirements” (WMA, 2013).

3.9.1 Informed consent (Umbrella study)

The section below explains the ethical considerations that were adhered to in the umbrella study. In keeping with the Helsinki Declaration, all participants were provided with a patient information leaflet that explained the process of the study in greater detail (see **Appendix 7**) and written informed consent forms were obtained prior to their enrolment and the original copy was filed (see **Appendix 8**). Consent forms were obtained in English and were verbally interpreted in Xhosa or Afrikaans, when needed. The permission to use images was granted by the participants where and if the need arose. All participants had the right to withdraw at any time without prejudice (WMA, 2013). The WMA (2013) Declaration of Helsinki states that, “The subject should be informed of the right to abstain from participation in the study or to withdraw consent to participate at any time without reprisal. After ensuring that the subject has understood the information, the physician should then obtain the subject's freely given informed consent, preferably in writing.

3.9.2 Data confidentiality and management

The research data obtained was curated to ensure a high degree of validity and authenticity. Identifiers linked to the subject’s study codes, and consent forms were kept in a separate, password-protected file that only the study team had access to. The CUBIC-UCT server is in the access-controlled research office and is only made available to research personnel by means of a secure password providing web access. This security measure ensured confidentiality of the data stored. As this is a low-risk retrospective study, data from the CUBIC server was accessed by the researcher. All participant’s data were anonymized, and study participants were given a unique study ID as explained under 3.5 in this chapter. No identifying details such as personal names and hospital folder numbers were utilized in the analysis and the same will be upheld in subsequent publications. Data and analysis records were kept in a secure computer and through an online storage facility that requires encrypted login details and a password that was only known to the researcher. As a back-up, data was transferred to an external hard drive, which was stored by the researcher in a locked cupboard.

3.9.3 Data integrity

The data collected were entered into an Excel spreadsheet. Study clinicians and project leaders met regularly to discuss data quality checks. Data collection and recording were done accurately.

Moreover, analysing, interpreting, and communicating findings was done honestly, avoiding convenient reading, data manipulation and biases. The research results are presented in an honest manner whether positive or negative, in a timely, accessible, responsible, and competent manner.

3.10 Summary

In summary, this chapter reviewed the procedures taken to investigate the research question. The study design used to elucidate the research objectives were described. Further, CMR sequences and the protocols that were used for this research study were outlined. The methods used for image analysis were demonstrated using different types of quantitative analysis, T1-weighted, T2-weighted, T2 STIR, T1 mapping and ECV, and T2 mapping, strain imaging, PAT and ParaAT volumes and LGE. Furthermore, this chapter described the ethical considerations that were relevant to this cross-sectional study such as, informed consent, data confidentiality, management and integrity. The next chapter describes the results of the study.

CHAPTER FOUR

RESULTS

4.1 Introduction

This chapter describes the demographical and clinical characteristics of HIV-infected participants (untreated and those on ART) and uninfected, matched controls. This chapter also presents the CMR findings of study participants which include the findings related to left and right ventricular function, left ventricular deformational characteristics, tissue characterisation, pericardial and paracardiac adipose deposits and late gadolinium enhancement as observed. Other topics discussed are the ART regimen which leads to durable suppression of the HIV including, NRTIs, NNRTIs and PIs. The chapter ends with a discussion of the bivariate correlates of myocardial function and tissue characterisation with pericardial adiposity and a chapter summary.

4.2 Demographic characteristics

The study participants (n=198) were classified into participants with HIV infection and those that were uninfected (Table 4.1). Participants infected with HIV infection and not on ART were younger, (36.4±8.2 years) than participants with HIV infection and on ART (45.0±8.3 years) and uninfected controls (41.7±11.5 years) respectively (p<0.001). Of 198 participants in the study, 81 (61.8%) were females with HIV infection on ART, 12 (63.2%) with HIV infection not on ART, and 37 (77.1%) were females that were uninfected controls (p=0.16). There were significant differences when comparing heart rate, weight, BMI and BSA-between the three groups (p<0.05). Patients infected with HIV infection and not on ART had a lower infection duration as compared to those infected with HIV and receiving ART (0.5±2.3 years, p<0.001).

Table 4.1. Demographic characteristics separated by HIV infection status and uninfected controls

Demographic characteristics							
Parameters mean± SD	HIV on ART (n=131)		HIV not on therapy (n=19)		Controls (n=48)		P-value (p<0.05)
Female, n (%)	81	(61.8)	12	(63.2)	37	(77.1)	0.16
Male, n (%)	50	(38.2)	7	(36.8)	11	(22.9)	0.16
Age, years	45.0	±8.3	36.4	±8.2	41.7	±11.5	<0.001 ^{a,b}
Heart rate, bpm	74.7	±14.6	83.9	±19.2	71.8	±16.1	0.02 ^{a,b,c}
Height, m	1.6	±0.1	1.7	±0.1	1.6	±0.1	0.15
Weight, kg	71.9	±18.0	74.4	±21.5	63.4	±10.9	<0.01 ^{a,c}
BMI, kg/m ²	26.8	±6.8	26.8	±8.2	23.4	±3.3	<0.01 ^{a,c}
BSA, m ²	1.8	±0.2	1.8	±0.3	1.7	±0.2	0.03 ^{a,c}
HIV duration, years	9.0	±6.0	0.5	±2.3	-	-	<0.001 ^{a,b}

Continuous data are shown as mean ± SD. ANOVA post-hoc tests (p<0.05): (a) HIV on ART, (b) HIV not on ART, (c) controls. (Legends: % = percentage; bpm = beats per minute; m = meter; kg = kilograms; BMI = body mass index; BSA = body surface area).

4.3 Clinical Characteristics

The clinical parameters of the participants are presented in Table 4.2. Of the 131 HIV-infected participants on ART, 41 (31.3%) were current smokers, 14 (10.7%) were prior smokers, and 76 (58%) were non-smokers. Moreover, among participants with HIV infection but not on ART, two (10.5%) were current smokers, one (5.3%) had a prior smoking history and, 16 (84.2%) were non-smokers (p=0.03). Further, amongst uninfected controls nine (18.8%) were current smokers, one (2.1%) prior smoker and 38 (79.2%) non-smokers. Among the patients with HIV infection cohort and not on ART, hypertension was present in 16 (84.2%), was diagnosed in 47 (35.9%) HIV-infected individuals on ART, and in 6 (12.5) uninfected controls (p<0.001). Uninfected controls (two) (4.2%) were less likely to have type 2 diabetes compared to HIV-infected individuals on ART (21) (16%) or HIV-infected not on ART (15) (78.9%).

Table 4. 2. Clinical characteristics separated by HIV infection status and uninfected controls

Clinical Characteristics (%)	HIV on ART (n=131)	HIV not on therapy (n=19)	Controls (n=48)	P-value (p<0.05)
Smokers, n;				0.03
Current	41(31.3%)	2(10.5%)	9(18.8%)	
Prior	14(10.7%)	1(5.3%)	1(2.1%)	
Never smoked	76(58%)	16(84.2%)	38(79.2%)	
Hypertension, n	47 (35.9)	16 (84.2)	6 (12.5)	<0.001
Diabetes, n	21 (16.0)	15 (78.9)	2 (4.2)	<0.001

ANOVA post-hoc tests (p<0.05)

4.4 Cardiovascular magnetic resonance findings

4.4.1 Left and right ventricular function

As shown in Table 4.3, there were no significant differences in LV function between the HIV-infected groups and the uninfected controls LVEDV, LVEDVi, LVESV, LVESVi, LVSV, LVSVi, LVEF, LVM, LVMi and LVEDD, all p>0.05). Participants with HIV infection on ART had increased LVM compared to uninfected controls (100.9 ± 28.5 g versus 87.6 ± 19.3 g; p<0.01).

On the other hand, HIV-infected individuals on ART exhibited lower RVEDVi compared to HIV-uninfected controls (69.7 ± 15.13 ml/m² versus 80.2 ± 31.3 ml/m², p = 0.01). HIV-infected individuals not on ART had elevated RVESV compared to HIV-uninfected controls (64.3 ± 21.3 ml versus 50.8 ± 15.0 , p=0.02). RVSVi was decreased in HIV-infected individuals not on ART compared to HIV-infected individuals on ART and uninfected controls (33.3 ± 0.3 ml/m² versus 39.4 ± 9.0 ml/m² and 41.9 ± 6.9 ml/m², respectively, p<0.001). HIV-infected individuals not on ART had significantly lower RVEF compared to HIV-infected people on ART or uninfected controls ($48.4 \pm 8.3\%$ versus $56.9 \pm 8.7\%$ versus $59.1 \pm 6.5\%$, p<0.001).

Table 4. 3. CMR functional characteristics of HIV-infected participants and uninfected controls

Characteristic	HIV on ART (n=131)	HIV not on therapy (n=19)	Controls (n=48)	P-value (p<0.05)
LVEDV, ml	139.5 ± 36.4	135.7 ± 39.3	128.0 ± 21.3	0.13
LVEDVi, ml/m ²	77.6 ± 17.7	73.9 ± 19.5	75.03 ± 11.3	0.50
LVESV, ml	59.1 ± 26.0	60.7 ± 24.1	53.1 ± 11.2	0.26
LVESVi, ml/m ²	32.9 ± 13.4	33.2 ± 12.9	31.2 ± 6.4	0.65
LVSV, ml	80.1 ± 18.9	75.3 ± 21.4	73.3 ± 13.4	0.07
LVSVi, ml/m ²	45.6 ± 9.3	40.7 ± 9.8	42.6 ± 6.5	0.07
LVEF, %	58.3 ± 8.0	55.8 ± 8.0	58.0 ± 5.0	0.40
LV Mass, g	100.9 ± 28.5	103.2 ± 29.7	87.6 ± 19.3	<0.01 ^{a,c}
LVMi, g/m ²	56.0 ± 13.3	55.9 ± 13.9	51.2 ± 10.0	0.07
LVEDD, cm	51.4 ± 32.2	49.7 ± 6.9	47.1 ± 4.5	0.64
RVEDV, ml	124.9 ± 29.4	124.9 ± 36.2	122.6 ± 24.5	0.89
RVEDVi, ml/m ²	69.7 ± 15.1	68.0 ± 18.2	80.2 ± 31.3	<0.01 ^{a,c}
RVESV, ml	54.4 ± 19.2	64.3 ± 21.3	50.8 ± 15.0	0.03 ^{b,c}
RVESVi, ml/m ²	30.3 ± 10.1	35.0 ± 11.3	29.7 ± 8.1	0.12
RVSV, ml	70.6 ± 17.6	61.3 ± 20.6	71.0 ± 13.5	0.07
RVSVi, ml	39.4 ± 9.0	33.3 ± 10.3	41.9 ± 6.9	<0.01 ^{a,b,c}
RVEF, %	56.9 ± 8.7	48.4 ± 8.3	59.1 ± 6.5	<0.001 ^{a,b,c}

Continuous data are shown as mean ± SD. ANOVA post-hoc tests (p<0.05): (a) HIV on ART, (b) HIV not on ART, (c) controls. (Legends: LV = left ventricular; RV = right ventricular; EDV = end-diastolic volume; ESV = end-systolic volume; SV = stroke volume; EF = ejection fraction; LVM = left ventricular mass; LVEDD = left ventricular end-diastolic diameter. Characteristics with an *i* are indexed to body surface area).

4.4.2 Left ventricular deformational characteristics

Myocardial deformational characteristics of HIV-infected participants and uninfected controls are presented in Table 4.4. HIV-infected individuals not on ART demonstrated impaired peak global circumferential and longitudinal strain compared to HIV-infected persons on ART and HIV-uninfected controls (p<0.001 for both comparisons). Similarly, HIV-infected individuals not on ART demonstrated impaired peak systolic longitudinal strain rate compared to HIV-infected

persons on ART and HIV-uninfected controls ($p < 0.001$ for both comparisons). In addition, HIV-infected individuals not on ART had reduced peak diastolic circumferential and longitudinal strain compared to uninfected controls ($p = 0.03$, $p = 0.01$, respectively).

Table 4. 4. Myocardial deformation characteristics

Parameter (mean \pm SD)	HIV on ART (n=131)	HIV not on therapy (n=19)	Controls (n=48)	P-value (p<0.05)
Peak global circumferential strain, %	-21.0 \pm 3.7	-17.3 \pm 2.9	-19.8 \pm 2.8	<0.001 ^{a,b,c}
Peak global radial strain, %	31.9 \pm 9.9	28.4 \pm 6.9	34.5 \pm 9.3	0.06
Peak global longitudinal strain, %	-19.8 \pm 5.5	-15.8 \pm 3.3	-18.2 \pm 2.9	<0.01 ^{a,b}
Systolic circumferential strain rate, s ⁻¹	-1.1 \pm 0.3	-1.0 \pm 0.2	-1.0 \pm 0.3	0.38
Diastolic circumferential strain rate, s ⁻¹	1.2 \pm 0.6	1.0 \pm 0.2	1.3 \pm 0.3	0.04 ^{b,c}
Systolic longitudinal strain rate, s ⁻¹	-1.0 \pm 0.3	-0.9 \pm 0.1	-1.3 \pm 0.5	<0.001 ^{a,b,c}
Diastolic longitudinal strain rate, s ⁻¹	1.2 \pm 0.4	1.0 \pm 0.2	1.3 \pm 0.4	0.01 ^{b,c}
Systolic radial strain rate, s ⁻¹	1.8 \pm 0.7	1.6 \pm 0.2	1.8 \pm 0.8	0.28
Diastolic radial strain rate, s ⁻¹	-2.1 \pm 1.4	-1.7 \pm 0.8	-2.4 \pm 0.8	0.08

Continuous data are shown as mean \pm SD. ANOVA post-hoc tests ($p < 0.05$): (a) HIV on ART, (b) HIV not on ART, (c) controls. s⁻¹, per second.

4.4.3 Tissue characterisation

Tissue characterisation results are summarised in Table 4.5. HIV-infected participants not on ART had elevated native T1 and LV LGE volume compared to HIV-infected persons on ART and uninfected controls ($p < 0.001$ for both controls). HIV-infected individuals not on ART demonstrated higher T2 times compared to HIV-infected persons on ART (42.0 ± 4.2 ms versus 39.4 ± 2.9 ms; $p=0.2$). However, ECV measures showed no differences between the three groups ($p=0.21$).

Table 4. 5. Myocardial tissue characteristics

Parameter (mean ± SD)	HIV on ART (n=131)	HIV not on therapy (n=19)	Controls (n=48)	P-value (p<0.05)
ECV, %	30.6 ± 5.3	31.8 ± 4.6	29.1 ± 9.2	0.21
Native T1, ms	1251 ± 47	1301 ± 58	1224 ± 48	<0.001 ^{a,b,c}
Native T2, ms	39.4 ± 2.9	42.0 ± 4.2	39.2 ± 2.2	<0.01 ^{a,b}
T1- weighted SIR, %	0.9 ± 0.2	0.8 ± 0.2	0.9 ± 0.1	0.03 ^{a,b,c}
T2- weighted SIR, %	1.4 ± 0.3	1.3 ± 0.4	1.4 ± 0.2	0.03
LV LGE volume fraction 2d, %	28.4 ± 6.7	32.9 ± 10.2	25.1 ± 8.3	<0.001 ^{a,b,c}

Continuous data are shown as mean ± SD. ANOVA post-hoc tests (p<0.05): (a) HIV on ART, (b) HIV not on ART, (c) controls. (Legends: ECV = Extracellular volume fraction; T1-w = T1-weighted imaging; SIR = signal intensity ratio; T2-w = T2-weighted imaging; LV LGE volume fraction = left ventricular late gadolinium enhancement volume fraction; ms, milliseconds s⁻¹ = per second).

4.4.4 Pericardial and paracardiac adipose deposits

Compared with participants with HIV and not on therapy and uninfected controls, participants with HIV on ART had higher PAT and ParaAT volumes as well as PATi and ParaATi (all p-values <0.001; Table 4.6). Figure 4.1 demonstrate the distribution of both PATi and ParaATi volumes in three sub-groups.

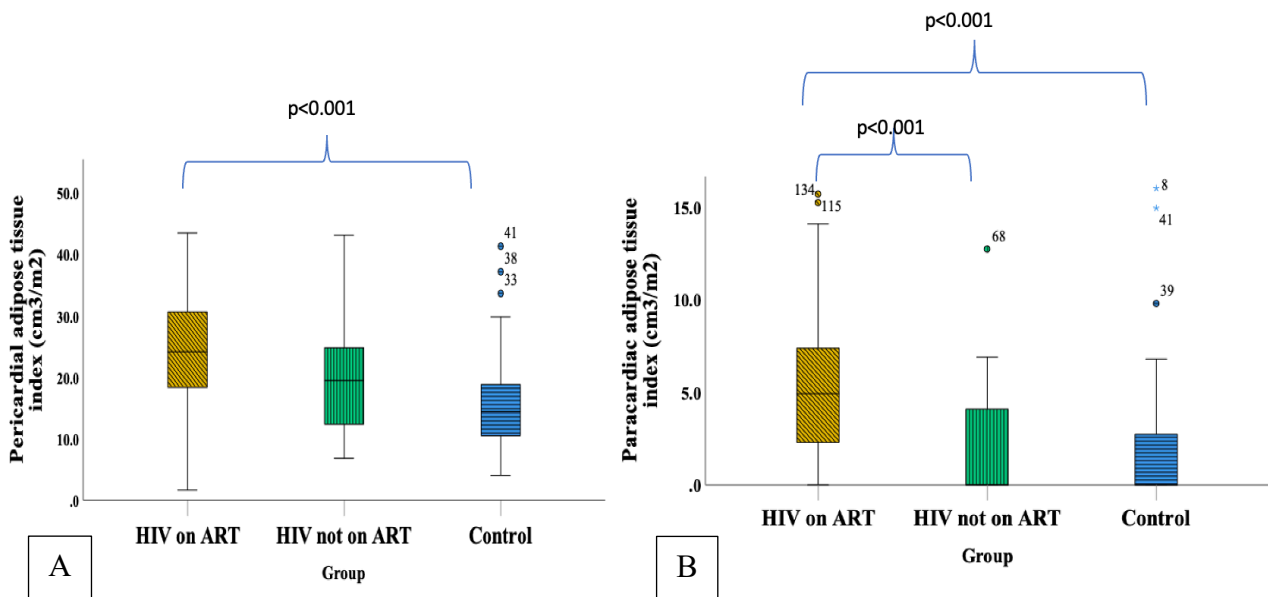


Figure 4.1. Box plot comparison of PATi (A) and ParaATi (B) fat between the three sub-groups, including HIV on ART, HIV not on therapy and uninfected controls.

Table 4.6 describe the findings of the quantification of pericardial and paracardiac adipose tissue in HIV-infected participants and uninfected controls (n=198) for all three cohorts. PLHIV on ART had greater whole-heart PAT volumes 43.1 cm³ (30.7- 54.8 IQR) compared to untreated PLHIV 32.1 cm³ (22.8-52.8 IQR) or uninfected controls 23.0 cm³ (17.2-31.7 IQR), p<0.001. PLHIV on ART had higher whole-heart ParaAT volume 9.0 cm³ (3.8-13.4 IQR) compared to untreated PLHIV 0 cm³ (0.0-11.0 IQR) or uninfected controls 0 cm³ (0.0-5.2 IQR), p<0.001.

Table 4.6. Quantification of pericardial and paracardiac adipose tissue in HIV-infected participants and uninfected controls

Parameters Median (IQR)	HIV on ART (n=131)	HIV not on therapy (n=19)	Controls (n=48)	P-value (p<0.05)
PAT, cm ³	44.6 ± 22.8	40.1 ± 25.8	27.1 ± 16.0	<0.001 ^{a,c}
PATi, cm ³ /m ²	24.6 ± 11.3	21.4 ± 13.7	15.8 ± 8.8	<0.001 ^{a,c}
PARA-AT, cm ³	9.9 ± 8.6	5.8 ± 10.5	3.9 ± 7.0	<0.001 ^{a,c}
PARA_ATi, cm ³ /m ²	5.4 ± 4.4	2.7 ± 4.9	2.2 ± 3.8	<0.001 ^{a,b,c}

Continuous data are shown as mean ± SD. ANOVA post-hoc tests (p<0.05): a) HIV on ART, b) HIV not on ART, c) controls. (Legends: PAT = pericardial adipose tissue; PATi = pericardial adipose tissue index; ParaAT = paracardiac adipose tissue; ParaATi = paracardiac adipose tissue index).

4.4.5 Late gadolinium enhancement

Different patterns of LGE were present in all 3 groups. HIV-infected individuals on ART showed diffuse/patchy LGE (n=35, 26.7%), linear midwall LGE (n=63, 48.1%) and focal LGE (n=1, 0.8%). HIV-infected persons not on ART showed diffuse/patchy LGE (n=11, 57.9%) and linear LGE (n=11, 52.6%) as seen in Table 4.7 and Figure 4.2. HIV-uninfected controls had diffuse/patchy LGE (n=5, 10.4%) and linear LGE (n=9, 18.8%), with the rest not demonstrating any focal fibrosis.

Table 4.7. LGE patterns in HIV-infected participants and uninfected controls

Parameters n (%)	HIV on ART (n=131)	HIV not on therapy (n=19)	Controls (n=48)	P-value (p<0.05)
Presence LV LGE	95 (72.5)	17 (89.5)	23 (47.9)	<0.001
LV LGE diff/patch	35 (26.7)	11 (57.9)	5 (10.4)	<0.001
LV LGE linear	63 (48.1)	10 (52.6)	9 (18.8)	<0.01
LV LGE focal	1 (0.8)	0	0	0.77

Continuous data are mean \pm SD. LV, left ventricular; LGE, late gadolinium enhancement; diff/patch, diffused and patchy LGE.

Figure 4.2 Below illustrates the patterns of LGE in participants with HIV and on ART, those not on therapy and uninfected controls.

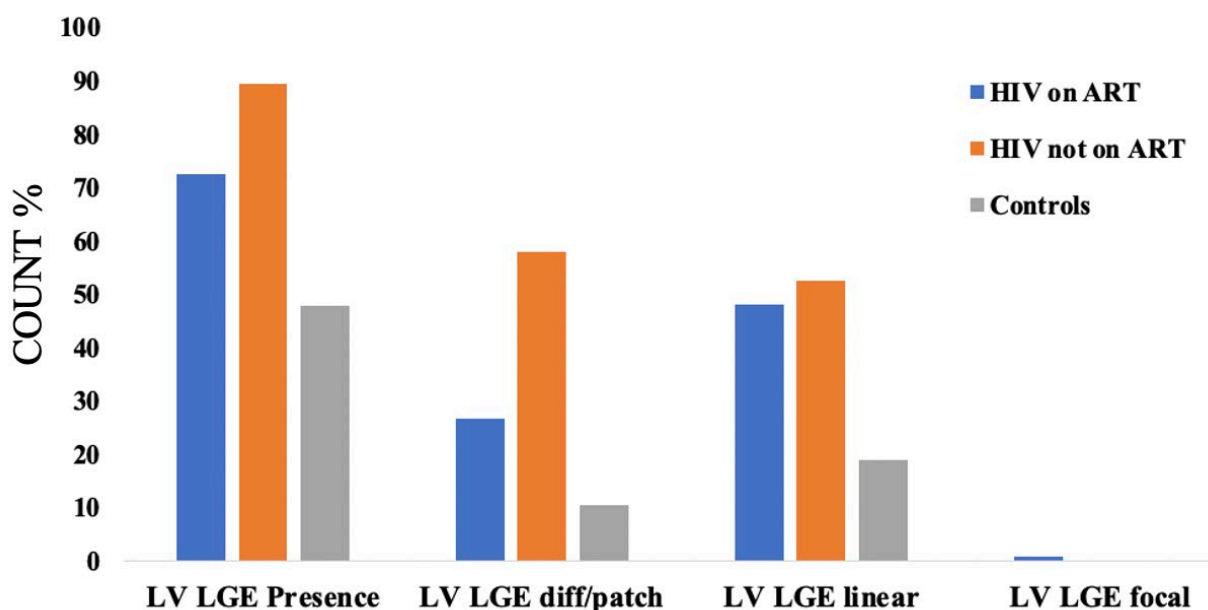


Figure 4.2. Bar graph illustrating percentage of patterns of late gadolinium enhancement amongst participants with HIV and on ART, those not on therapy and uninfected controls.

4.5 ART regimen

A total of 131/198 participants were on combination ART, which included NRTIs, NNRTIs and PI – Table 4.8. The most commonly prescribed NRTIs were emtricitabine (n=102) (77.9%), tenofovir disoproxil (n=94) (71.8%) and lamivudine (n=14) (10.7%). NNRTIs prescribed included efavirenz (n=94) (71.8%) and nevirapine (n=8) (6.1%). The PI prescribed were atazanavir, darunavir,

lopinavir and ritonavir (n=17) (13%). None of the participants included in this study were receiving an integrase inhibitors.

These participants were on antiretroviral combination therapy treatment including nucleoside reverse transcriptase inhibitors, non-nucleoside reverse transcriptase inhibitors and protease inhibitors. The commonest of the nucleoside reverse transcriptase inhibitors was emtricitabine (n=102) (77.9%), followed by tenofovir disoproxil (n=94) (71.8%), lamivudine (n=14) (10.7%). Non-nucleoside reverse transcriptase inhibitors that was most frequently used was Efavirenz (n=94) (71.8%) and the least was nevirapine (n=8) (6.1%). Protease inhibitors were used on few participants (n=17) (13%) and none were using integrase inhibitors.

Table 4. 8. Classification of PLHIV by ART regimens (n=131).

HIV-related characteristics	HIV on ART (n=131)	Percentage (%)
Nucleoside reverse transcriptase inhibitor		
Abacavir	4	3.1
Emtricitabine	102	77.9
Lamivudine	14	10.7
Tenofovir alafenamide (TAF)	9	6.9
Tenofovir disoproxil (TDF)	94	71.8
Stavudine	2	1.5
Zidovudine	11	8.4
Other	10	7.6
Non-nucleoside reverse transcriptase inhibitor		
Efavirenz	94	71.8
Nevirapine	8	6.1
Protease inhibitor		
Atazanavir	1	0.8
Darunavir	1	0.8
Lopinavir	8	6.1
Ritonavir	7	5.3
Integrase inhibitor		
Dolutegravir	0	-
Elvitegravir	0	-

4.6 Bivariate correlates of myocardial function and tissue characteristics with pericardial adiposity.

There were significant positive weak correlations between the PATi and LVESVi ($r = 0.3$, $p = 0.002$), LVMi ($r = 0.3$, $p < 0.003$), peak diastolic circumferential strain rate ($r = 0.2$, $p = 0.02$) and peak diastolic longitudinal strain rate ($r = 0.2$, $p = 0.01$) – Table 4.9. Further, significant negative weak correlations were observed between PATi and peak global circumferential strain ($r = -0.2$, $p = 0.02$) and peak radial diastolic strain rate ($r = -0.2$, $p = 0.01$).

Table 4.9. Correlation between PATi and CMR parameters in HIV-infected participants and uninfected controls.

CMR Parameters	HIV on ART		HIV not on therapy		Controls	
	Pearson' r = value	P-value	Pearson' r = value	P-value	Pearson' r = value	P-value
LVEDVi, ml/m ²	0.18*	0.04	0.4	0.1	-0.06	0.7
LVSVi, ml/m ²	0.3**	0.002	0.1	0.6	0.2	0.2
LVMi, g/m ²	0.3**	0.003	0.5 *	0.3	0.2	0.2
RVEDVi, ml/m ²	0.2*	0.4	0.3	0.2	-0.1	0.4
RVSVi, ml/m ²	0.2*	0.06	0.13	0.5	0.7	0.6
ECV, %	-0.2*	0.06	-0.3	0.3	-0.2	0.1
Peak global circumferential strain, %	-0.2*	0.02	0.03	0.8	-0.2	0.1
Diastolic circumferential strain rate, s ⁻¹	0.2*	0.02	-0.05	0.8	-0.1	0.5
Diastolic longitudinal strain rate, s ⁻¹	0.2*	0.01	-0.4	0.1	0.2	0.2
Diastolic radial strain rate, s ⁻¹	-0.2*	0.01	-0.05	0.8	-0.2	0.1

*Correlation is significant at the 0.05 level. ** correlation is significant at the 0.01 level. Correlation was analysed by Pearson's correlation.

4.7 Bivariate correlates of myocardial function and tissue characteristics with paracardiac adiposity.

On bivariate correlations analysis, ParaATi demonstrated a significant weak positive correlation in HIV on ART participants with LVEF ($r = 0.2$, $p = 0.03$), RVEF ($r = 0.3$, $p = 0.003$), peak global radial strain ($r = 0.2$, $p = 0.003$), and peak systolic radial strain rate ($r = 0.21$, $p = 0.004$). In contrast, ParaATi demonstrated significant weak negative correlations with RVESVi ($r = -0.2$, $p = 0.04$), ECV ($r = -0.2$, $p = 0.04$), peak global circumferential strain ($r = -0.2$, $p < 0.001$), peak global longitudinal strain ($r = -0.3$, $p < 0.001$), peak systolic circumferential strain rate ($r = -0.2$, $p = 0.04$), and peak diastolic radial strain rate ($r = -0.2$, $p = 0.04$). While those not on ART showed a moderately positive correlation with LVEF ($r = 0.5$, $p = 0.05$) and a negative correlation with peak

global longitudinal strain ($r = -0.5$, $p = 0.03$). However, uninfected controls demonstrated a moderately negative correlation with LVEDVi, LVESVi, RVESVi, RVSVi and ECV (Table 4.10).

Table 4.10. Correlation between ParaATi and CMR parameters in HIV-infected participants and uninfected controls.

CMR Parameters	HIV on ART		HIV not on therapy		Controls	
	Pearson' r = value	P-value	Pearson' r = value	P-value	Pearson' r = value	P-value
LVEDVi, ml/m ²	-0.04	0.6	-0.09	0.7	-0.4**	0.01
LVSVi, ml/m ²	-0.1	0.3	-0.3	0.3	-0.4**	0.01
LVEF, %	0.2*	0.03	0.5 *	0.05	0.3	0.05
RVESVi, ml/m ²	-0.2*	0.04	-0.2	0.4	-0.3*	0.03
RVSVi, ml/m ²	0.1	0.2	0.2	0.4	-0.3*	0.04
RVEF, %	0.3**	0.003	0.4	0.1	0.2	0.3
ECV, %	-0.2*	0.04	-0.1	0.7	-0.3*	0.02
Peak global circumferential strain, %	-0.2**	<0.001	-0.4	0.07	-0.02	0.8
Peak global radial strain, %	0.2**	0.003	0.4	0.06	0.02	0.8
Peak global longitudinal strain, %	-0.3**	<0.001	-0.5*	0.03	0.04	0.7
Systolic circumferential strain rate, s ⁻¹	-0.2*	0.04	0.2	0.4	0.03	0.8
Systolic radial strain rate, s ⁻¹	0.21**	0.004	-0.01	0.9	-0.06	0.6
Diastolic radial strain rate, s ⁻¹	-0.2*	0.04	-0.3	0.2	-0.02	0.9

*Correlation is significant at the 0.05 level. ** correlation is significant at the 0.01 level. Correlation was analysed by Pearson's correlation.

ParaAT demonstrated weak negative correlations with peak global circumferential and longitudinal strain ($r = -0.23$, $p < 0.001$ and $r = -0.21$, $p < 0.01$, respectively). PAT had shown a weak negative correlation with peak circumferential strain ($r = -0.18$, $p < 0.01$). However, PAT had been found to have a moderately positive correlation with LV mass ($r = 0.45$, $p < 0.001$) (Figure 4.3).

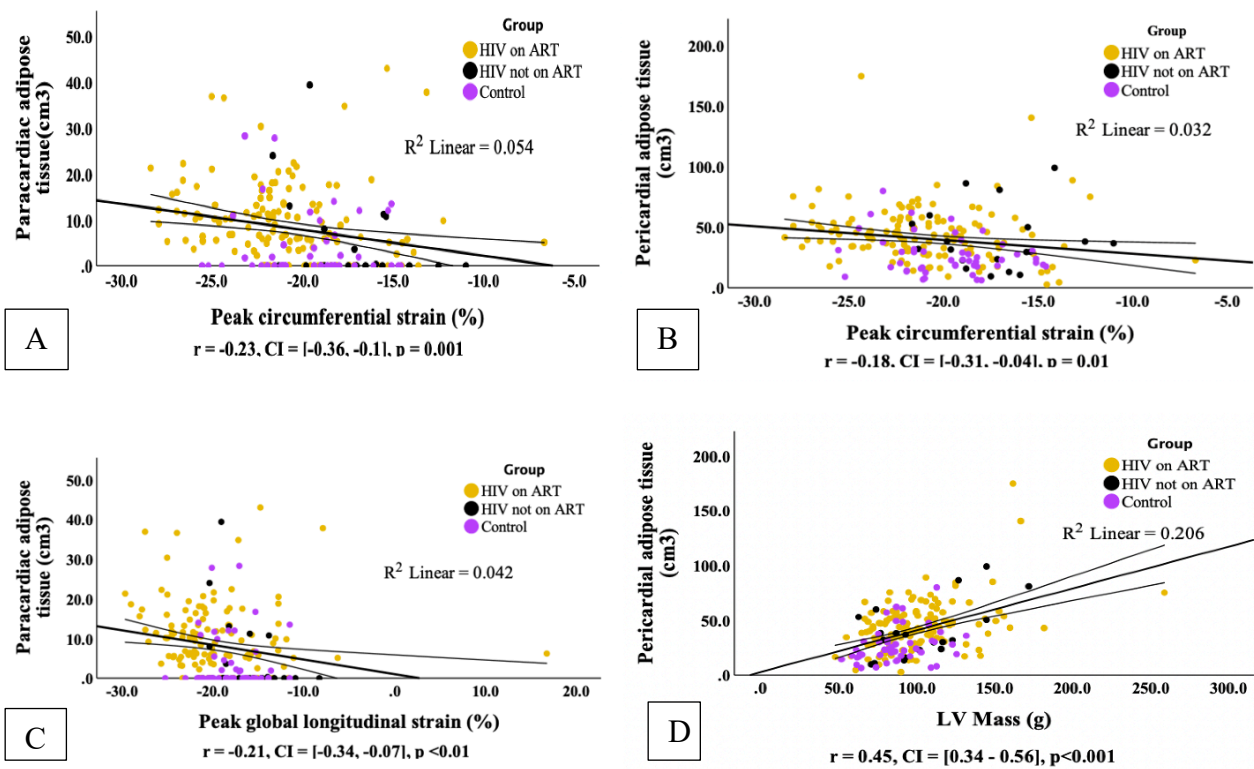


Figure 4.3. Scatter plots illustrating the correlation between (A) ParaAT and peak circumferential strain, (B) PAT and peak circumferential strain, (C) PAT and peak longitudinal strain and (D) PAT and LV mass in HIV-infected sub-groups and HIV-uninfected controls.

4.8 Summary

The results of this study demonstrated that cardiovascular structure and function, and tissue characterisation could be accurately measured and quantified using CMR. The results have been reported in such a way that it answers the research question and objectives of the study. The results showed increased PAT and ParaAT in PLHIV on ART compared to HIV-uninfected controls, with untreated PLHIV having an intermediate phenotype. For PLHIV not on ART, myocardial inflammation is associated with more significant impairment in strain and tissue characteristics, but not PAT and ParaAT volume. The chapter that follows describes the main findings which are placed within the context of other similar studies in literature

CHAPTER FIVE

DISCUSSION

This chapter discusses the findings of this study as it relates to the objectives of this study. The aim of this cross-sectional study was to quantify, using cardiovascular magnetic resonance, PAT and ParaAT in ART-treated and untreated PLHIV and matched controls without HIV. Furthermore, the study investigated the relationship of PAT and ParaAT volume to HIV disease duration, ART regimen, and myocardial phenotypes of ventricular function, deformational characteristics, inflammation, and fibrosis.

This study demonstrated a significantly higher BMI, BSA and weight in both patients receiving ART and untreated PLHIV compared to matched HIV-uninfected controls. However, a gradient of PAT and ParaAT volume, which is more remarkable in PLHIV on ART, has an intermediate phenotype in untreated PLHIV, and is lowest in HIV- uninfected persons. Untreated PLHIV had higher T1 and T2 times, and ECV compared to PLHIV on ART and untreated controls. Global RV ejection fraction was reduced in untreated PLHIV. Abnormalities in strain, strain rate, LVM, myocardial inflammation and fibrosis are commonest in untreated PLHIV compared to PLHIV on ART and uninfected controls. Both PAT and ParaAT showed weak correlations with indices of myocardial function and tissue characteristics.

Cardiovascular disease is a major contributor to morbidity and mortality in PLHIV. In the general population, increased PAT is associated with poor cardiovascular outcomes, but its role in HIV-associated CVD is not well described. The widescale availability and use of ART has dramatically decreased the number of HIV/AIDS-related deaths and improved quality of life; however, ART may also be associated with the development of CVD (Tsabedze *et al.*, 2018; Pejković *et al.*, 2019). In particular, heart failure with preserved ejection fraction, myocardial inflammation, myocardial fibrosis, and myocardial steatosis are common phenotypes in ART-treated PLHIV (Ntusi & Ntsekhe, 2016). This study revealed the magnitude of the effect of inflammation in untreated PLHIV is greater than that of visceral cardiac adiposity on impairments in LV function and myocardial tissue characteristics. In recent years, native T1 and T2 mapping techniques have been proven to be more reliable in the diagnosis of inflammation (Russo *et al.*, 2020). Therefore, native T1 and T2 times, and ECV assist in relevant decision-making concerning patient management and risk stratification, due to its ability to uniquely enhance the effect of cardiac adiposity on myocardial tissue (Choi, Park & Kim, 2017).

In this study, both HIV-infected groups demonstrated high BMI measure, which is an indicator of total body adiposity; however, the BMI only considers the individual's height and weight and does not measure visceral adiposity like waist-hip ratio. Therefore, there is no indication of the degree of intra-abdominal adiposity in these HIV-infected groups but weight loss can be a potential therapy in these patients because it is associated with the reduction of PAT burden (Goudis et al., 2018). Prior data as suggested that BMI and WHR as a measure to assess the fat distribution for predicting CVD risks (Yu et al., 2017).

In PLHIV on ART, we observed higher volumes of ectopic PAT and ParaAT deposition. The vast majority of studies investigating adiposity in HIV-infected persons reported that the development of adiposity in PLHIV is due to ART secondary effects, direct viral effects and complex interaction of chronic inflammation (Buggey & Longenecker, 2018; Buggey *et al.*, 2020; Song *et al.*, 2020). Importantly, it is believed that pericardial fat is a source of proinflammatory cytokine stimulation; and elaboration of proinflammatory factors leads to endothelial dysfunction and CAD (Selthofer-Relatić & Bošnjak, 2015). This study showed that, HIV participants on ART had a higher amount of fat deposition than those who were naïve to treatment /uninfected controls. In theory, the increase in pericardial adipose tissue may be associated with decreased LV global longitudinal strain and increased LV mass, even in the absence of other risk factors; and may contribute to identifying risks of cardiac dysfunction in PLHIV (Buggey *et al.*, 2020). However, in this study, LV global longitudinal strain is lower in those who were naïve to treatment than uninfected controls. In the meanwhile, the LV mass was significant high for both HIV-infected groups. Therefore, were shown that the elevated levels of PAT can be associated with increased LV mass in PLHIV.

Furthermore, Lo *et al.* published a study which included 78 HIV-infected men and 32 controls, who had increased pericardial fat volumes measured by computed tomography and suggested that increased adiposity in PLHIV is associated with ART (Lo *et al.*, 2010). Pericardial fat was greater in HIV patients than in controls (Guaraldi *et al.*, 2011). More work is needed to investigate clinical significance of epicardial fat accumulation in HIV patients. However, elevated fat volumes in PLHIV could be caused by NRTIs because they have been implicated in the body's fat redistribution (Hemkens & Bucher, 2014). PIs stimulate the synthesis of hepatic triglycerides leading to high levels of triglyceride (Rodriguez & Tan, 2017).

It has been postulated that the increase in cardiac adiposity in PLHIV on ART occurs in response to high volume adipose tissue deposition around the heart. This lipodystrophy have been linked to

ART use (Brener *et al.*, 2014). Increased epicardial adiposity have multiple clinical implications. Often PLHIV on ART tend to have an increased risk of incident cardiovascular events and CAD (Guaraldi *et al.*, 2011). Increased amount of plaque in the coronary arteries from HIV-infected men with increased fat deposition was thought to be the result of increased duration of ART (Brener *et al.*, 2014). Currently ART is being investigated as the mechanistic link between increased adiposity and cardiac dysfunction. Further, this study sought to define clearly the association that has been described between increased adiposity in HIV and the effects on cardiac function and structure.

A previous study looking at cardiac steatosis and LV dysfunction in PLHIV on ART indicated that ectopic fat deposition in the myocardium might contribute to cardiac disease in patients with HIV infection treated with Highly Active Antiretroviral Therapy (HAART) (Nelson, 2014). The presence of fat deposition in the myocardium in their HIV-infected group was associated with ART exposure, these findings provides significant clinical relevance in the prediction of LV dysfunction in PLHIV as it provide mechanical insight into the pathogenesis of CVD in patients using ART (Nelson, 2014).

The increase in adiposity redistribution appears to be a source of inflammatory cells and mediators, and these inflammatory cells lead to endothelial dysfunction (Murphy *et al.*, 2020; Kim *et al.*, 2021). Fat deposits have been recognised as a rich source of free fatty acids and a number of bioactive molecules, such as inflammatory cytokines which might significantly affect cardiac pathology such as lipodystrophy, coronary heart disease, atherosclerosis and metabolic syndrome (Hemkens & Bucher, 2014). The prevalence of lipodystrophy in the use of ART may be associated with fat redistribution syndrome, characterised by fat deposits in the abdomen and neck (Buggley & Longenecker, 2018). Additionally, the complications caused by these fat deposits are multifactorial with local inflammation, fibrosis and structural remodelling (Bonou *et al.*, 2021). An increase in pericardial fat can reliably help identify PLHIV at high risk of myocardial dysfunction and prevent clinical consequences like silent ischemic heart disease (Kristoffersen *et al.*, 2013). Given the pathogenic role of the increased amount of pericardial fat in PLHIV, future screening protocols for PAT as a CV risk factor can be useful in the management of these myocardial changes in PLHIV. Development of new therapies which plays a crucial role in lowering concentrations of lipids, i.e. statin therapy can aid in clinical intervention for managing cardiovascular events in PLHIV (Uthman *et al.*, 2018). Our findings can be useful for policy marking in identifying persons at higher cardiovascular risk in-order to prioritise them for clinical interventions.

Untreated PLHIV had higher T1 and T2 times, and ECV compared to PLHIV on ART and untreated controls. These observations revealed that the magnitude of the effect of inflammation in untreated PLHIV is greater than that of visceral cardiac adiposity on impairments in LV function and myocardial tissue characteristics. Further, this suggests that HIV participants naïve to treatment have higher indices of extracellular matrix remodelling compared with HIV on ART, and this may be due to high viral load in HIV participants not on ART since they are not taking any ART yet (Deeks *et al.*, 2015; Hsue & Waters, 2017).

Elevated native T1 times highlight the presence of diffuse fibrosis and /or inflammation in participants with HIV on ART and those naïve to treatment. Most studies suggest that increased native T1 and expanded ECV are also observed in the presence of myocardial oedema, infiltration and infarction (Holloway *et al.*, 2013; Taylor *et al.*, 2016). Evidence of clinical and experimental studies shows increased interstitial space and oedema as biological determinants of an increase in native T1 times (Haaf *et al.*, 2016; Luetkens *et al.*, 2016). Native T1 time has been used to assess several different clinical contexts for measurement of myocardial tissue composition in the setting of HIV-related CVD. In fact, native T1 times play a major role in the early detection of myocardial fibrosis and has been utilised for the study of many cardiac pathologies, including oedema, dilated cardiomyopathy, valvular heart disease, infarction, hypertrophic cardiomyopathy (Holloway *et al.*, 2013; Ferreira *et al.*, 2014; Choi *et al.*, 2017; Radenkovic *et al.*, 2017). Differences were also noted in native T2 time between the HIV participants on ART and those naïve to treatment however, these were within the normal range (de Louw, 2021).

ECV may enable the characterisation of myocardial tissue remodelling and early fibrotic changes that can be missed on LGE imaging (Karamitsos *et al.*, 2020). Moreover, HIV is associated with a high degree of inflammation (Subramanian *et al.*, 2012). PLHIV on ART are at an increased risk of developing ischemic LV dysfunction, atherosclerosis and myocardial infarction due to inflammation (Belkin & Uriel, 2018). A number of studies conducted in HIV-infected patients reveal that increased native T1 time and ECV are correlated with histologic measures of interstitial myocardial fibrosis (Haaf *et al.*, 2016; Mandoli *et al.*, 2021). Similar to Saad *et al.* (2020), we report a slightly insignificant elevated ECV values in the HIV-infected groups than uninfected controls, which may indicate an ongoing inflammatory process in our cohort.

Untreated PLHIV had the largest burden of LGE (Figure 3) these include diffuse/patchy, linear and focal patterns, which is a good indicator of myocardial fibrosis. These results suggest that HIV-

untreated participants are at a high risk of cardiac events, while in HIV on ART participants might be linked to ART toxicity (myocardium) after a long period of exposure (Rosito *et al.*, 2008; Deeks *et al.*, 2015). It is difficult to estimate or determine the root cause of LGE in our healthy controls, but this could be linked to lack of adequate access to health care, malnutrition, as well as social and environmental factors as our cohort was from low-income communities as shown in another study (So-Armah & Freiberg, 2018). LGE has been shown to be significantly more sensitive in evaluating myocardial viability and distinguishing between ischaemic and non-ischaemic aetiologies of myocardial dysfunction (Lee *et al.*, 2011; Lewis, Burrage & Ferreira, 2020).

Current LGE models appear robust and good at identifying differing volumes of distribution and extent of myocardial involvement, because gadolinium accumulates in areas of abnormal myocardium within minutes following contrast injection (Earls *et al.*, 2002). Clinically, LGE shines a spotlight on cardiomyopathies, pathological conditions like infarction, myocarditis, amyloidosis, sarcoidosis, Anderson-Fabry and systemic sclerosis, thereby providing relevant insight for diagnostic and prognostic purposes (Lintingre *et al.*, 2020). One of the strengths of LGE is the ability to predict cardiovascular mortality (von Knobelsdorff-Brenkenhoff & Schulz-Menger, 2016). However, LGE has limitations for assessment of diffuse interstitial fibrosis because image contrast relies on the differences in signal intensity between the normal and fibrotic myocardium (Li *et al.*, 2021).

Further, we report abnormal RV function in the untreated PLHIV. The mechanism for RV dysfunction in HIV-untreated participants is unclear, but may likely be due to direct toxic effect from the virus (Simon *et al.*, 2014). RV dysfunction has been associated with a poorer prognosis, which is a risk factor for cardiovascular mortality (Guazzi, 2020). Moreover, untreated PLHIV had the greatest impairments in myocardial strain and strain rates, which strongly suggest that early effects of HIV infection on the heart can lead to cardiac inflammation may be due to immune dysregulation and opportunistic infection and not PAT and ParaAT volume. This observation may be due to early marker of myocardial dysfunction (Sood *et al.*, 2017). The myocardial changes are as a result of LV or deformation due to LV myocardial contractile dysfunction (in either circumferential, radial longitudinal strain) (Geyer *et al.*, 2010). Therefore, strain measures are useful and can be reliable for risk stratification in various cardiac abnormalities in PLHIV (Amzulescu *et al.*, 2019). Impaired cardiac strain is a consequence of immune activation and several chronic inflammatory conditions, which may serve as a sensitive imaging marker for the development of therapeutic strategies for CV health in PLHIV (Thiara *et al.*, 2015).

Feature tracking is an emerging technique particularly strong in assessing myocardial strain which can detect the impaired relaxation of the ventricle and myocardial dysfunction (Mangion *et al.*, 2019). Myocardial strain has been shown to be a robust technique in the measurement of the degree of change in the measurement of the tissue from resting length to maximum length (Rajiah *et al.*, 2022). While strain rate measures the rate at which these deformations occur during the cardiac cycle (Amzulescu *et al.*, 2019). Strain imaging has been utilised for the studies of different heart disease (ischemic and non-ischemic) for early detection of subclinical myocardial dysfunction (Lim *et al.*, 2021). Most studies found a significant decrease in strain values in various cardiomyopathies (Emrich *et al.*, 2021; Rajiah *et al.*, 2022). A recent study from the American College of Cardiology Foundation has shown a significant rise in the development of diastolic dysfunction and heart failure in PLHIV compared with the noninfected population (de Leuw *et al.*, 2021).

Interestingly, there were no differences in LV volumes and LVEF between all three groups. This echoes the findings of Scholtz at the University of Pretoria, who stated that strain becomes abnormal before the ejection fraction does (Scholtz, 2019). Similarly, prior studies conducted on the impact of HIV/ART on cardiovascular structure and function, confirm that strain can be used as an early marker of myocardial dysfunction (Thiara *et al.*, 2015; Ntusi *et al.*, 2016; Taylor *et al.*, 2016; Mangion *et al.*, 2019). Rodrigues and colleagues using echo, evaluated 68 HIV-infected patients (11 not using ART, 33 on NNRTI and 24 using PI), compared with 30 healthy controls and also normal LV ejection fraction were noted (Rodrigues *et al.*, 2019).

In this study, HIV-infected sub-groups had significantly higher LV mass, suggesting the effects of excessive pericardial adipose tissue deposits, resulting in increased metabolic demand on the heart leading to LV hypertrophy (Lu *et al.*, 2022). Similar to our report, a CMR study comparing 103 PLHIV on ART compared with 92 healthy controls, showed that myocardial mass was elevated, while ejection fraction and strain rates were lower in the HIV on ART group compared to healthy controls and these results were associated with changes in the myocardial structure and function (Ntusi *et al.*, 2016).

On univariate regression analysis in the pooled population, ParaAT demonstrated a weak negative correlation with peak global circumferential strain and longitudinal strain. At the same time PAT showed a weak negative correlation with peak circumferential strain and a moderate positive correlation with LVM (Figure 4.3). The poor correlation between PAT and ParaAT with functional parameters, confirm that PAT and ParaAT had no significant effect on impairments in LV function

and myocardial tissue characteristics and which did not allow the researchers to draw significant conclusions.

The discussion above highlights a gradient of PAT and ParaAT volume, which is greatest in PLHIV on ART, has an intermediate phenotype in untreated PLHIV, and is lowest in HIV-uninfected persons. Abnormalities in strain, strain rate, LVM, myocardial inflammation and fibrosis are commonest in untreated PLHIV compared to PLHIV on ART and uninfected controls. Both PAT and ParaAT showed weak correlations with indices of myocardial function and tissue characteristics.

CHAPTER SIX

STRENGTHS, LIMITATIONS, RECOMMENDATIONS AND CONCLUSION

6.1 Introduction

All research studies are subject to factors that can influence the data collection and main findings and subsequent conclusions drawn from such a study. Therefore, this chapter describes the strengths and limitations of this study and provides probable assumptions the limitations could have had on the results and subsequent findings of the study. These strengths of this study are presented here and limitations are placed within the context for which recommendations are made for future similar studies. The chapter further ends with a conclusion.

6.2 Strengths

This cross-sectional study had many strengths including the ability to compare three sub-groups which presented the opportunity to evaluate the impact of cardiac adiposity on the CV structure and function in PLHIV on ART and those that are untreated as well as in HIV-negative individuals. This study also had a large sample size of PLHIV on ART, which provided important information on myocardial phenotype and outcomes in PLHIV within the South African context. This study further provided new insight which showed that myocardial inflammation is associated with impairment in strain and tissue characteristics using the state-of-the-art imaging. The umbrella and subsidiary study were conducted under the guidance and leadership of Prof Ntusi, a specialist consultant cardiologist, with years of experience in cardiology and CMR. Furthermore, the author also had the privilege of support from a solid group of researchers who provided support to self during the data collection, image analysis and interpretation of the data.

6.3 Limitations

Nonetheless, this study had limitations which are in 2-fold: first, a relatively small sample size of PLHIV who were untreated, resulting in data lacking age-matched HIV on ART/uninfected controls. During recruitment, the greatest challenge the umbrella study had was to enrol HIV-infected persons not on therapy because the national HIV treatment program has made it difficult to recruit this cohort in our setting.

6.4 Recommendations

Based on the above-mentioned major findings and limitations of the present study, the following recommendations are proposed to strengthen CMR findings in PLHIV. Another study will be

needed to confirm the reason why RV parameters were abnormal for the HIV naïve participants. In future, the use of fat suppression imaging sequence may provide additional insight for cardiac adipose tissue assessment and new post-processing tools should be developed for the quantification of cardiac adiposity which would improve diagnostic accuracy. PLHIV with fat redistribution might benefit in CVD screening, but little is known about the abnormal findings in uninfected controls. Therefore, future prospective randomised studies should be undertaken to prioritise screening of CVD in these communities. Future studies with an equal number of participants in each cohort for example, those PLHIV on ART and those not on treatment, as well as healthy volunteers are recommended.

6.5 Conclusion

HIV/AIDS is a major public health issue in South Africa, but the increase in ART roll-out has decreased the number of HIV/AIDS-related deaths, while increasing risk factors associated with heart failure such as myocardial inflammation, myocardial fibrosis, myocardial steatosis, and lipid metabolic abnormalities.

The study highlights that pericardial and paracardial fat can drive cardiometabolic risk factors and directly promote cardiac dysfunction in HIV patients. The adipokines and cytokines secreted by pericardial fat exert detrimental effects on cardiovascular vessels, leading to the development of atherosclerosis. CMR offers a non-invasive means of assessing ventricular function, anatomical structure, tissue characterisation and the presence of LGE in asymptomatic HIV-infected patients.

The study showed that pericardial and paracardial fat volumes were elevated in HIV patients on ART, which can have deleterious effects on cardiovascular structure and function. But a weak correlation was determined between cardiac adiposity and myocardial tissue characteristics.

Myocardial strain impairment was evident in participants with HIV not on ART, which strongly suggest the presence of diastolic dysfunction and thus, leads to early treatment of CVD. The elevated native T1 values in HIV-infected participants reflect the sequel of chronic inflammation in PLHIV and ART. The results of this study demonstrate that strain imaging and native T1 mapping can be reliable method for evaluating cardiac function and myocardial fibrosis in patients with HIV-associated CVD. The remarkably increased LV mass in HIV-infected participants make it possible to identify LV hypertrophy in the diagnosis of HIV-related CVD. Significantly, we were able to detect the presence of LGE, which is known to be the predicator of adverse events in PLHIV. With this known, patients will be able to receive appropriate management to avoid adverse events.

REFERENCE LIST

- Agoston-Coldea, L., Zlibut, A., Revnic, R., Florea, M. & Muntean, L. 2021. Current advances in cardiac magnetic resonance imaging in systemic sclerosis. *European Review for Medical and Pharmacological Sciences*, 25(10): 3718-3736.
- Aldweib, N., Farah, V. & Biederman, R.W.W. 2018. Clinical utility of cardiac magnetic resonance imaging in pericardial diseases. *Current Cardiology Reviews*, 14(3): 200-212.
- Amzulescu, M.S., Craene, M. D., Langet, H., Pasquet, A., Vancraeynest, D., Pouleur, A.C., Vanoverschelde, J.L. & Gerber, B.L. 2019. Myocardial strain imaging: review of general principles, validation, and sources of discrepancies. *European Heart Journal Cardiovascular Imaging*, 20(6): 605-619.
- Antonopoulos, A.S. & Antoniades, C. 2017. The role of epicardial adipose tissue in cardiac biology: classic concepts and emerging roles. *Journal of Physiology*, 595(12): 3907-3917.
- Aus dem Siepen, F., Baumgartner, C., Muller-Hennessen, M., Andre, F., Messroghli, D., Ochs, M., Riffel, J., Giannitsis, E.M., Katus, H.A., Friedrich, M.G. & Buss, S. 2018. Variability of cardiovascular magnetic resonance (CMR) T1 mapping parameters in healthy volunteers during long-term follow-up. *Open Heart*, 5(1): e000717. Available at: <http://dx.doi.org/10.1136/openhrt-2017-000717>
- Autenrieth, C.S., Beck, E.J., Stelzie, D., Mallouris, C., Mahy, M. & Ghys, P. 2018. Global and regional trends of people living with HIV aged 50 and over: estimates and projections for 2000-2020. *PLoS ONE*, 13(11): e0207005. Available at: <https://doi.org/10.1371/journal.pone.0207005>
- Baker, J.V., Wolfson, J., Collins, G., Morse, C., Rhame, F., Liappis, A., Rizza, S., Temesgen, Z., Mystakelis, H., Deeks, S., Neaton, J., Schacker, T., Sereti, I. & Russell, P. 2021. Losartan to reduce inflammation and fibrosis endpoints in HIV disease. *AIDS*, 35(4): 575-583.
- Bangsberg, D.R., Acosta, E.P., Gupta, R., Guzman, D., Riley, E.D., Harrigan, P.R., Parkin, N. & Deeks, S. 2006. Adherence-resistance relationships for protease and non-nucleoside reverse transcriptase inhibitors explained by virological fitness. *AIDS*, 20(2): 223-231.

Barbaro, G. & Boccara, F. 2005. Cardiovascular disease in AIDS. Second. *Department of Medical Pathophysiology University of Rome*, 1st ed. Springer Link, [online] Available at: <https://doi.org/10.1007/b138963>.

Bekker, L., Alleyne, G., Baral, S., Cepeda, J., Daskalakis, D., Dowdy, D., Dybul, M., Eholie, S., Esom, K., Garnett, G., Grimsrud, A., Hakim, J., Havlir, D., Isbell, M., Johnson, L., Kamarulzaman, A., Kasaie, P., Kazatchkine, M., Kilonzo, N., Klein, M., Lewin, S., Luo, C., Makofane, K., Martin, N.K., Mayer, K., Millett, G., Ntusi, N., Pace, L., Pike, C., Piot, P., Pozniak, A., Quinn, T.C., Rockstroh, J., Ratevosian, J., Ryan, O., Sippel, S., Spire, B., Soucat, A., Starrs, A., Strathdee, S.A., Thomson, N., Vella, S., Schechter, M., Vickerman, P., Weir, B. & Beyrer, C. 2018. Advancing global health and strengthening the HIV response in the era of the sustainable development goals: the international AIDS society-Lancet commission. *The Lancet Global Health*, 392(10144): 312-358.

Belkin, M.N. & Uriel, N. 2018. Heart health in the age of highly active antiretroviral therapy: a review of HIV cardiomyopathy. *Current Opinion in Cardiology*, 33(3): 317-324.

Bertaso, A.G., Bertol, D., Duncan, B.B. & Foppa, M. 2013. Epicardial fat: definition, measurements and systematic review of main outcomes. *Arquivos Brasileiros de Cardiologia*, 101(1): 18-28.

Bière, L., Behaghel, V., Mateus, V., Assuncao, A., Grani, C., Ouerghi, K., Grall, S., Willoteaux, S., Prunier, F., Kwong, R. & Furber, A. 2017. Relation of quantity of subepicardial adipose tissue to infarct size in patients with ST-elevation myocardial infarction. *American Journal of Cardiology*, 119(12): 1972-1978.

Bloomfield, G. S., Khazanie, P., Morris A. & Hicks, C. 2014. HIV and non-communicable cardiovascular and pulmonary diseases in low-and middle-income countries in the ART era: what we know and best directions for future research. *Journal of Acquired Immune Deficiency Syndromes and Human Retrovirology*, 67(01): S40-S53.

Bonou, M., Kapelios, C.J., Athanasiadi, E., Mavrogeni, S.I., Psychogiou, M. & Barbetseas, J. 2021. Imaging modalities for cardiovascular phenotyping in asymptomatic people living with HIV. *Vascular Medicine*, 26(3): 326-337.

Brener, M., Ketlogetswe, K., Budoff, M., Jacobson, L., LI, X., Rezaeian, P., Razipour, A., Palella, F.J., Kingsley, L., Witt, M.D., George, R.T. & Post, W.S. 2014. Epicardial fat is associated with duration of antiretroviral therapy and coronary atherosclerosis. *AIDS*, 28(11): 1635-1644.

Buckberg, G.D., Nanda, N.C., Nguyen, C. & Kocica, M.J. 2018. What is the heart? Anatomy, function, pathophysiology, and misconceptions. *Journal of Cardiovascular Development and Disease*, 5(2): 33.

Buggey, J., Yun, L., Hung, C.L., Kityo, C., Mirembe, G., Erem, G., Truong, T., Ssinabulya, I., Tang, W.H.W., Hoit, B.D., McComsey, G.A. & Longenecker, C.T. 2020. HIV and pericardial fat are associated with abnormal cardiac structure and function among Ugandans. *Heart*, 106(2): 147-153.

Buggey, J. & Longenecker, C.T. 2018. Heart fat in HIV: marker or mediator of risk? *Current Opinion HIV AIDS*, 12(6): 572-578.

Bune, G.T., Yalew, A.W. & Kumie, A. 2019. The global magnitude of metabolic syndrome among antiretroviral therapy (ART) exposed and ART-naïve adult HIV-infected patients in gedio-zone, southern Ethiopia: comparative cross-sectional study, using the adult treatment panel III criteria. *Diabetes and Metabolic Syndrome: Clinical Research and Reviews*, 13(5): 2833-2841.

Butler, J., Kalogeropoulos, A.P., Anstrom, K.J., Hernandez, A.F., Desvigne-Nickens, P. & Braunwald, E. 2018. Dysfunction in individuals with human immunodeficiency virus infection: literature review, rationale and design of the characterizing heart function on antiretroviral therapy (CHART) Study. *Journal of Cardiac Failure*, 24(4): 255-265.

Cai, J., Hatsukami, T.S., Ferguson, M.S., Small, R., Polissar, N.L. & Yuan, C. 2002. Classification of human carotid atherosclerotic lesions with in vivo multicontrast magnetic resonance imaging. *American Heart Association*, 106(11): 1368-1373.

Captur, G., Manisty, C. & Moon, J.C. 2016. Cardiac MRI evaluation of myocardial disease. *Heart*, 102(18): 1429-1435.

Castillo, E.C., Vazquez-Garza, E., Yee-Trejo, D., Garcia-Rivas, G. & Torre-Amione, G. 2020. What is the role of the inflammation in the pathogenesis of heart failure. *Current Cardiology Reports*, 22(11): 139.

Choi, E.Y., Park, C.H. & Kim, T.H. 2017. The prognostic role of T1 mapping sequences: can T1 mapping parameters have a role in risk stratification. *Cardiovascular Imaging Asia*, 1(3): 193-204.

Cohen, J. (2016). A power primer. Methodological issues and strategies in clinical research, *American Psychological Association*, (279-284).

Available at: <https://doi.org/10.1037/14805-018>

Cojan-Minzat, B.O., Zlibut, A. & Agoston-Coldea, L. 2020. Non-ischemic dilated cardiomyopathy and cardiac fibrosis. *Heart Failure Reviews*, 26(5): 1081-1101.

Dastidar, A.G., Rodrigues, J.C.L., Baritussio, A. & Bucciarelli-Ducci, C. 2016. Education in heart MRI in the assessment of ischaemic heart disease. *Heart*, 102(3): 239-252.

de Cock, K.M., Jaffe, H.W. & Curran, J.W. 2012. The evolving epidemiology of HIV/AIDS. *AIDS*, 26(10): 1205-1213

de Leuw, P., Arendt, C.T., Haberl, A.E., Frodinadl, D., Kann, G., Wolf, T., Stephan, C., Schuettfort, G., Vasquez, M., Arcari, L., Zhou, H., Zainal, H., Gawor, M., Vidalakis, E., Kolentinis, M., Albrecht, M.H., Escher, F., Vogl, T.J. & Puntmann, V. 2021. Myocardial fibrosis and inflammation by CMR predict cardiovascular outcome in people living with HIV. *JACC: Cardiovascular Imaging*, 14(8): 1548-1557.

Deeks, S.G., Overbaugh, J., Phillips, A. & Buchbinder, S. 2015. HIV infection. *Nature Reviews Disease Primers*, 1(2015): 15035-15035.

Earls, J.P., Ho, V.B., Foo, T.K., Castillo, E. & Flamm, S. D. 2002. Cardiac MRI: recent progress and continued challenges. *Journal of Magnetic Resonance Imaging*, 16(2): 111-127.

Elsaka, O., Noureldean, M.A., Gamil, M.A., Ghazali, M.T. & Al-Razik, A.H. 2022. A Review on pericardial effusion. *Asian Journal of Advances in Research*, 12(1): 25-40.

Emrich, T., Halfmann, M., Schoept, J. & Kreitner, K. 2021. CMR for myocardial characterization in ischemic heart disease: state-of-the-art and future developments. *European Radiology Experimental*, 5(1): 14.

Fernandez-Jimenez, R., Barreiro-Perez, M., Martin-Garcia, A., Sanchez-Gonzalez, J., Agüero, J., Galan-Arriola, C., Garcia-Prieto, J., Diaz-Pelaez, E., Vara, P., Martinez, I., Zamarro, I., Garde, B., Sanz, J. & Fuster, V. 2017. Dynamic edematous response of the human heart to myocardial infarction. *Circulation*, 136(14): 1288-1300.

Ferreira, A.M., Costa, F., Tralhao, A., Marques, H., Cardim, N. & Andragao, P. 2014. MRI-conditional pacemakers: current perspectives. *Medical Devices: Evidence and Research*, 7(2014): 115-124.

Frangogiannis, N.G. 2019. Cardiac fibrosis: cell biological mechanisms, molecular pathways and therapeutic opportunities. *Molecular Aspects of Medicine*, 65(2): 70-99.

Fricke, A.C.V. & Iacobellis, G. 2019. Epicardial Adipose Tissue: clinical biomarker of cardio-metabolic risk. *International Journal of Molecular Science*, 20(23): 5989.

Gagliardi, M.G., Panebianco, M. & Formigari, R. 2021. 54 54.1. Available at: file:///C:/Users/01455852/OneDrive - University of Cape Town/CMR/Dissemination/Gagliardi2021_Chapter_HemodynamicsInPericardialAndMy.pdf%0D.

Geyer, H., Caracciolo, G., Abe, H., Wilansky, S., Carerj, S., Gentile, F., Nesser, H., Khandheria, B., Narula, J. & Sengupta, P.P. 2010. Assessment of myocardial mechanics using speckle tracking echocardiography: fundamentals and clinical applications. *Journal of the American Society of Echocardiography*, 23(4): 351-369.

Goebel, J., Seifert, I., Nensa, F., Schemuth, H.P., Maderwald, S., Quick, H.H., Schlosser, T., Jesnsen, C., Bruder, O. & Nassenstein, K. 2016. Can native T1 mapping differentiate between healthy and diffuse diseased myocardium in clinical routine cardiac MR imaging? *PLoS ONE*, 11(5): e0155591. Available at: <https://doi.org/10.1371/journal.pone.0155591>

Goudis, C.A., Vasileiadis, I.E. & Liu, T. 2018. Epicardial adipose tissue and atrial fibrillation: pathophysiological mechanisms, clinical implications, and potential therapies. *Current Medical Research and Opinion*, 34(11): 1933-1943.

Greenstein, A.S., Khavandi, K., Withers, S.B., Sonoyama, K., Clancy, O., Jeziorska, M., Laing, I., Yates, A.P., Pemberton, P.W., Malik, R.A. & Heagerty, A.M. 2009. Local inflammation and hypoxia abolish the protective anticontractile properties of perivascular fat in obese patients. *Circulation: American Heart Association*, 119(12): 1661-1670.

Guaraldi, G., Scaglioni, R., Zona, S., Orlando, G., Carli, F., Ligabue, G., Besutti, G., Bagni, P., Rossi, R., Modena, M. & Raggi, P. 2011. Epicardial adipose tissue is an independent marker of cardiovascular risk in HIV-infected patients. *AIDS*, 25(9): 1199-1205.

Guazzi, M. 2020. The alarming association between right ventricular dysfunction and outcome: Aetiology matters. *European Heart Journal*, 44(12): 1283-1285.

Haaf, P., Garg, P., Messroghli, D.R., Broadbent, D.A., Greenwood, J.P. & Plein, S. 2016. Cardiac T1 mapping and extracellular volume (ECV) in clinical practice: a comprehensive review. *Journal of Cardiovascular Magnetic Resonance*, 18(89): 1-12.

Hadigan, C., Meigs, J.B., Wilson, P.W.F., D'Agostino, R.B., Davis, B., Basgoz, N., Sax, P.E. & Grinspoon, S. 2003. Prediction of coronary heart disease risk in HIV-infected patients with fat redistribution. *Clinical Infectious Diseases*, 36(7): 909-916.

Hafez, M. S. & Missiri, A. M. E. L. 2021. Left atrial ejection force as a marker for the diagnosis of heart failure with preserved ejection fraction. *Journal of Cardiovascular Echography*, 31(3): 125-130.

Hassanabad, A.F., Zarzycki, A., Deniset, J.F. & Fedak, P.W.M. 2021. An overview of human pericardial space and pericardial fluid. *Cardiovascular Pathology*, 53(2021): 107346.

Hegazy, M.A., Mansour, K., Alzyat, A.M., Mohammad, M.A. & Hegazy, A.A. 2022. A systematic review on normal and abnormal anatomy of coronary arteries. *European Journal Anatomy*, 26(3): 355-368.

- Hemkens, L.G. & Bucher, H.C. 2014. HIV infection and cardiovascular disease. *European Heart Journal*, 35(21): 1373-1381.
- Higuchi, K., Akkaya, M., Akoum, N. & Marrouche, N.F. 2014. Cardiac MRI assessment of atrial fibrosis in atrial fibrillation: implications for diagnosis and therapy. *Heart*, 100(7): 590-596.
- Hoit, B.D. 2017. Anatomy and physiology of the pericardium. *Cardiology Clinics*, 35(4): 481-490.
- Holloway, C.J., Ntusi, N., Suttie, J., Mahmood, M., Wainwright, E., Clutton, G., Hancock, G., Beak, P., Tajar, A., Piechnik, S.K., Schneider, J.E., Angus, B., Clarke, K., Dorrell, L. & Neubauer, S. 2013. Comprehensive cardiac magnetic resonance imaging and spectroscopy reveal a high burden of myocardial disease in HIV patients. *Circulation*, 128(8): 814-822.
- Homsy, R., Meier-Schroers, M., Gieseke, J., Dabir, D., Luetkens, J.A., Kuetting, D.L., Naehle, C.P., Marx, C., Schild, H.H., Thomas, D.K. & Sprinkart, A.M. 2016. 3D-Dixon MRI based volumetry of peri- and epicardial fat. *The International Journal of Cardiovascular Imaging*, 32(9): 291-299.
- Hsue, P.Y. & Waters, D.D. 2017. Heart failure in persons living with HIV infection. *Current Opinion in HIV and AIDS*, 12(6): 534-539.
- Hutchison, S.J. 2009. Pericardial disease: clinical diagnostic imaging atlas. Philadelphia: Elsevier Health Sciences.
- Iaizzo, P.A. 2015. Handbook of cardiac anatomy, physiology, and devices. 3rd ed. Minneapolis: Springer, 1-33.
- Ishida, M., Kato, S. & Sakuma, H. 2009. Cardiac MRI in ischemic heart disease. *Circulation Journal*, 73(9): 1577-1588.
- Jennings, L., Robbins, R., Nguyen, N., Ferraris, C., Leu, C., Dolezal, C., Hsiao, N., Mgbako, O., Joska, J., Castillo-Mancilla, J., Myer, L., Anderson, P.L., Remien, R.H. & Orrell, C. 2022. Tenofovir diphosphate in dried blood spots predicts future viremia in persons with HIV taking antiretroviral therapy in South Africa. *AIDS*, 36(7): 933-940.

Karamitsos, T.D., Arvanitaki, A., Karvounis, H., Neubeauer, S. & Ferreira, V.M. 2020. Myocardial tissue characterization and fibrosis by imaging. *Journal of the American College of Cardiology: Cardiovascular Imaging*, 13(5): 1221-1234.

Kitterer, D., Latus, J., Henes, J., Birkmeier, S., Backes, M., Braun, N., Sechtem, U., Alscher, M.D., Mahrholdt, H. & Greulich, S. 2015. Impact of long-term steroid therapy on epicardial and pericardial fat deposition: a cardiac MRI study. *Cardiovascular Diabetology*, 14(130): 1-11.

Kong, P., Christia, P. & Frangogiannis, N.G. 2014. The pathogenesis of cardiac fibrosis. *Cellular and Molecular Life Sciences*, 71(5): 549-574.

Kramer, C.M., Barkhausen, J., Flamm, S. D., Kim, R.J., & Nagel, E., Society for Cardiovascular Magnetic Resonance. & Board of Trustees Task Force on Standardized Protocol. 2013. Standardized cardiovascular magnetic resonance (CMR) protocols 2013 update. *Journal of Cardiovascular Magnetic Resonance*, 15:91.

Available at: <https://doi.org/10.1186/1532-429X-15-91>

Krishnamurthy, R., Cheong, B. & Muthupillai, R. 2014. Tools for cardiovascular magnetic resonance imaging. *Cardiovascular Diagnosis Therapy*, 4(2): 104-125.

Kristoffersen, U.S., Lebech, A., Wiinberg, N., Petersen, C.L., Hasbak, P., Gutte, H., Jensen, G.B., Hag, A.M.F., Ripa, R.S. & Kjaer, A. 2013. Silent ischemic heart disease and pericardial fat volume in HIV-infected patients: a case-control myocardial perfusion scintigraphy study. *PLoS ONE*, 8(8): e72066.

Kroll, L., Nassenstein, K., Jochims, M., Koitka, S. & Nensa, F. 2021. Assessing the role of pericardial fat as a biomarker connected to coronary calcification- a deep learning based approach using fully automated body composition analysis. *Journal of Clinical Medicine*, 10(2): 356.

Lee, J.J., Liu, S., Nacif, M.S., Ugander, M., Han, J., Kawel, N., Sibley, C.T., Kellman, P., Arai, A.E. & Bluemke, D.A. 2011. Myocardial T1 and extracellular volume fraction mapping at 3 Tesla. *Journal of Cardiovascular Magnetic Resonance*, 13(75): 1-10.

- Leo, L.A., Paiocchi, V.L., Schlossbauer, S.A., Ho, S.Y. & Faletra, F.F. 2019. The intrusive nature of epicardial adipose tissue as revealed by cardiac magnetic resonance. *Journal of Cardiovascular Echography*, 29(2): 45-51.
- Lewis, A.J.M., Burrage, M.K. & Ferreira, V.M. 2020. Cardiovascular magnetic resonance imaging for inflammatory heart diseases. *Cardiovascular Diagnosis and Therapy*. 10(3): 598-609.
- Lintingre, P., Nivet, H., Clement-Guinaudeau, S., Camaioni, C., Sridi, S., Corneloup, O., Gerbaud, E., Coste, P., Dournes, G., Latrabe, V., Laurent, F., Montaudon, M. & Cochet, H. 2020. High-resolution late gadolinium enhancement magnetic resonance for the diagnosis of myocardial infarction with nonobstructed coronary arteries. *Journal of the American College of Cardiology: Cardiovascular Imaging*, 13(5): 1135-1148.
- Li, X., Lai, L., Luo, R., Yang, H., Ma, H., Yang, Z., Zhao, S., Su, W. & Hua, W. 2021. The clinical prognosis of presence and location of late gadolinium enhancement by cardiac magnetic resonance imaging in patients with hypertrophic cardiomyopathy: a single-center cohort study. *Journal of Cardiovascular Translational Research*, 14(5): 1001-1016.
- Lim, C., Blaszczyk, E., Riazzy, L., Wiesemann, S., Schuler, J., von Knobelsdorff, F. & Schulz-Menger, J. 2021. Quantification of myocardial strain assessed by cardiovascular magnetic resonance feature tracking in healthy subjects-influence of segmentation and analysis software. *European Radiology*, 31(16): 3962-3972.
- Liu, M., López de Juan Abad, B. & Cheng, K. 2021. Cardiac fibrosis: myofibroblast-mediated pathological regulation and drug delivery strategies. *Advanced Drug Delivery Reviews*, 173: 504-519.
- Lo, J., Abbara, S., Rocha-Filho, J.A., Shturman, L., Wei, J. & Grinspoon, S.K. 2010. Increased epicardial adipose tissue volume in HIV-infected men and relationships to body composition and metabolic parameters. *AIDS*, 24(13): 2127-2130.
- Longenecker, C.T., Margevicius, S., Liu, Y., Yun, C., Bezerra, H.G. & McComsey, G.A. 2017. Effect of pericardial fat volume and density on markers of insulin resistance and inflammation in

patients with human immunodeficiency virus infection. *American Journal of Cardiology*, 120(8): 1427-1433.

Lu, Z., Jiang, Z., Tang, J., Lin, C. & Zhang, H. 2022. Functions and origins of cardiac fat. *Federation of European Biochemical Societies Journal*, 16388. Available at: <https://doi.org/10.1111/febs.16388>

Luetkens, J.A., Doerner, J., Schwarze-Zander, C., Wasmuth, J., Boesecke, C., Sprinkart, A.M., Schmeel, F.C., Homsy, R., Gieseke, J., Schild, H.H., Rockstroh, J.K. & Naehle, C.P. 2016. Cardiac magnetic resonance reveals signs of subclinical myocardial inflammation in asymptomatic HIV-infected patients. *Circulation: Cardiovascular Imaging*, 9(3): e004091.

Ma, Z.G., Yuan, Y., Wu, H., Zhang, X. & Tang, Q. 2018. Cardiac fibrosis: new insights into the pathogenesis. *International Journal of Biological Sciences*, 14(12): 1645-1657.

Mahrholdt, H., Klem, I. & Sechtem, U. 2007. Cardiovascular MRI for detection of myocardial viability and ischaemia. *Heart*, 93(1): 122-129.

Mandoli, G.E., D'Ascenzi, F., Vinco, G., Benfari, G., Ricci, F., Focardi, M., Cavigli, L., Pastore, M.C., Sisti, N., Vivo, O D., Santoro, C., Mondillo, S. & Cameli, M. 2021. Novel approaches in cardiac imaging for non-invasive assessment of left heart myocardial fibrosis. *Frontiers in Cardiovascular Medicine*, 8(614235); 1-15.

Manga, P. 2017. HIV and ischemic heart disease. *Journal of the American College of Cardiology*, 69(1): 73-82.

Manga, P., McCutcheon, K., Tsabedze, N., Vachiat, A. & Zachariah, D. 2017. HIV and nonischemic heart disease. *Journal of the American College of Cardiology*, 69(1): 83-91.

Mangion, K., Burke, N.M.M., McComb, C., Carrick, D., Woodward, R. & Berry, C. 2019. Feature-tracking myocardial strain in healthy adults- a magnetic resonance study at 3.0 Tesla. *Scientific Reports*, 9(1): 3239.

Margolis, A.M., Heverling, H., Pham, P.A. & Stolbach, A. 2014. A Review of the toxicity of HIV Medications. *Journal of Medical Toxicology*, 10(1): 26-39.

Marra, M.P., Lima, A.C. & Iliceto, S. 2011. MRI in acute myocardial infarction. *European Heart Journal*, 32(3): 284-293.

Martini, F., Timmons, M. J., Tallitsch, R.B., Ober, W.C., Garrison, C.W., Welch, K.B. & Hutchings, R.T. 2015. *Human anatomy*. Italy: Prentice Hall. 545-554.

Matloch, Z., Kotulák, T. & Haluzík, M. 2016. The Role of epicardial adipose tissue in heart disease. *Physiological Research*, 65(1): 23-32.

Mazurek, T., Kobylecka, M., Zielenkiewicz, M., Kurek, A., Kochman, J., Filipiak, K.J., Mazurek, K., Huczek, Z., Krolicki, L. & Opolski, G. 2017. PET/CT evaluation of 18F-FDG uptake in pericoronary adipose tissue in patients with stable coronary artery disease: independent predictor of atherosclerotic lesions' formation? *Journal of Nuclear Cardiology*, 24(3): 1075-1084.

Menacho, K., Seraphim, A., Ramirez, S., Falcon, L., Bhuvu, A., Alave, J., Banda, C., Mejia, F., Salazar, D., Putri, A., Mosto, F., Gonzales, P., Culotta, V., Herrey, A.S., Ntusi, N.A.B., Walker, J.M. & Moon, J.C. 2020. Myocardial inflammation and edema in people living with human immunodeficiency virus. *Journal of the American College of Cardiology: Cardiovascular Imaging*, 13(5): 1278-1280.

Mondy, V.C., Peter, S.B. & Ravi, R. 2021. Native T1 mapping in diffuse myocardial diseases using 3 - Tesla MRI: an institutional experience. *Indian Journal of Radiology and Imaging*, 30(4): 465-472.

Murphy, S.P., Kakkar, R., McCarthy, C.P. & Januzzi, J.L. 2020. Inflammation in heart failure: JACC State-of-the-Art Review. *Journal of the American College of Cardiology*, 75(11): 1324-1340.

Myerson, S.G., Francis. M. J. & Neubauer, S. 2010. *Oxford specialist handbook in cardiology: cardiovascular magnetic resonance*. 1st ed. Oxford: Oxford University Press.

Nacheha, J.B., Hislop, M., Dowdy, D.W., Chaisson, R.E., Regensberg, L. & Maartens, G. 2007. Adherence to nonnucleoside reverse transcriptase inhibitor-based HIV therapy and virologic outcomes. *Annals of Internal Medicine*, 146(8): 564-573.

Nelson, A.J., Worthley, M., Psaltis, P.J., Carbone, A., Dundon, B.K., Duncan, R.F., Piantadosi, C., Lau, D.H., Sanders, P., Wittert, G.A & Wortley, S.G. 2009. Validation of cardiovascular magnetic resonance assessment of pericardial adipose tissue volume. *Journal of Cardiovascular Magnetic Resonance*, 11(15). Available at: <https://doi.org/10.1186/1532-429X-11-15>

Nelson, M.D., Szczepaniak, L.S., LaBounty, T.M., Szczepaniak, E., Li, D., Tighiouart, M., Li, Q., Dharmakumar, R., Sannes, G., Fan, Z., Yumul, R., Hardy, W.D. & Conte, A.H. 2014. Cardiac steatosis and left ventricular dysfunction in HIV-infected patients treated with highly active antiretroviral therapy. *Journal of the American College of Cardiology: Cardiovascular Imaging*, 7(11): 1175-1177.

Nix, L. 2015. Metabolic syndrome, diabetes, and cardiovascular risk in HIV. *National Institutes of Health*, 11(3): 271-278.

Ntusi, N.A.B. 2017. HIV and myocarditis. *Current Opinion in HIV and AIDS*, 12(6): 561-565.

Ntusi, N.A.B. & Ntsekhe, M. 2016. Human immunodeficiency virus-associated heart failure in sub-Saharan Africa: evolution in the epidemiology, pathophysiology, and clinical manifestations in the antiretroviral era. *European Society of Cardiology Heart Failure*, 3(3): 158-167.

Ntusi, N., O'Dwyer, E., Dorrell, L., Wainwright, E., Piechnik, S., Clutton, G., Hancock, G., Ferreira, V., Cox, P., Badri, M., Karamitso, T., Emmanuel, S., Clarke, K., Neubauer, S. & Holloway, T. 2016. HIV-1-related cardiovascular disease is associated with chronic inflammation, frequent pericardial effusions, and probable myocardial edema. *Circulation: Cardiovascular Imaging*, 9(3): e004430. Available at: <https://doi.org/10.1161/CIRCIMAGING.115.004430>

Ntusi, N.A.B., Piechnik, S.K., Francis, J.M., Ferreira, V.M., Rai, A.B.S., Matthews, P.M., Robson, M.D., Moon, J., Wordsworth, P.B., Neubauer, S. & Karamitsos, T. D. 2014. Subclinical myocardial inflammation and diffuse fibrosis are common in systemic sclerosis - a clinical study using

myocardial T1-mapping and extracellular volume quantification. *Journal of Cardiovascular Magnetic Resonance*, 16(21). Available at: <https://doi.org/10.1186/1532-429X-16-21>

Osuji, F.N., Onyenekwe, C.C., Ahaneku, J.E. & Ukibe, N.R. 2018. The effects of highly active antiretroviral therapy on the serum levels of pro-inflammatory and anti-inflammatory cytokines in HIV infected subjects. *Journal of Biomedical Science*, 25(88). Available at: <https://doi.org/10.1186/s12929-018-0490-9>

Özer, T., Mehmet, A. & Kirali, K. 2020. Inflammatory pericardial effusion. *Thoracic surgery*. Switzerland: Springer, 645-653. [online]. Available at: <https://doi.org/10.1007/978-3-030-40679-0> [Accessed 5 July 2022].

Patel, V.B., Shah, S., Verma, S. & Oudit, G.Y. 2017. Epicardial adipose tissue as a metabolic **transducer**: role in heart failure and coronary artery disease. *Heart Failure Reviews*, 22(6): 889-902.

Pejković, M., Stojić, V. & Popovska-Jovičić, B. 2019. Risk assessment for the development of metabolic syndrome in patients with AIDS, after the first year of antiretroviral therapy. *Medicinski podmladak*, 70(1): 48-52.

Petersen, S.E., Aung, N., Sanghvi, M.M., Zemrak, F., Fung, K., Paiva, J.M., Francis, J.M., Khanji, M.Y., Lukaschuk, E., Lee, A.M., Carapella, V., Kim, Y.J., Leeson, P., Piechnik, S.K. & Neubauer, S. 2017. Reference ranges for cardiac structure and function using cardiovascular magnetic resonance (CMR) in caucasians from the UK Biobank population cohort. *Journal of Cardiovascular Magnetic Resonance*, 19(1). Available at: <https://doi.org/10.1186/s12968-017-0327-9>

Philip, C., Seifried, R., Peterson, P.G., Liotta, K. & Steel, K. 2021. Cardiac MRI for patients with increased cardiometabolic risk. *Radiology: Cardiothoracic Imaging*, 3(2): e200575. Available at: <https://doi.org/10.1148/ryct.2021200575>

Pinto, A.R., Llinikh, A., Ivey, M.J., Kuwabara, J.T., D'Antoni, M., Debuque, R., Chandran, A., Wang, L., Arora, K., Rosenthal, N.A. & Tallquist, M.D. 2016. Revisiting cardiac cellular composition. *Circulation Research*, 118(3): 400-409.

Radenkovic, D., Weingartner, S., Ricketts, L., Moon, J.C. & Captur, G. 2017. T1 mapping in cardiac MRI. *Heart Failure Reviews*, 22(4): 415-430.

Rajiah, P., Canan, A., Saboo, S.S., Restrepo, C.S. & Bolen, M.A. 2019. MRI of the pericardium. *Radiographics*, 39(7): 1921-1922.

Rider, O.J., Asaad, M., Ntusi, N., Wainwright, E., Clutton, G., Hancock, G., Banerjee, R., Pitcher, A., Samaras, K., Clarke, K., Neubauer, S., Dorrell, L. & Holloway, C.J. 2014. HIV is an independent predictor of aortic stiffness. *Journal of Cardiovascular Magnetic Resonance*, 16(57). Available at: <https://doi.org/10.1186/s12968-014-0057-1>

Ridgway, J.P. 2010. Cardiovascular magnetic resonance physics for clinicians: part 1. *Journal of Cardiovascular Magnetic Resonance*, 12(71). Available at: <https://doi.org/10.1186/1532-429X-12-71>

Ripley, D.P., Musa, T.A., Dobson, L.E., Plein, S. & Greenwood, J.P. 2016. Cardiovascular magnetic resonance imaging: what the general cardiologist should know. *Heart*, 102(19): 1589-1603.

Risher, K.A., Cori, A., Reniers, G., Marston, M., Calvet, C., Crampin, A., Dadirai, T., Dube, A., Gregson, S., Herbst, K., Lutalo, T., Moorhouse, L., Mtenga, B., Nabukalu, D., Newton, R., Price, A.J., Tlhajoane, M., Todd, J., Tomlin, K., Urassa, M., Vandormael, A., Fraser, C., Slaymaker, E. & Eaton, J.W. 2021. Age patterns of HIV incidence in eastern and southern Africa: a modelling analysis of observational population-based cohort studies. *The Lancet HIV*, 8(7): e429-e439. Available at: [https://doi.org/10.1016/S2352-3018\(21\)00069-2](https://doi.org/10.1016/S2352-3018(21)00069-2)

Rodrigues, R.C., Azevedo, K.M.L., Moscavitch, S.D., Setubal, S. & Mesquita, C.T. 2019. The use of two-dimensional strain measured by speckle tracking in the identification of incipient ventricular dysfunction in HIV-infected patients on antiretroviral therapy, untreated HIV patients and healthy controls. *Arquivos Brasileiros de Cardiologia*, 113(4): 737-745.

Rodriguez, E.R. & Tan, C.D. 2017. Structure and anatomy of the human pericardium. *Progress in Cardiovascular Diseases*, 59(4): 327-340.

Rosito, G.A., Massaro, J.M., Hoffmann, U., Ruberg, F.L., Mahabadi, A.A., Vasan, R.S., O'Donnell, C.J. & Fox, C.S. 2008. Pericardial fat, visceral abdominal fat, cardiovascular disease risk factors, and vascular calcification in a community-based sample the Framingham heart study. *Circulation*, 117(5): 605-613.

Russo, V., Lovato, L. & Ligabue, G. 2020. Cardiac MRI: technical basis. *Radiologia Medica*, 125(11): 1040-1055.

Rutka, K., Garkowski, A., Karaszewska, K. & Lebkowska, U. 2021. Imaging in diagnosis of systemic sclerosis. *Journal of Clinical Medicine*, 10(2): 248.

Sacks, H.S. & Fain, J.N. 2007. Human epicardial adipose tissue : a review. *American Heart Journal*, 153(6): 907-917.

Salerno, M., Sharif, B., Arheden, H., Kumar, A., Axel, L., Li, D. & Neubauer, S. 2017. Recent advances in cardiovascular magnetic resonance: techniques and applications. *Circulation: Cardiovascular imaging*, 10(6): e003951. Available at: <https://doi.org/10.1161/CIRCIMAGING.116.003951>

Saremi, F., Grizzard, J.D. & Kim, R.J. 2008. Optimizing cardiac MR imaging: practical remedies for artefacts. *Radiographics*, 28(40): 1161-1187.

Schiattarella, G.G., Sequeira, V. & Ameri, P. 2020. Distinctive patterns of inflammation across the heart failure syndrome. *Heart Failure Reviews*, 26(3): 133-1344.

Scholtz, M.E.L. 2019. Cardiovascular Magnetic Resonance in patients with HIV Infection: assessing the structural and functional abnormalities associated with remodelling of the myocardium. [online]. Thesis (PhD) University of Pretoria. Available at: <https://repository.up.ac.za/handle/2263/72681> [Accessed 30 September 2022].

Selthofer-Relatić, K. & Bošnjak, I. 2015. Myocardial fat as a part of cardiac visceral adipose tissue: physiological and pathophysiological view. *Journal of Endocrinological Investigation*, 38(9): 933-939.

Simon, M.A., Lacomis, C.D., George, M.P., Kessinger, C., Weinman, R., McMahon, D., Gladwin, M.T., Champion, H.C. & Morris, A. 2014. Isolated right ventricular dysfunction in patients with human immunodeficiency virus. *Journal of Cardiac Failure*, 20(6): 414-421.

Singh, R., Chakraborty, M., Gautam, A., Roy, S.K., Halder, I., Barber, J. & Garg, A. 2021. Residual immune activation in HIV-Infected individuals expands monocytic-myeloid derived suppressor cells. *Cellular Immunology*, 362(10): 104304.

So-Armah, K. & Freiberg, M.S. 2018. HIV and cardiovascular disease: update on clinical events, special populations , and novel biomarkers. *Current HIV/AIDS Report*, 15(3): 233-244.

Song, G., Qiao, W., Sun, L. & Yu, X. 2020. A Meta-Analysis of different types of cardiac adipose tissue in HIV patients. *BioMed Research International*, 8234618: 1-8.

Sood, V., Stephen, J., Saad, H., Samuels, P., Moosa, S. & Ntusi, N. 2017. Review of cardiovascular magnetic resonance in human immunodeficiency virus-associated cardiovascular disease. *South African Journal of Radiology*, 21(2): 1-10.

STATS SA (Statistic South Africa). 2019. *Statistical Release P0302*: mid-year population estimates. [online]. Available at: www.statssa.gov.za,info@statssa.gov.za. [Accessed 30 March 2020].

Staunton, C., Adams, R., Anderson, D., Croxton, T., Kamuya, D., Munene, M. & Swanepoel, C. 2020. Protection of Personal Information Act 2013 and data protection for health research in South Africa. *International Data Privacy Law*, 10(2): 160-179.

Steckman, D.A., Schneider, P.M., Schuller, J.L., Aleong, R.G., Nguyen, D.T., Sinagra, G., Vitrella, G., Brun, F., Cova, M.A., Pagnan, L., Mestroni, L., Varosy, P.D. & Sauer, W.H. 2012. Utility of cardiac magnetic resonance imaging to differentiate cardiac sarcoidosis from arrhythmogenic right ventricular cardiomyopathy. *American Journal of Cardiology*, 110(4): 575-579.

Subramanian, S., Tawakol, A., Burdo, T.H., Abbara, S., Wei, J., Vijayakumar, J., Corsini, E., Abdelbaky, A., Zanni, M.V., Hoffmann, U., Williams, K.C., Lo, J. & Grinspoon, S.K. 2012.

Arterial inflammation in patients with HIV. *Journal of American Medical Association*, 308(4): 379-386.

Suliman, A. 2011. The state of heart disease in Sudan. *Cardiovascular Journal of Africa*, 22(4): 191-196.

Suthahar, N., Meijers, W.C., Sillje, H.H.W. & de Boer, R.A. 2017. From inflammation to fibrosis - molecular and cellular mechanisms of myocardial tissue remodelling and perspectives on differential treatment opportunities. *Current Heart Failure Reports*, 14(4): 235-250

Taylor, A.J., Salerno, M., Dharmakumar, R., & Jerosch-Herold. 2016. T1 mapping basic techniques and clinical applications. *Journal of the American College of Cardiology: Cardiovascular Imaging*, 9(1): 67-81.

Thanassoulis, G., Massaro, J.M., O'Donnell, C.J., Hoffmann, U., Levy, D., Ellinor, P.T., Wang, T.J., Schnabel, R.B. & Vasan, R.S. 2010. Pericardial fat is associated with prevalent atrial fibrillation. *Circulation Arrhythmia Electrophysiology*, 3(4): 345-350.

Thiara, D.K., Liu, C.Y., Raman, F., Mangat, S., Purdy, J.B., Duarte, H.A., Schmidt, N., Hur, J., Sibley, C.T., Bluemke, D.A. & Hadigan, C. 2015. Abnormal myocardial function is related to myocardial steatosis and diffuse myocardial fibrosis in HIV-infected adults. *Journal of Infectious Diseases*, 212(10): 1544-1551.

Thomas, T.P. & Grisanti, L.A. 2020. The dynamic interplay between cardiac inflammation and fibrosis. *Frontiers in Physiology*, 11(529075).

Available at: <https://doi.org/10.3389/fphys.2020.529075>

Tikhomirov, R., Reilly-O'Donnell, B., Catapano, F., Faggian, G., Grelik, J., Martelli, F. & Emanueli, C. 2020. Exosomes: from potential culprits to new therapeutic promise in the setting of cardiac fibrosis. *Cell*, 9(3): e721.

Tsabedze, N., Vachiat, A., Zachariah, D. & Manga, P. 2018. A new face of cardiac emergencies: human immunodeficiency virus-related cardiac disease. *Cardiology Clinics*, 36(1): 161-170.

UNAIDS (United Nations Programme on HIV/AIDS). 2021. Confronting inequalities lessons for pandemic responses from 40 years of AIDS.

Available at: https://www.unaids.org/sites/default/files/media_asset/2021-global-aids-update_en.pdf [Accessed 22 January 2022].

Urban, C.F., Lourido, S. & Zychlinsky, A. 2006. How do microbes evade neutrophil killing? *Cellular Microbiology*, 8(14): 1687-1696.

Uthman, O.A., Nduka, C., Watson, S.I., Mills, E.J., Kengne, A.P., Jaffar, S.S., Clarke, A., Moradi, T., Ekström, A.M. & Lilford, R. 2018. Statin use and all-cause mortality in people living with HIV: a systematic review and meta-analysis. *BMC infectious diseases*, 18(258). Available at: <https://doi.org/10.1186/s12879-018-3162-1>

van der Graaf, A.W.M., Bhagirath, P., Ghoerbien, S. & Gotte, M.J.W. 2014. Cardiac magnetic resonance imaging: artefacts for clinicians. *Netherlands Heart Journal*, 22(10): 542-549.

van Schalkwyk, C., Dorrington, R.E., Seathodi, T., Velasquez, C., Feizzadeh, A. & Johnson, L.F. 2021. Modelling of HIV prevention and treatment progress in five South African metropolitan districts. *Scientific Reports*, 11(1): 5652.

Vermes, E., Pantaléon, C., Auvet, A., Cazeneuve, N., Machet, M. C., Delhommiais, A., Bourguignon, T., Aupart, M. & Brunereau, L. 2018. Cardiovascular magnetic resonance in heart transplant patients: diagnostic value of quantitative tissue markers: T2 mapping and extracellular volume fraction, for acute rejection diagnosis. *Journal of Cardiovascular Magnetic Resonance*, 20(1):59.

Volberding, P.G.W.L., Joep, M.A.G. & Joel, E.S.N. 2013. *Sande's HIV/AIDS Medicine: Medical Management of AIDS 2012*. 2nd ed. San Francisco: Elsevier, 1-57.

von Knobelsdorff-Brenkenhoff, F. & Schulz-Menger, J. 2016. Role of cardiovascular magnetic resonance in the guidelines of the European Society of Cardiology. *Journal of Cardiovascular Magnetic Resonance*, 18(6): 1-18.

Weber, K.T., Sun, Y., Bhattacharya, S.K., Ahokas, R.A. & Gerling, I.C. 2013. Myofibroblast-mediated mechanisms of pathological remodelling of the heart. *Nature Reviews Cardiology*, 10(1): 15-26.

Whittaker, R., Case, K.K., Nilsen, O., Blystad, H., Cowan, S., Klovstad, H. & Van Sighem, A. 2020. Monitoring progress towards the first UNAIDS 90-90-90 target in key populations living with HIV in Norway. *BMC Infectious Diseases*, 20(451). Available at: <https://doi.org/10.1186/s12879-020-05178-1>.

WHO (World Health Organization). 2021. Service delivery for the treatment and care of people living with HIV. [online]. Available at: <https://www.who.int/publications/i/item/9789240023581> [Accessed 23 February 2022].

WMA (World Medical Association). 2013. Declaration of Helsinki Ethical Principles for Medical Research Involving Human Subjects. [online]. Available at: <https://www.uni-goettingen.de/de/document/download/a91ef4324cf47306d6dbf334687e70dc.pdf/helsinki.pdf> [Accessed 3 March 2022].

Wong, C.X., Ganesan, A.N. & Selvanayagam, J.B. 2017. Epicardial fat and atrial fibrillation: current evidence, potential mechanisms, clinical implications, and future directions. *European Heart Journal*, 38(17): 1294-1302.

Yang, M., He, Y., Ma, M., Zhao, Q., Xu, H., Xia, C., Peng, W., Li, Z., Li, h., Guo, Y. & Yang, Z. 2021. Characterization of infarcted myocardium by T1-mapping and its association with left ventricular remodeling. *European Journal of Radiology*, 137:109590. Available at: <https://doi.org/10.1016/j.ejrad.2021.109590>

Yu, Q., Pang, B., Liu, R., Rao, W., Zhang, S. & Yu, Y. 2017. Appropriate body mass index and waist-hip ratio cutoff points for overweight and obesity in adults of Northeast China. *Iranian Journal of Public Health*, 46(8):1038-1045.

Zhu, Y., Yang, D., Zou, L., Chen, Y., Liu, X. & Chung, Y. 2019. T2STIR preparation for single-shot cardiovascular magnetic resonance myocardial edema imaging. *Journal of Cardiovascular Magnetic Resonance*, 21(72). Available at: <https://doi.org/10.1186/s12968-019-0583-y>

APPENDICES

APPENDIX 1: MRI SAFETY SCREENING FORM

Cape Universities Body Imaging Centre (CUBIC)

University of Cape Town

MRI Participant Screening Form

Study:	_____		
Participant Code:	_____		
Date Of Birth:	_____	Weight:	_____
		Height:	_____

The following information is very important to ensure your safety and to prevent any interference during the MR procedure.

Please answer the following questions (mark with a X):

		Yes	No	Don't Know
1.	Do you have a cardiac pacemaker/defibrillator?			
2.	Do you have a neuro-stimulator?			
3.	Do you have a cochlea implant/surgery to your ears? (If yes, please specify)			
4.	Have you ever had heart surgery such as a valve replacement? (If yes, please specify)			
5.	Have you ever had any type of electronic, mechanical, or magnetic implant? (If yes, please specify)			
6.	Do you have any foreign body in your eyes or body? (Bullet fragments etc..)			
7.	Do you have a vena cava filter?			
8.	Do you have a prosthetic limb, eye or other artificial device not already mentioned? (If yes, please specify)			
9.	Are you pregnant or breast feeding?			
10.	Are you claustrophobic?			
11.	Do you have aneurism clips?			
12.	Do you have renal impairment?			
13.	Do you have asthma?			
14.	Do you have allergies? (If yes, please specify)			
15.	Do you have any other implants? (e.g. screws, plates, joint replacements)			
18.	Other			

I hereby acknowledge that the potential risks of the examination have been explained to me and that during the course of the investigation it may for the intravenous injection of a contrast agent.

Attention: It is the policy of this institution not to discuss results of the MR Investigation with the patients for ethical reasons. All enquiries in this regard should be directed to the referring physician.

Participant Signature: _____

Date: _____

Consented by: _____

Please remove all loose metallic objects, including metallic body piercings, hearing aids and dentures.

APPENDIX 2: CMR SCANNING PROTOCOL

Sequences	Views	Role in assessment
Localizers: body	<ul style="list-style-type: none"> ● Axial view ● Coronal view ● Sagittal view 	To determine whether patient position is correct in the scanner. And allow general survey of the chest.
Half Fourier acquired single-shot turbo spin-echo (HASTE):	<ul style="list-style-type: none"> ● Axial view ● Coronal-view 	<p>Allows the assessment of thoracic pathology, pericardium and general anatomical survey and relationship of vessels and cardiac chambers.</p> <p>Axial: Coverage from neck vessels to the inferior border of the right ventricle.</p> <p>Coronal: coverage from posterior border of the descending aorta to the anterior border of the right ventricle</p>
Pilot cine imaging:	<ul style="list-style-type: none"> ● Horizontal long axis (HLA) 4-chamber view ● Vertical long axis (VLA) 2-chamber view ● Short axis (SA) 	Positioning according to the heart axis.
Trufi-scout	<ul style="list-style-type: none"> ● HLA view 	Delta-frequency (off-resonance effect in bSSFP)
Cine imaging:	<ul style="list-style-type: none"> ● HLA view ● VLA view ● Left ventricular outflow track (LVOT) view ● Paracoronal LVOT view ● Right ventricle (RV) - 2 chamber view ● Right ventricular outflow tract (RVOT) view ● Paracoronal RVOT view ● SA stack 	<p>Ventricular and atrial function</p> <p>Size</p> <p>Regional wall motion.</p> <p>Valves</p> <p>Myocardial invasion</p>
T1-weighted	<ul style="list-style-type: none"> ● Basal slice ● Mid-ventricular slice ● Apical slice 	<p>Inflammation</p> <p>Diffuse fibrosis</p> <p>Infiltration</p> <p>Pericardial morphology</p>
T2- weighted-STIR	<ul style="list-style-type: none"> ● Basal slice ● Mid-ventricular slice ● Apical slice 	Acute inflammation
T1 mapping	<ul style="list-style-type: none"> ● Basal slice ● Mid-ventricular slice ● Apical slice 	<p>Inflammation</p> <p>Diffuse fibrosis</p> <p>Infiltration</p> <p>Pericardial morphology</p>
T2 mapping	<ul style="list-style-type: none"> ● Basal slice ● Mid-ventricular slice ● Apical slice 	<p>edema</p> <p>Infiltration</p> <p>Fibrosis</p> <p>Inflammation</p>
Cine tagging	<ul style="list-style-type: none"> ● Basal slice ● Mid-ventricular slice ● Apical slice 	<p>Diastolic function</p> <p>Deformation (strain)</p> <p>Extent of fibrocalcific process</p>
Administration of gadolinium-DTPA contrast		
Early Gad - 90 seconds (s) – 2 minutes (min)	<ul style="list-style-type: none"> ● Basal slice ● Mid-ventricular slice ● Apical slice 	Early GAD uptake by myocardium
Inversion time mapping (TI) scout (5-6 minutes after giving Gad)	<ul style="list-style-type: none"> ● Mid-ventricular slice 	Optimal image contrast (best suppression of the normal myocardium)
LGE (washout kinetics from myocardial circulation) 5 - 20 minutes	<ul style="list-style-type: none"> ● SA stack ● HLA view ● LVOT view ● VLA view 	<p>Myocardial viability</p> <p>Scar detection</p> <p>Inflammation</p> <p>Fibrosis</p>
T1 mapping (post Gad)	<ul style="list-style-type: none"> ● Basal slice ● Mid-ventricular slice ● Apical slice 	Pericardial layer and fluid characterization
Through-plane flow through:	<ul style="list-style-type: none"> ● Pulmonary valve (PV) view ● Aortic valve (AV) view 	CV haemodynamics

APPENDIX 3: CMR SEQUENCES AND PARAMETERS USED TO SCAN PARTICIPANTS

CMR sequences	Parameters										
	TR (ms)	TE (ms)	Flip angle (deg)	FOV read (mm)	FOV phase (%)	Base resolution (%)	Phase resolution (%)	PAT mode	Voxel size (mm)	Sequence type	Bandwidth (Hz/Px)
Haste_tra_db_2bh_iPAT	989.0	49	160	340	75.0%	256	56	GRAPPA	1.3x1.3x8.0	GRE	651
Haste_cor_db_2bh_iPAT	872.0	49	160	360	100 %	256	56	GRAPPA	1.4x1.4x8.0		514
Loc_chambers_iPAT	992.80	1.26	10	360	91.7	192	75	GRAPPA	1.9x1.9x8.0	GRE	651
Trufi_freq-Scout	377.73	1.45	50	340	89.8	256	76	GRAPPA	1.3x1.3x6.0	Trufi	751
Cine_4-chamber_retro	45.00	1.67	40	360	83.7	208	80	GRAPPA	1.7x1.7x6.0	Trufi	962
Cine_2-chamber_retro	37.9	1.38	35	380	83.7	208	80	GRAPPA	1.8x1.8x6.0	Trufi	962
Cine_LVOT_retro	45	1.67	45	360	83.7	208	80	GRAPPA	1.7x1.7x6.0	Trufi	962
Cine_cor_LVOT_retro	45	1.67	45	360	89.4	208	80	GRAPPA	1.7x1.7x6.0	Trufi	962
Cine_RVOT_retro	45	1.67	45	360	83.7	208	80	GRAPPA	1.7x1.7x6.0	Trufi	962
Cine_cor_RVOT_retro	45	1.67	45	360	83.7	208	80	GRAPPA	1.7x1.7x6.0	Trufi	962
Cine_RV_2chamber_retro	45	1.67	45	360	84.9	208	80	GRAPPA	1.7x1.7x6.0	Trufi	962
Cine_RV_3chamber_retro	45	1.67	45	360	89.4	208	80	GRAPPA	1.7x1.7x6.0	Trufi	962
Cine_retro_SAX1(8-12 slices)	44.88	1.67	44	360	89.4	208	80	GRAPPA	1.7x1.7x8.0	Trufi	962
9_db_t1_SA_(B, M,A)	750.0	11.0	180	340	81.3	256	100	GRAPPA	1.3x1.3x5.0	TSE	849
9_db_t2_lpat_SA_(B, M, A)	800.00	44.0	180	340	78.1	256	65	GRAPPA	1.3x1.3x10	tir	849
Tagging_grid_SA-(B, M, A, HLA)	48.33	2.55	10	320	80.40	224	80		1.4x1.4x6.0	GRE	446
T1Map_LongT1_SA_(B, M, A)	280.56	1.12	35	360	85.2	256	66		1.4x1.4x8.0	Trufi	1085
T2Map_FLASH_SA_(B, M, A)	207.39	1.32	12	360	80.2	192	75	GRAPPA	1.9x1.9x8.0	GRE	1184
T1-Scout@6min post Gad	28.71	1.41	35	340	81.3	192	50		1.8x1.8x8.0	Trufi	965
DE_high-res-psir_seg_SAX1, HLA, VLA, LVOT	750.00	1.96	20	350	75	256	73	GRAPPA	1.4x1.4x8.0	GRE	287
T1Map_ShortT1_SA_(B, M, A)	360.56	1.12	35	360	85.2	256	66		1.4x1.4x8.0	Trufi	1085
Flow_retro_tp_fb_200_(PV/AV)	20.36	2.8	20	340	68.8	256	100		1.3x1.3x5.0	GRE	454

APPENDIX 4: MICROSOFT EXCEL SPREADSHEET WITH PARTICIPANT INFORMATION AND CMR MEASUREMENTS

	A	B	D	E	F	G	H	I	J	K	L	M	N	O	P	Q	R	S	T	U	V	W	X	Y	Z	AA	AB
1	Group	ID	Age	Sex	Weight	Height	BMI(kg/m ²)	BSA(m ²)	HR	HIV_Du	PAT	PAT_inc	PARA	PARA_I	LVEDV	LVEDVi	LVESV	LVESVi	LVSV	LVSVi	LVEF	LVMass	LVMASS	LVEDD	RVEDV	RVEDVi	RVESV
2	2	HNT001	26	1	68	185	20	1,9	69	0	80,9	43,2	0	0	222	119	119	64	103	55	46	172	92	61	195	104	105
3	1	HTG001	50	2	140	180	43	2,6	94	13	73,2	27,7	20,5	7,7	113	43	34	13	79	30	70	109	41	48	105	40	53
4	1	HTG002	28	1	38	166	14	1,3	83	5	4,5	3,4	2,9	2,2	87	66	52	40	35	26	40	61	46	40	75	57	30
5	2	HNT002	33	2	55	150	24	1,5	112	10	10,7	7,1	0,3	0,2	94	62	43	28	51	34	54	73	48	38	99	65	52
6	1	HTG003	58	2	72	160	28	1,8	80	6	27,8	15,6	13,7	7,7	148	93	50	28	98	55	66	132	74	55	116	65	63
7	1	HTG004	42	1	67	174	22	1,8	92	0	26,9	15,0	10,9	6,1	129	72	47	26	82	46	64	98	55	42	153	85	74
8	1	HTG005	40	1	50	170	17	1,5	95	5	12,8	8,3	2,5	1,6	103	67	49	32	55	36	53	100	65	48	103	67	59
9	1	HTG006	46	2	89	160	35	2,0	78	0	17,1	8,6	8,8	4,4	109	55	36	18	72	36	67	131	66	48	107	54	69
10	1	HTG007	19	1	33	160	13	1,2	83	7	13,9	9,8	5,0	3,6	128	91	61	43	67	55	52	97	80	49	122	101	64
11	1	HTG008	57	1	56	170	19	1,6	66	13	13,3	8,2	0,0	0,0	112	69	45	28	67	41	60	95	58	49	95	58	42
12	2	HNT003	52	1	85	180	26	2,1	76	0	86,3	41,9	8,0	3,9	154	75	57	28	97	47	63	127	62	52	148	72	85
13	1	HTG009	31	2	85	160	33	1,9	122	6	22,8	11,7	5,1	2,6	286	147	235	121	51	26	18	140	72	64	180	93	142
14	2	HNT004	35	2	132	165	48	2,5	84	0	50,1	19,5	11,2	4,3	174	68	90	35	85	35	49	145	59	56	136	55	75
15	1	HTG010	32	2	94	177	30	2,1	78	0	88,8	39,7	37,8	16,9	147	66	83	37	64	30	44	106	49	52	108	50	61
16	1	HTG011	39	1	54	190	15	1,7	62	10	2,7	1,6	0,0	0,0	133	79	68	41	64	38	48	90	53	54	122	72	67
17	1	HTG012	48	1	77	185	22	2,0	77	0	43,1	21,7	12,0	6,0	157	79	57	29	100	50	64	160	80	47	121	61	60
18	1	HTG013	46	2	59	170	20	1,7	66	0	23,5	14,1	0,0	0,0	120	72	52	31	68	41	57	83	50	43	93	56	42
19	1	HTG014	42	2	75	169	26	1,9	81	0	60,6	32,3	0,0	0,0	194	103	80	43	114	61	59	113	60	54	157	84	72
20	2	HNT005	37	1	60	180	19	1,7	84	0	99,1	57,2	0	0	176	102	107	62	69	40	39	145	84	58	154	89	90
21	2	HNT006	43	2	75	170	26	1,9	62	0	52,84	28,08	23,97	12,74	119	64	45	24	74	39	62	63	34	47	111	58	55
22	2	HNT007	32	2	67	165	25	1,8	81	0	23,7	13,5	3,6	2	179	102	75	43	105	60	58	116	66	57	138	79	68
23	2	HNT008	27	2	44	162	17	1,4	94	0	9,5	6,8	0	0	91	65	42	30	50	36	55	71	50	39	78	55	35
24	1	HTG015	31	2	68	151	30	1,7	79	0	27,2	16,1	10,0	5,9	116	68	59	35	57	34	49	69	41	52	107	63	55
25	2	HNT009	48	2	65	165	24	1,7	105	0	36,79	21,32	0	0	62	36	32	19	30	17	48	93	54	44	68	39	47
26	1	HTG016	35	1	60	172	20	1,7	66	0	37,1	21,9	0,0	0,0	149	88	66	39	82	48	55	92	54	51	154	91	89
27	2	HNT010	31	1	100	170	35	2,2	90	0	29,79	13,71	10,75	4,95	146	69	64	30	82	38	56	117	54	54	147	68	81
28	2	HNT011	53	2	90	165	33	2,0	76	0	22,78	11,22	0	0	121	62	40	20	81	40	67	102	50	57	78	38	37
29	1	HTG017	48	1	68	168	24	1,8	69	0	37,8	21,2	16,8	9,5	206	116	98	55	108	61	53	146	82	56	193	108	110
30	2	HNT012	31	2	64	155	27	1,7	68	0	15,88	9,57	0	0	147	90	65	40	81	49	56	93	56	53	111	67	62
31	1	HTG018	32	2	43	160	17	1,4	83	0	17,2	12,4	5,8	4,2	106	75	58	42	47	34	45	58	42	54	104	75	54
32	1	HTG019	29	2	69	165	25	1,8	70	0	34,2	19,3	0,0	0,0	75	42	41	23	34	19	46	90	51	39	68	38	50
33	1	HTG020	49	1	82	170	28	2,0	113	0	48,2	24,5	0,0	0,0	98	50	44	22	54	27	56	120	61	38	83	42	45
34	1	HTG021	34	1	50	170	17	1,5	77	0	37,2	24,2	0,0	0,0	145	94	59	39	85	55	59	95	62	53	109	71	57
35	2	HNT013	37	2	78	155	32	1,8	125	0	38,22	20,85	0	0	88	48	37	20	52	28	59	87	47	44	68	37	34
36	1	HTG022	52	1	75	179	23	1,9	66	0	84,1	43,6	0,0	0,0	170	88	74	38	97	50	57	125	65	45	170	88	87
37	2	HNT014	26	1	60	190	17	1,8	70	0	38,38	21,57	0	0	125	70	65	36	61	34	48	77	43	45	143	80	79
38	1	HTG023	35	1	84	180	26	2,0	97	0	57,8	28,2	18,8	9,2	122	60	49	24	74	36	60	87	42	44	124	61	61
39	2	HNT015	34	2	77	167	28	1,9	62	0	59,89	31,69	13,04	6,9	115	61	41	22	75	40	65	74	39	47	109	58	46
40	2	HNT016	39	2	112	168	40	2,3	64	0	31,64	13,84	39,38	17,23	178	78	61	27	118	52	66	123	54	56	183	80	71
41	1	HTG024	50	1	65	165	24	1,7	60	0	43,7	25,3	0,0	0,0	118	69	54	31	65	38	54	93	54	47	117	68	63
42	2	HNT017	42	1	60	170	21	1,7	66	0	13,1	7,8	0	0	138	82	67	40	70	42	51	92	55	44	149	89	96

APPENDIX 5: UCT HREC ETHICAL APPROVAL



UNIVERSITY OF CAPE TOWN
Faculty of Health Sciences
Human Research Ethics Committee



Room G50- Old Main Building
Groote Schuur Hospital
Observatory 7925
Telephone (021) 406 6492
Email: hrec-enquiries@uct.ac.za
Website: www.health.uct.ac.za/fhs/research/humanethics/forms

21 August 2020

HREC REF: 493/2020

Prof N Ntusi
Department of Medicine
1-Floor, OMB
Email: ntobeko.ntusi@uct.ac.za
Student: patricia.malshi@uct.ac.za

Dear Prof Ntusi

PROJECT TITLE: IMPACT OF PERICARDIAL AND PARACARDIAC FAT ON CARDIOVASCULAR STRUCTURE AND FUNCTION IN HIV INFECTED PERSONS ON ART: A CARDIOVASCULAR MAGNETIC RESONANCE STUDY (M DEGREE - MRS PATRICIA MAISHI) (SUB-STUDY 140/2017)

Thank you for submitting your study to the Faculty of Health Sciences Human Research Ethics Committee (HREC) for review.

It is a pleasure to inform you that the HREC has **formally approved** the above-mentioned study, subject to updating the annual approval of 140/2017.

This approval is subject to strict adherence to the HREC recommendations regarding research involving human participants during COVID -19, dated 17 March 2020 & 06 July 2020.

Approval is granted for one year until the 30 August 2021.

Please submit a progress form, using the standardised Annual Report Form if the study continues beyond the approval period. Please submit a Standard Closure form if the study is completed within the approval period.

(Forms can be found on our website: www.health.uct.ac.za/fhs/research/humanethics/forms)

We acknowledge that the student: Mrs Patricia Malshi will also be involved in this study.

Please quote the HREC REF in all your correspondence.

Please note that the ongoing ethical conduct of the study remains the responsibility of the principal investigator.

Please note that for all studies approved by the HREC, the principal investigator **MUST** obtain appropriate Institutional approval, where necessary, before the research may occur.

HREC/REF:493/2020sa

Yours sincerely

PROFESSOR M BLOCKMAN
CHAIRPERSON, FHS HUMAN RESEARCH ETHICS COMMITTEE

Federal Wide Assurance Number: FWA00001637.
Institutional Review Board (IRB) number: IRB00001938
NHREC-registration number: REC-210208-007

This serves to confirm that the University of Cape Town Human Research Ethics Committee complies to the Ethics Standards for Clinical Research with a new drug in patients, based on the Medical Research Council (MRC-SA), Food and Drug Administration (FDA-USA), International Council for Harmonisation of Technical Requirements for Pharmaceuticals for Human Use: Good Clinical Practice (ICH GCP), South African Good Clinical Practice Guidelines (DoH 2006), based on the Association of the British Pharmaceutical Industry Guidelines (ABPI), and Declaration of Helsinki (2013) guidelines. The Human Research Ethics Committee granting this approval is in compliance with the ICH Harmonised Tripartite Guidelines E6: Note for Guidance on Good Clinical Practice (CPMP/ICH/135/95) and FDA Code Federal Regulation Part 50, 56 and 312.

HREC/REF:493/2020sa

APPENDIX 6: CPUT HWS FACULTY RESEARCH ETHICS CERTIFICATE



HEALTH AND WELLNESS SCIENCES RESEARCH ETHICS COMMITTEE (HW-REC)
Registration Number NHREC: REC- 230408-014

P.O. Box 1906 • Bellville 7535 South Africa
Symphony Road Bellville 7535
Tel: +27 21 959 6917
Email: sethn@cput.ac.za

18 February 2021
REC Approval Reference No:
CPUT/HW-REC 2021/H4

Faculty of Health and Wellness Sciences

Dear Ms P Maishi

Re: APPLICATION TO THE HW-REC FOR ETHICS CLEARANCE

Approval was granted by the Health and Wellness Sciences-REC to **Ms P Maishi** for ethical clearance. This approval is for research activities related to research for **Ms P Maishi** at Cape Peninsula University of Technology.

TITLE: Impact of Pericardial and Paracardiac Fat on the Cardiovascular Structure and Function in HIV Infected Persons: A Cardiovascular Magnetic Resonance Study

Supervisor: Mr A Speelman

Comment: Ethics approval is conditional to the obtaining of permission to conduct research at the Grootte Schuur Hospital in writing and supplying it to the committee secretariat.

Approval will not extend beyond 19February 2022. An extension should be applied for 6 weeks before this expiry date should data collection and use/analysis of data, information and/or samples for this study continue beyond this date.

The investigator(s) should understand the ethical conditions under which they are authorized to carry out this study and they should be compliant to these conditions. It is required that the investigator(s) complete an **annual progress report** that should be submitted to the HWS-REC in December of that particular year, for the HWS-REC to be kept informed of the progress and of any problems you may have encountered.

Kind Regards



Carolynn Lackay
Chairperson – Research Ethics Committee
Faculty of Health and Wellness Sciences

APPENDIX 7: SUBJECT INFORMATION LEAFLET

Predictors of Diffuse Myocardial Fibrosis in HIV Infected Persons: A Multiparametric Cardiovascular Magnetic Resonance Study

You are invited to take part in a research study. Before you decide, it is important for you to understand why the research is being done and what it will involve. Please take time to read the following information carefully and discuss it with friends, relatives, and your doctor, if you wish. This leaflet will tell you the purpose of the study, what will happen to you when you take part and gives you detailed information about the conduct of the study. Ask us if there is anything that is not clear or if you would like more information. Thank you for reading this.

What is the purpose of the study?

Patients with HIV infection have inflammation of the heart muscle which may lead to scarring of fibrosis. We would like to assess the frequency of scarring in the heart muscle in HIV-infected patients, as assessed by MRI and to see what effect antiretroviral therapy and common blood pressure medication have on improving or preventing this fibrosis. Finally, we are also interested to assess the relationship of myocardial scarring on MRI with cardiovascular outcomes.

If you take part in this study, you will be seen at a visit, where you will be examined, have a resting electrocardiogram (ECG), have your blood pressure measured (BP), have an analysis of your blood vessel function by placing a sensor at your wrist, and be asked to provide us with a blood sample. We will also examine the function of your heart with an MRI scan. You will not be asked to take any additional long-term pill or alter your regular medication in any way.

Why have I been invited?

You have been invited because either you have HIV infection or have tested negative for HIV.

Do I have to take part?

It is up to you to decide whether to take part. If you decide to take part, you are free to withdraw consent at any time without giving a reason. Your decision will not affect further treatment for your condition. If you decide that you no longer wish to continue with the study, we will keep all the test results that we got from you up to the point of your withdrawal.

What will happen to me if I take part?

You would attend a visit that will last about 2 hours. At this visit, we will ask some general questions about your health and regular medication. After that, we will do a quick check of your pulse, blood pressure, weight and height. We will also do an ECG trace of your heart's electrical impulse. After that, we may perform an ultrasound scan of your heart. We will then scan your heart, using cardiac MRI. If your ultrasound or MRI scan suggests abnormalities, we will advise your doctors to refer you to a cardiologist for review.

Below, all the above-mentioned tests are discussed in a little bit more detail:

1. Clinical assessment

The assessment will start by asking you a set of questions about your health and previous medical conditions, using a structured questionnaire. The physical examination will include measurement of your pulse, blood pressure, weight, and height, as well as an examination of the heart and the vessels.

2.The heart MRI scan

The MRI scan of your heart will be the most important part of this study and will last about 60 minutes. MRI scans are painless but involve the use of a strong magnetic field, so if you have any of the following, you would not be suitable for a scan, and would not be able to take part in this study:

- a permanent pacemaker
 - metal clips in blood vessels of the brain
 - an injury to the eye involving fragments of metal

 - shrapnel injuries, bullet fragments other metal or electronic implants
 - stimulators
 - cochlear implant
 - insulin pump
-

➤

The MRI scanner is shaped like a doughnut, the hole inside is about 70 centimetres wide, with a table that slides in and out.

You will be asked to change into a hospital gown and lie on your back for the scan. We will clean your skin with gel to put special ECG stickers on your chest. Your heart rate will be measured during the scan, and it is important to lie very still while your heart is being scanned. You will also be asked to breathe in and out and hold your breath for several seconds for most of the scans. Pictures of the heart are created using a magnetic field, radio waves and computers. When images are being taken, the MRI scanner makes a loud noise, and you will be provided with earphones to protect your ears. It is important that you lie still for the duration of the scan. We will give you a buzzer that you can squeeze should you feel any pain or discomfort during the scan. To do a complete assessment of the heart, we need to examine the blood circulation and your heart muscle to check for inflammation and scarring. We also need to assess the appearance of the tissue of the heart. In order to do this, we shall inject some contrast dye, called gadolinium, through a drip into your arm. This will only be done towards the last 15 minutes of the scan. The scans will be stored for up to 10 years and may be used in future research as our understanding of heart and blood vessel function and inflammation improves.

The Electrocardiogram (ECG)

We will take an electrocardiogram (ECG) of your heart which will last about 5 minutes. An ECG is a tool that uses surface electrodes on certain points on your chest and arms to monitor the electrical properties of your heart.

3.The ultrasound of the heart (15-20 minutes)

An echocardiogram or ultrasound of your heart is a safe and painless procedure to study heart structure and function. You will be asked to lie on a couch on your left side, and a probe will be placed on your chest. Lubricating jelly is used so the probe makes good contact with the skin. Ultrasound waves then create images of your heart on the scanner monitor. It normally takes 15-20 minutes to acquire these images.

What about travel expenses?

We will reimburse travel expenses to and from the hospital. Lunch will be provided or reimbursed.

What will I have to do if I agree to take part in this study?

- Attend a visit at Groote Schuur Hospital for the assessment, blood tests and for the scans.
- Consent to taking part in this study by signing a form.
- We will ask that you do not have anything to eat 4-6 hours before the visit.
- Undergo the procedures as described above.

Are there any other possible risks from taking part?

The scanning is done using an MRI scanner which is also used routinely in clinical practice to acquire images of various body parts. MRI scans are safe, non-invasive and do not involve any ionizing radiation (X-rays). Some people find the space limitation in the scanner uncomfortable, but you will be given a chance to see the scanner to make sure that you are comfortable in it before the study starts. The scan is noisy, and we provide headphones to protect your ears. The whole time that you are in the scanner you will be given a buzzer which you will be able to use at any time if you wish to stop the study. As the scanner consists of a powerful magnet, it may attract certain metallic objects. You must not have a scan if you have had metallic objects or medical devices (e.g., pacemaker) or surgical implants such as stainless-steel screws, hip replacements inserted into your body during an operation. Please inform us if you have any of these metal implants anywhere in your body. MRI is safe in pregnancy, because this is a research study, as a precaution we advise you to tell us if there is any chance you might be pregnant. The doctor or radiographer will go through a list of possible risks with you before you go into the scanner.

In the unlikely event of us seeing any structural abnormalities on your MRI scan, a member of our research team will discuss the implications with you, and, with your permission, your doctor may be notified. However, it is important to note that we do not carry out scans for diagnostic purposes, and therefore these scans are not a substitute for a clinical appointment. Rather, our scans are intended for research purposes only. Some people find having a drip in their arm uncomfortable and there can be bruising at the site of needle entry. Our staff is trained in drip insertion and we will make sure you are as comfortable as possible.

Gadolinium, the dye used for the MRI scans, has been in clinical use for over 20 years. As the dye is being injected, some people report a sensation of warmth at the injection site. It is unusual to feel pain, and in this case, we would stop the injection immediately. Rarely, some people feel slightly nauseous or have a metallic taste following the injection, but vomiting is very rare. Occasionally, people have developed a rash; however, severe allergic reactions are very rarely experienced. Again, this dye is injected through a drip in the arm. There is no pain associated with the injection at the site. There is a small risk of an allergic reaction to the dye.

ECG and ultrasound are safe, non-invasive tests, with no known serious risks/harm. Rarely, individuals having either test may develop an allergic reaction to placement of electrodes that results in a mild rash. This rash disappears in a few days without any treatment.

It is important to note that in a large-volume MRI Centre like Groote Schuur Hospital, where our experienced staff has been doing MRI scans for many years, the risk of harm from the MRI and other tests is exceedingly small.

What are the possible benefits?

There is no direct benefit for you as an individual taking part in this study. We hope that by studying people with your condition using cardiac MRI, we may be able to improve understanding of this condition and help to inform screening and or treatment of future patients.

What happens when the research study stops?

The end of the study will not affect the care you receive from your doctors. The end of the study will mark the official end of your participation in this project. Copies of any publications connected

to this study will be available on request from Professor Ntusi. Please inform us should you wish to have copies of the findings of this research project.

Will my taking part in the study be kept confidential?

Yes. We will follow ethical and legal practice and all information about you will be handled in confidence. If you take part in the study, some of the data collected from the study would be looked at by authorized persons from the University of Cape Town, to check that the study is being carried out correctly. All investigators have a duty of confidentiality to you as a research participant, and nothing that could reveal your identity would be disclosed outside the research site. The data collected from the study will be recorded anonymously and you would not be identifiable from this.

What if relevant new information becomes available?

Sometimes, we (the study investigators) get new information about the procedures being studied. If this happens, one of us will tell you and discuss whether you should continue in the study. If there is sufficient evidence to suggest you may be harmed from participating in this study, the study could be stopped.

Unexpected findings on your scan

In the unlikely event of us seeing any structural abnormalities on your MRI scan, a designated clinical specialist will discuss the implications with you and may arrange for further investigations as necessary. However, it is important to note that we do not carry out scans for diagnostic purposes, and therefore these scans are not a substitute for a clinical appointment. Rather, our scans are intended for research purposes only. So if we find anything unusual, it would be appropriate for us to contact your GP/specialist so that they can arrange on-going clinical care for you. But we would only do this after we and the specialist had discussed your options and gained your permission.

What will happen if I don't want to carry on with the study?

You are free to withdraw from the study at any time. Anonymised data will be kept till the point you choose to end your participation in the study. Data collected till the point of your withdrawal will be included in the analysis.

What will happen to the results of the research study?

We anticipate that the results will be published in a scientific journal for the benefit of the wider medical community. However, individual patients will not be identified in any publication and your personal and clinical details will remain strictly confidential. Any scientific publications arising from the study will be available on request to all participants. You would have no legal right to a share of any profits that may arise from the research.

Will your test results be shared with you?

We will show you the images we acquire from the ultrasound and MRI scans when we finish performing the scans. The results of the other tests will only be available on publication of the results. If, however, results of any of the tests are grossly abnormal, we will contact you to discuss these with you before suggesting a course of action and contacting your doctor/specialist.

Who is organizing and funding the research?

The study is organized and conducted by researchers from the University of Cape Town and Groote Schuur Hospital. The studies are funded, in part, by a grant from the National Research Foundation of South Africa.

Who has reviewed the study?

The University of Cape Town Human Research Ethics Committee as well as the Research Ethics Committee of the Cape Peninsula University of Technology has reviewed and approved the study.

Further information and contact details

Should you wish to know more about any aspects of this study, please contact:

Professor Ntusi at: (021) 406 6200

APPENDIX 8: INFORMED CONSENT FORM

Study Full Title	Predictors of Diffuse Myocardial Fibrosis in HIV-Infected Persons: A Multiparametric Cardiovascular Magnetic Resonance Study.
Patient ID	
Principal investigator	Prof. Ntusi

	I agree	I disagree
I confirm that I have read and understand the information sheet for the above study. I have had the opportunity to consider the information, ask questions and have had these answered satisfactorily.	<input type="checkbox"/>	<input type="checkbox"/>
I understand that my participation is voluntary and that I am free to withdraw at any time without giving any reason, without my medical care or legal rights being affected.	<input type="checkbox"/>	<input type="checkbox"/>
I understand that relevant sections of my medical notes and data collected during the study may be looked at by authorized individuals from the University of Cape Town, where it is relevant to my taking part in this research.	<input type="checkbox"/>	<input type="checkbox"/>
I understand that my doctor will, with my permission, be informed of the results of medical tests performed as part of the research, which are important for my health care.	<input type="checkbox"/>	<input type="checkbox"/>
I also understand that I may be invited to return for a second MRI scan, which is optional and that I will not pay for any of these procedures.	<input type="checkbox"/>	<input type="checkbox"/>
I agree to being contacted in the future to ask if I am interested in future related studies.	<input type="checkbox"/>	<input type="checkbox"/>

Name of participant	Signature	Date
Name of person taking consent	Signature	Date